

A Preliminary Prospectivity Map for the Tellus Border region

Final project report

29th October 2013

Sarah Coulter and Joshua Stinson

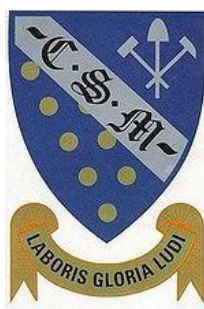
This research is supported by the EU INTERREG IVA-funded Tellus Border project. The views and opinions expressed in this research report do not necessarily reflect those of the European Commission or the SEUPB.



A project supported by the EU's INTERREG IVA
Programme managed by the Special EU Programmes Body



GALÁNTAS
G O L D C O R P O R A T I O N



Acknowledgements

The outstanding work conducted by Tellus Border teams associated with GSNI and GSI has provided the foundation for this project. In particular, we are grateful for the guidance and supervision afforded to us by Ray Scanlon and Kate Knights (GSI), and Mark Patton (GSNI). This research is supported by the EU INTERREG IVA-funded Tellus Border project.

Table of Contents

1. Introduction.....	12
2. Geology and Mineral deposits	15
3. Tellus Border data analysis	19
3.1. Analytical approach and statistical methods	19
3.2. Controls on geochemistry.....	23
3.2.1. Element concentration in relation to pH	23
3.2.2. Element Concentration in relation to Lithology	27
3.2.3. Element concentrations in relation to faulting	28
3.3.Evaluation of Geochemical data	30
4. Target Area Generation.....	31
4.1. Target Area selection	35
4.2. Target Area Analysis.....	36
4.2.1. Knowledge Driven Exploration:.....	36
4.2.2. Data Driven Exploration:.....	36
5. Exploration Methods and Analysis	38
5.1. Sample collection strategy	38
5.2. Sample preparation.....	39
5.2.1. QA/QC.....	39
5.3. Sample analyses	40
6. Analysis of Target areas.....	41
6.1. Manorhamilton.....	41
6.1.1. Introduction.....	41
6.1.2. Local geology	42
6.1.3. Existing Data Analysis	44
6.1.3.1. Knowledge Driven Exploration	44
6.1.3.2. Data Driven Exploration	45
6.1.4. Fieldwork	48
6.1.5. Results.....	49
6.2. Glenties.....	56
6.2.1. Introduction.....	56
6.2.2. Local Geology	57
6.2.3. Existing Data Analysis	60

6.2.3.1. Knowledge Driven Exploration	60
6.2.3.2. Data Driven Exploration	61
6.2.3.3.Target A	62
6.2.3.4.Target B.....	65
6.2.4. Fieldwork	68
6.2.5. Results.....	72
6.3. Millford	78
6.3.1. Introduction.....	78
6.3.2. Local geology	79
6.3.3. Existing data analysis	81
6.3.3.1. Knowledge driven Exploration	81
6.3.3.1. Data Driven Exploration	82
6.3.4. Fieldwork	87
6.3.5. Results.....	89
6.4. Shercock	96
6.4.1. Introduction.....	96
6.4.2. Local Geology	96
6.4.3. Existing data analysis	98
6.4.3.1.Knowledge Driven Exploration	98
6.4.3.2. Data Driven Exploration	99
6.4.4. Fieldwork	104
6.4.5. Results.....	107
7. Summary and Conclusion	112
8. References	114

List of Figures

Figure 1: Map showing the generalised geology and known mineral deposits in Ireland with the Tellus Border region highlighted.

Figure 2: Map of the Tellus Border region showing the status of PL areas

Figure 3: Summary map of geological provinces of the north of Ireland (GSI, 2006)

Figure 4: Map displaying the main deep seated lineaments, major faults and significant geological features for the north of Ireland

Figure 5: Box and whisker diagram displaying variability of As associated with major bedrock units

Figure 6: Box and whisker diagram displaying relationship between As levels and fault orientation

Figure 7: Chart comparing the upper end values of As within each fault group

Figure 8: Stream sediment geochemical data analysis using nine selected pathfinder elements.

Figure 9: Top-soil geochemical data analysis using nine selected pathfinder elements.

Figure 10: Combined top-soil and stream sediment analysis for major pathfinder elements

Figure 11: Map showing Preliminary Target Areas.

Figure 12: Locality map for the Manorhamilton area, with subset image of its location within the border region.

Figure 13: Geological base map showing lithology and faulting in the Manorhamilton area.

Figure 14: Map for the glacial features in the Manorhamilton area

Figure 15: Map of sample locations for top-soil survey of Manorhamilton

Figure 16: Map indicating the locations of stream sediment samples within the Manorhamilton target

Figure 18: Graph representing main pathfinder anomalies for bedrock sample 025

Figure 19: Map showing the location of panned concentrate samples (above) and their relative levels of Au, Ag, Hg and Sb (below).

Figure 20: Locality map for the Glenties area, with a sub-set of its location in the border region

Figure 21: Detailed geological map of Glenties target areas A and B

Figure 22: Map displaying the trend of glacial movements in the Glenties target, with the dominant orientation being E-W using evidence from striae and NE-SW using drumlin evidence.

Figure 23: Summary map of stream sediment sample locations in the Glenties A target.

Figure 24: Summary map for top-soil samples within Glenties target A.

Figure 25: Map of stream sediment sample locations in Glenties target area B.

Figure 26: Summary map for top-soil data in Glenties area B.

Figure 27: photographs displaying two forms of mineralisation in the Glenties region

Figure 28: Stereonet of the main structural features within pod of dolerite within the Glenties target

Figure 29: Map showing location of new samples taken in the Glenties target

Figure 30: Map displaying location of significant Au anomalies in the Glenties target

Figure 31: Quartz vein sample OM-13-PS-032 containing pyrite with minor galena

Figure 32: Locality map of the Millford target area, with a sub-set of its location within the border region

Figure 33: Geological map of the Millford target area

Figure 34: Map displaying the trend of glacial movements in Millford

Figure 35: Location map of top-soil samples in the Millford target area.

Figure 36: Location map of stream sediment sample points for the Millford target area

Figure 37: Map showing the location of new sample sites within Millford.

Figure 38: Sample locations of high stream sediment anomalies (top), with graphical representation of the data showing the overprint of topography and mapped lithology (bottom).

Figure 39: The relationship between ranked anomalies and pH for soil samples in Millford

Figure 40: Locality map of the Shercock target area, with a sub-set map of its location within the border region

Figure 41: Detailed Geological map of the Sherock target area

Figure 42: Map displaying the trend of glacial movements in the Shercock target

Figure 43: Map displaying sample locations for top-soil data in the Shercock target

Figure 44: Stream sediment sample locations in the Shercock target area

Figure 45: Photograph of typical overburden in Shercock area

Figure 46: photographs showing the occurrence of vein hosted mineralisation in the Shercock target area

Figure 47: Map showing location of new samples collected in the Shercock target.

List of Tables

Table 1: Key exploration criteria used with their associated mineralised regions.

Table 2: Summary for each element used in exploration process, showing comparison of values with crustal abundance.

Table 3: Statistics for Sb in top-soils

Table 4: Cumulative frequency plot for Sb, with bins selected at 0.1ppm. Bin ranges selected to best represent the variety in data.

Table 5: Histogram and percentile ranges, colour coded.

Table 6: Analysis of element concentrations in relation to pH >7 and 5-7.

Table 7: Analysis of element concentration in relation to pH 3-5 and <3.

Table 8: Data for three elements comparing the top 10 values of the total data set with data from the fault analysis.

Table 9: Summary table of each preliminary target area with its associated geochemical anomalies.

Table 10: Showing additional criteria for the derivation of final targets

Table 11: Example summary table for Au pathfinder elements

Table 12: Correlation matrix for Au pathfinder elements in top-soil data from the Millford target area

Table 13: Correlation matrix for high anomalies from both base metal and Au pathfinder groups, in top-soil data from Millford target area

Table 14: A comparison of Manorhamilton data with the complete Tellus Border geochemical dataset.

Table 15: Summary values of Au pathfinder elements from top-soil data in the Manorhamilton target.

Table 16: Correlation matrix for Au pathfinder elements in the Manorhamilton top-soil data.

Table 17: Summary table of Au pathfinder elements in stream sediment data for Manorhamilton

Table 18: Correlation matrix of Au pathfinder elements in stream sediments at Manorhamilton

Table 19: Summary of main lithologies in the Manorhamilton target area.

Table 20: The key results for new samples collected in the Manorhamilton target.

Table 21: Comparison of selected sub-soil and panned concentrate samples with associated top-soils and stream sediment samples in Manorhamilton

Table 22: Summary table for Tellus Border geochemical data for the Glenties target area.

Table 23: Summary table for Au pathfinder elements in stream sediment analyses for Glenties A

Table 24: Correlation matrix for stream sediment Au pathfinder data in Glenties A.

Table 25: Summary table for Au pathfinder elements in Glenties A top-soil data.

Table 27: Summary table for stream sediment Au pathfinder elements in Glenties area B

Table 28: Correlation matrix for stream sediment Au pathfinder elements in Glenties area B

Table 29: Summary table for Au pathfinder elements in top-soil samples for Glenties B

Table 30: Correlation matrix for Au pathfinder elements in top-soils for the Glenties B region

Table 31: Correlation matrix for Au pathfinder elements in stream sediment data for Glenties A and B

Table 32: Correlation matrix for top-soil Au pathfinder elements for Glenties areas A and B

Table 33: Summary of mapped units within the Glenties area.

Table 34: The results of analyses for new samples collected within the Glenties targets.

Table 35: Summary table of Tellus Border geochemical data for the Millford target area

Table 36: Summary table of Au pathfinder elements in top-soils for the Millford target area.

Table 37: Correlation matrix for Au pathfinder elements in the Millford top-soils.

Table 38: Summary of base metal pathfinder elements from top-soil data for the Millford target area

Table 39: Correlation matrix for base metal pathfinder element for the Millford target area.

Table 40: Summary table of base metal pathfinder elements from stream sediment data in the Millford target.

Table 41: Correlation matrix of Au pathfinder elements in stream sediments for the Millford area.

Table 42: Summary table of base metal pathfinder elements for Millford

Table 43: Correlation matrix of base metal pathfinder elements in stream sediments for Millford

Table 44: Correlation matrix combining Au and base metal pathfinder groups in stream sediments for Millford

Table 45: Summary table of mapped lithologies in the Millford area.

Table 46 Results of analyses on samples collected in the Millford target area.

Table 47: Summary table for Tellus Border geochemical data relating to the Shercock target area.

Table 48: Summary of Au pathfinder elements from top-soil data in the Shercock target.

Table 49: Correlation matrix for Au pathfinder elements in top-soils for the Shercock target

Table 50: Summary table of base metal pathfinder elements in top-soils for Shercock

Table 51: Correlation matrix for base metals in the Shercock area

Table 52: Correlation matrix for both pathfinder groups in Shercock top-soils.

Table 53: Stream sediment Au pathfinder data for the Shercock target

Table 54: Correlation matrix for Au pathfinder elements in the Shercock stream sediments

Table 55: Summary of base metal pathfinders in the Shercock target area stream sediments

Table 56: Correlation matrix for base metal pathfinders in the Shercock target area stream sediments

Table 57: Correlation matrix for both pathfinder groups in stream sediments of the Shercock target area.

Table 58: Summary of mapped units and formations in the Shercock area.

Table 59: Summary table showing new sample results for the Shercock target.

Table 60: Comparison of selected sub-soil and panned concentrate samples with the associated top-soil and stream sediment samples in the Shercock target

Table 61: Comparison between major element values in top- and sub-soils within the Shercock target.

Summary

Data derived during the original Tellus project (2004-2006) prompted significant interest in the mineral prospectivity of Northern Ireland. Mining and exploration companies were attracted to the region due to the availability of high quality geophysical and geochemical data. In 2011 a new phase of the project was initiated in the border counties of the Republic of Ireland. The Tellus Border project brought together teams from both the Geological Survey of Northern Ireland (GSNI), The Geological Survey of Ireland (GSI), Queen's University Belfast (QUB) and Dundalk Institute of Technology, in a joint initiative to extend high resolution geophysical and geochemical mapping into the counties of Counties Donegal, Leitrim, Sligo, Cavan, Monaghan and Louth and to integrate the results with datasets for the north. This EU funded work has generated new high quality datasets for a region which currently harbours only a single working mine (Kingscourt) and where only one significant Au deposit has been well documented (Clontibret). The aim of this project was to analyse the data in conjunction with historic geological records to assess the prospectivity of the Border region for precious and base metals.

The Border region is underlain by a diverse geology, similar geological associations elsewhere have yielded a wide range of mineral prospects including gold, silver and base metals such as copper, lead and zinc. Some such prospects have already been established within the Border zone. The new data has provided an ideal opportunity to apply the key geophysical and geochemical associations found at known deposits to a wider area. The research carried out during this project did not constrain the investigation to a single genetic model because of the size and inherent geological diversity of the Border zone. Instead, an open mind was adopted about many potential styles of mineralisation whilst maintaining objectivity in analysis. As such, the work has identified many areas and aspects of analysis which could provide the foundation for more detailed future research projects.

The project began by integrating all available geochemical data, the magnetic and electrical conductivity geophysical surveys, in ArcGIS. The geochemical data includes topsoil and stream sediment base metal analyses. Basic statistical methods were adopted to analyse the results and construct data ranges for the purposes of display of the main elements on base maps. The co-occurrence of multiple mineral pathfinder elements within single samples, or samples in close proximity, and between different sample types was used as one of the main criteria for identifying the most prospective areas. Other principal criteria were lithology and age of bedrock, structural features such as NE trending faults and deep seated lineaments. This information was gathered from geological base maps in conjunction with the new Tellus Border electrical conductivity and magnetic maps. The results isolated 19 areas within the Border zone. The scope of this project necessitated further screening of these Potential Target Areas (PTAs) in order to derive four sub-areas for further detailed follow up study. The criteria applied include status of Prospecting Licence Areas (PLAs), land accessibility, historical workings and potential environmental and anthropogenic contamination. Whether a PL area was designated as 'open' or already held under an exploration licence was a major concern during the shortlisting process. The main objective of this work is to promote the prospectivity potential of the region and ultimately lead to the uptake of new largely

unexplored licences. Therefore, any of the nineteen areas which were wholly or largely within 'held' licences were discounted at this stage. The four areas which were selected for further detailed sampling and mapping were: Glenties and Millford in Co. Donegal; Manorbhamilton in Co. Leitrim and Shercock in Co. Cavan. All four areas appear prospective for gold, with Shercock and Glenties also exhibiting potential for base metal mineralisation.

Each of the four target areas were investigated by Omagh Minerals' geologists, lithological and structural observations were made in the field and a range of sample types collected for geochemical analysis. Samples included: top-soils, sub-soils, float rock, bedrock, stream sediment and panned concentrates. All samples were subject to fire assay and ICP-MS analysis at the ALS laboratory in Galway. During analysis and interpretation of the datasets consideration was given to the association between certain element concentrations and local geological and environmental conditions e.g. lithology, fault orientation, soil and stream water pH and contamination. Furthermore, the passage of ice flow during the last glaciation was taken into consideration as this control will have redistributed material from its source and thus has an important bearing on element patterns. The new results indicate significant gold anomalies in stream sediments and rock samples, particularly within the Millford and Glenties targets.

The project has succeeded in highlighting the highly prospective nature of the Border region, particularly for gold. The new results generated during this work have enhanced the Tellus Border geochemistry datasets within specific zones. Geological observations and new data have informed discussions regarding genetic models for mineralisation and new areas for further research have been identified.

1. Introduction

The Tellus Border zone encompasses an area of around 13,300 km² this region has traditionally yielded coal and industrial mineral deposits. Historical records point towards barite and gypsum workings in the Carboniferous sediments around Benbulbin, Glengevlin and Kingscourt (Figure 1). The latter continues to support an active mine and has done since 1936 (EMD, 2005). Several Pb-Zn deposits are known on the southern and eastern fringes of the Border zone, namely at Salterstown, Clonabreeny, Oldcastle, Lough Sheelin and importantly in the vicinity of Navan which hosts Europe's largest Zinc mine (EMD, 2005). A porphyry style Cu-Mo prospect also exists in association with granite close to Crossdoney. Within Donegal three Pb prospects are documented at Glentogher, Glenaboghil and Keeldrum.

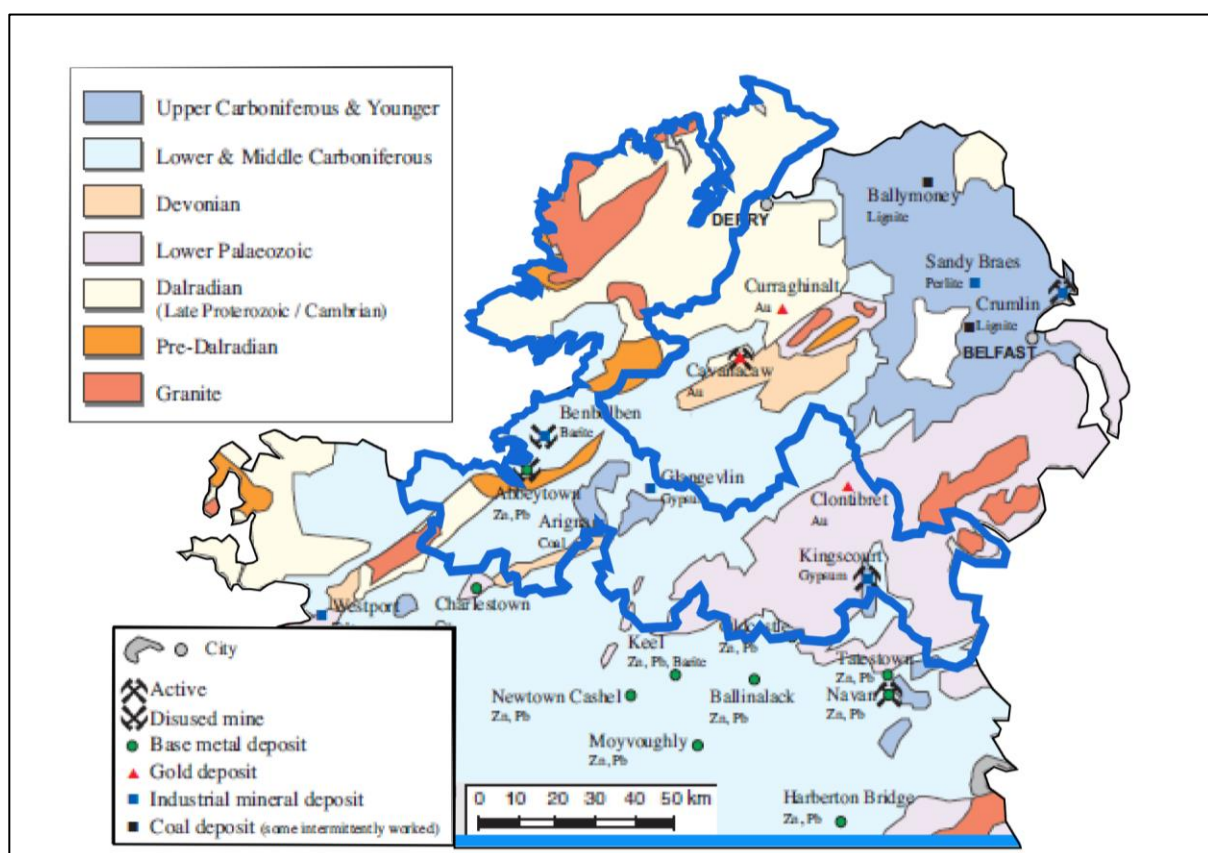


Figure 1: Map showing the generalised geology and known mineral deposits in Ireland with the Tellus Border region highlighted. Adapted from Exploration and Mining Division Ireland, 2005.

Figure 2 shows the current status for Prospecting Licence (PL) areas in the Border region. In total there are 287 areas, these are usually ~35km² and their margins are defined largely by townland boundaries. At the beginning of this project 86 PL areas were under licence principally by exploration companies, amounting to 30% of the total area.

On 15th February 2011 the Tellus Border project was launched. This regional mapping initiative included an intensive sampling and analysis programme in an effort to collect geological and environmental data for soils, stream sediment and water at ~3.5 km² centres

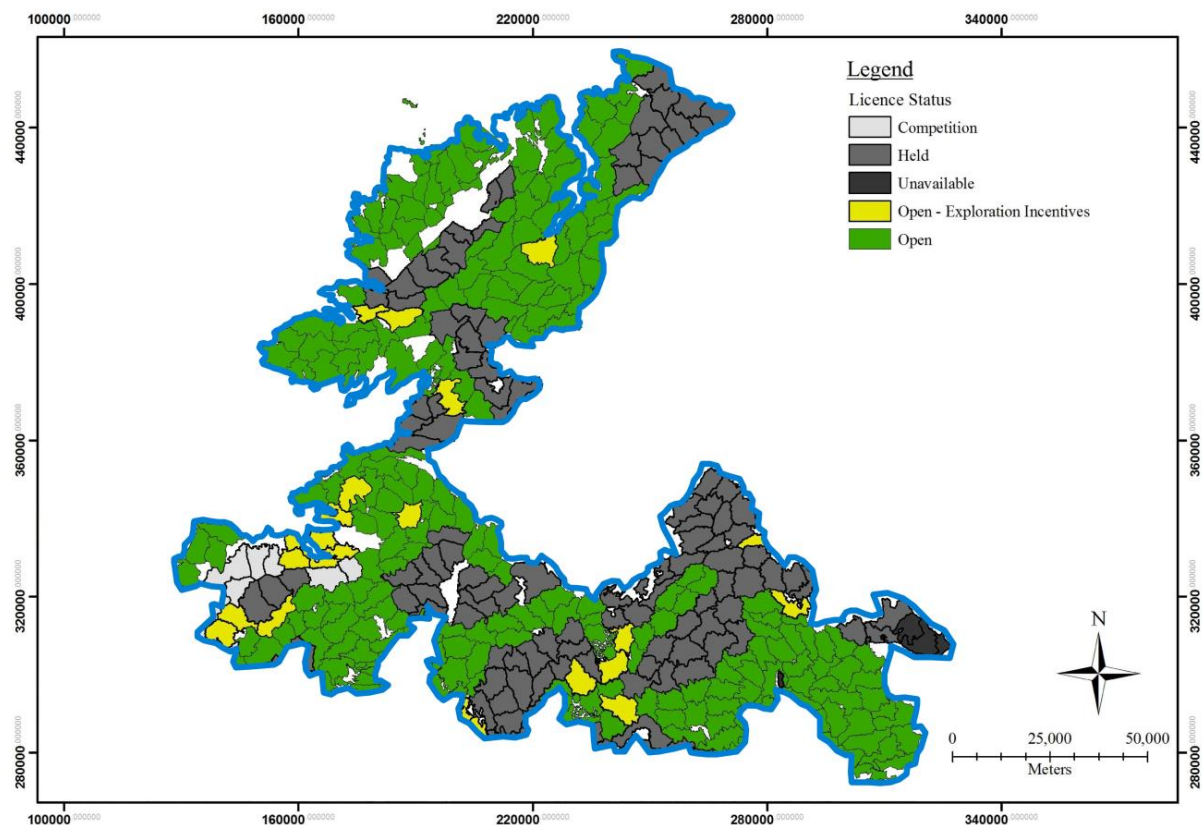


Figure 2: Map of the Tellus Border region showing the status of PL areas (source: EMD, Sept 2013)

including counties Donegal, Sligo, Leitrim, Cavan, Monaghan and Louth. Samples were taken from approximately 7,000 locations. A low flying aircraft was used to conduct magnetic, radiometric and electrical conductivity surveys on 200 m spaced lines during autumn 2011 and summer 2012 (www.tellusborder.eu). This cross border project aims to integrate data between countries to assess the natural resources, environmental conditions and improve geological understanding (Clennon, 2013).

The ultimate aim of this work was to use the new Tellus Border datasets to assess the potential for mineralisation associated with precious and base metals within the Border zone. This aim was devised with a view to encouraging inward investment from local and international exploration and mining companies. In order to make an effective and accurate assessment of prospectivity potential within the timeframe of this project we employed a range of data sources, however, most consideration was given to the geochemical results generated through the Tellus Border project. Secondary sources used to complement the new data include:

- Historical exploration reports
- Geological base maps (1:100,000)
- MinLocs database
- Geological publications

Following the integration and analysis of the Border region as a whole, the most prospective areas were isolated. Follow up fieldwork was conducted in four of these. This report is split largely into two main bodies of work, firstly the analysis of the Tellus Border datasets for the derivation of target areas (Sections 3 and 4); followed by the methods results and analyses for fieldwork (Sections 5 and 6).

2. Geology and Mineral deposits

The Tellus Border zone straddles two main mineral provinces, the North-Western Basement and the Longford-Down Massif (Figure 3). It is dissected by major structural features, the south-western continuation of the Highland Boundary Fault (HBF) and the Southern Upland Fault (SUF) as well as deep seated north-west trending lineaments. Recent work by Cooper *et al.* (2013) assesses the age of intrusions within the Grampian Terrane and investigates the relationship between major lineaments and magmatic events in the north of Ireland. Figure 4 (Cooper *et al.*, 2013) depicts the location of the deep seated lineaments and the major NE-SW trending faults which in some areas are known to be associated with significant gold deposits.

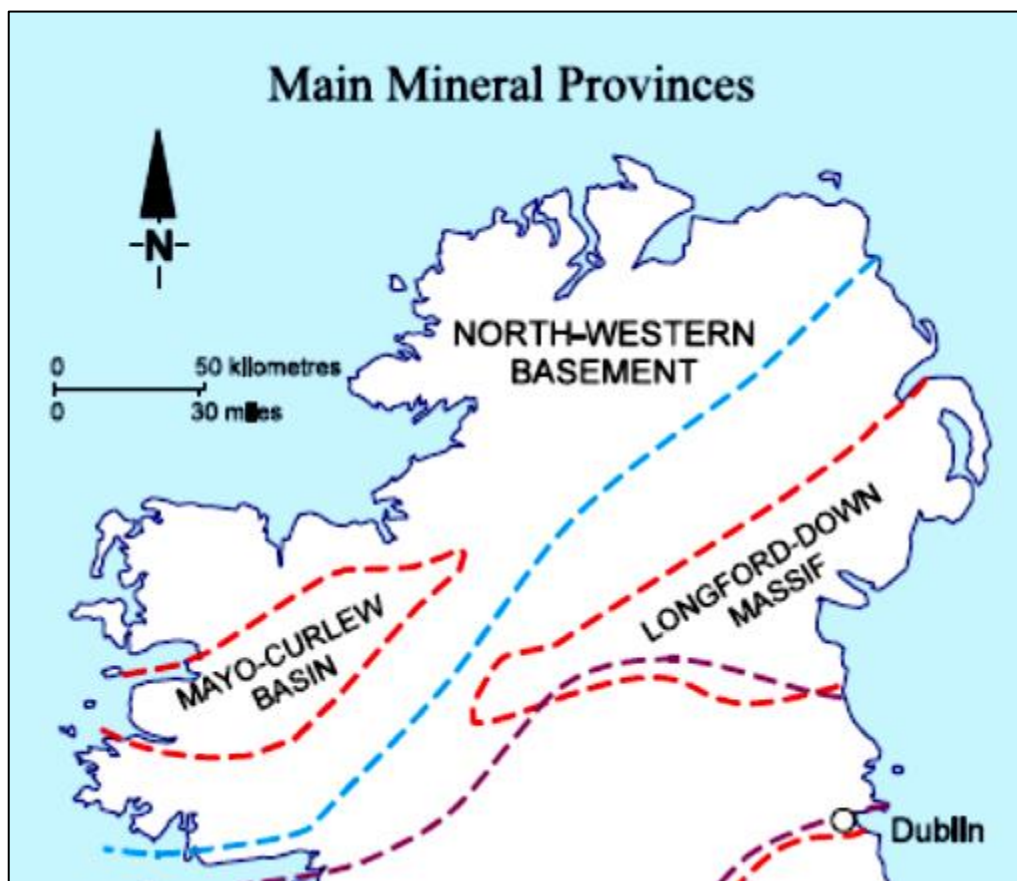


Figure 3: Summary map of geological provinces of the north of Ireland (GSI, 2006)

The Longford-Down Massif encompasses the eastern portion of the Border region. This geological inlier comprises Ordovician and Silurian rocks which can be traced through the Dunnage Zone (Newfoundland) in the west and the Scottish Southern Uplands (Stone *et al.*, 1995). It forms part of the Caledonian Orogenic belt which has been the focus of multiple mineral exploration projects. This area is host to lead, zinc, iron gold and antimony deposits the occurrences of which have been linked to movement on a major fault, namely the Orlock Bridge Fault, which separates the Ordovician and Silurian strata (Smith *et al.*, 2003). A current area of exploration interest is the Armagh-Monaghan Gold belt which sits at the intersection between the northeast – southwest trending Orlock Bridge Fault (OBF) and a north-south trending fault and is associated with igneous intrusive (Steed and Morris, 1997).

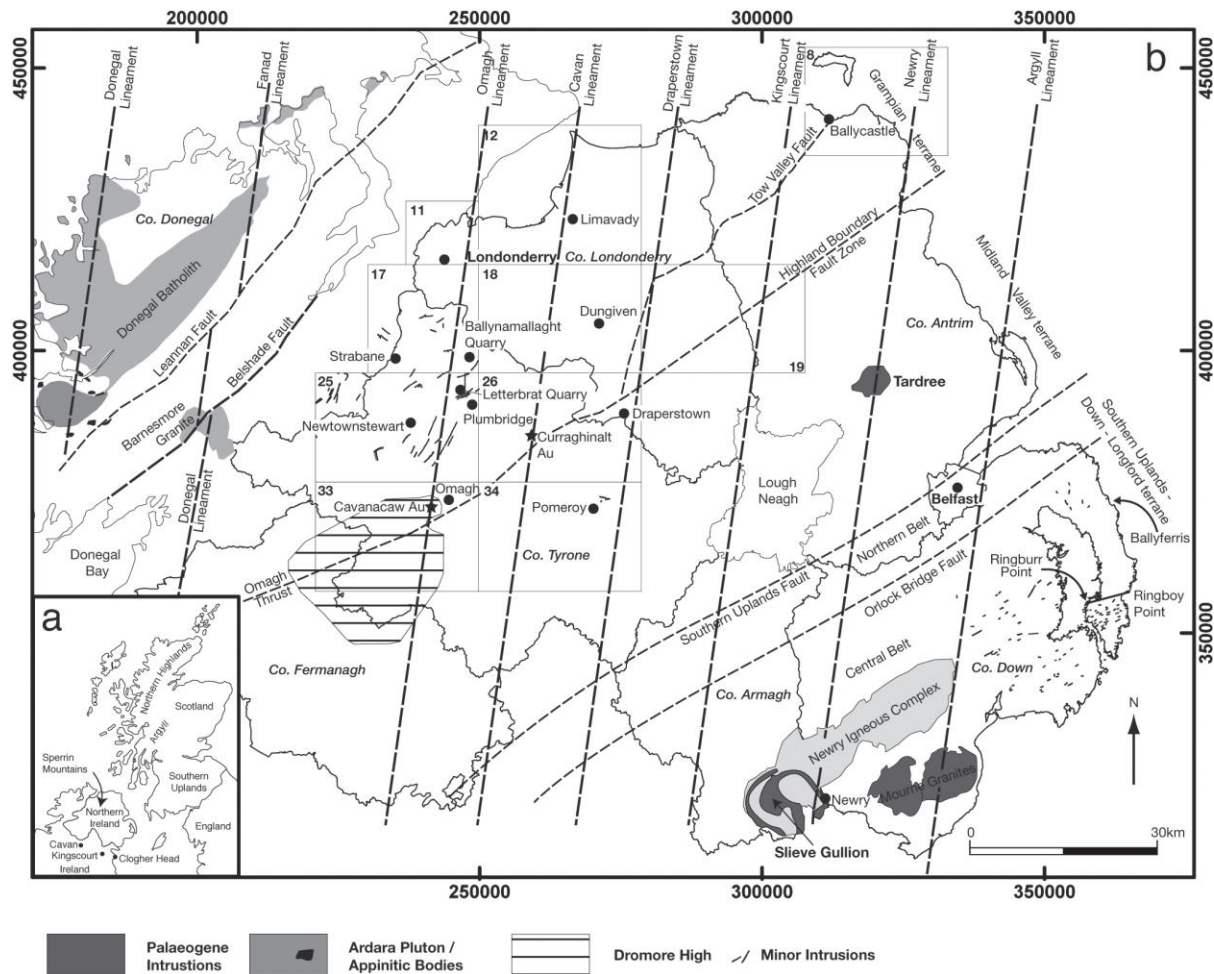


Figure 4 Map displaying the main deep seated lineaments, major faults and significant geological features for the north of Ireland (From: Cooper *et al.*, 2013).

A long history of mining stretching over the last 200 years is recorded for the Clontibret area. Gold is hosted in lenticular quartz carbonate veins proximal to the OBF, stringer veins and northwest trending lodes, and is associated principally with the sulphide minerals arsenopyrite and pyrite (Cruise and Farrell, 1993).

Some of the oldest rocks found in Ireland are hosted in the North-Western Basement, these comprise a range of lithologies including Proterozoic gneiss basement rocks and younger volcanic and intrusive igneous rocks, metamorphosed sandstones, limestones and mudstones (GSI, 2006). Many forms of mineralisation have been discovered in this highly diverse province. Base metals and barite occur as stratabound deposits and Palaeozoic granites are the focus of skarns and porphyry Mo-Cu (www.mineralsireland.ie). One style of mineralisation that has been the subject of detailed investigations in recent years is that of quartz vein hosted gold. These veins, related to shear zones, appear to be concentrated largely within Dalradian age rocks. Much of Donegal is underlain by Dalradian lithologies which have been associated with economically viable gold deposits in Northern Ireland, in particular the Cavanacaw and Curraghinault deposits.

Rocks of the Dalradian Supergroup, Grampian Terrane, were formed during the late Neo-Proterozoic continental break up and creation of the Iapetus Ocean (Soper, 1994). These underwent extensive deformation during the Grampian Orogeny (Woodcock & Strachan, 2000), the closure of the Iapetus and collision of Laurentia with an intra-oceanic volcanic arc resulted in the Fair-Head-Clew-Bay Line (Williams & Stevens, 1974). This is a western extension of the Highland Boundary Fault (HBF) and is a major structural feature which has been the focus for mineral exploration in Ireland and Scotland. Curraghinalt and Cavanacaw lie to the north of the FHCB line, locally called the Omagh Thrust (OT). Mineralisation in these areas has been linked to further structures: the Omagh Lineament and the Curraghinalt Lateral Ramp, the latter lies in the footwall of the OT (Parnell *et al.*, 2000). Both targets have yielded auriferous quartz veins associated with psammite and pelite lithologies, related to shear zones (Clifford *et al.*, 1992). Magmatic fluids are believed to be the source of sulphides and gold which were precipitated out during interaction with formation waters (Parnell *et al.*, 2000).

Within the North-Western Basement and near the south-western margin of the Border zone lies a significant Pb-Zn deposit which occurs within a stratabound carbonate sequence at Abbeytown (EMD, 2005). The Carboniferous rocks to the south of the Border are host to significant Pb-Zn deposits, some of these can be seen on the fringes of the southern border of the Tellus region. These are stratabound lower Carboniferous limestone hosted. The geological diversity of the Border zone means that there is potential for many different styles and types of mineralisation complicating an assessment of the prospectivity of the region and negating the use of any single model. However, consideration of prospects within and close to the Border was carried out in order to define the main exploration criteria, these are presented in Table 1.

Example	Criteria	Rationale
Cavanacaw Co. Tyrone, Northern Ireland. Au, Ag, Pb	Dalradian meta-sediments	All major known mineralisation of quartz veins associated with meta-sedimentary units of the Dalradian ¹
	Major crustal scale faults	Can be main conduit to fluid flow towards the surface, with hydrothermal activity being the near surface expression.
	Graphite hosted in schists	Acts as aid in thrusting of the lack inlier. Conductivity analysis best method of identification
	porphyritic, chlorite and sericite alteration	Alteration haloes can be used as a vector to mineralisation, from chlorite, porphyrite to sericite moving inwards
	Small scale fracture systems	Form the main basis of structural control on a local level, and can often show high levels of deformation
Clontibret Co. Monaghan, ROI Au-Sb	Large scale heat source	Au found most distally from heat source, with Pb and Ag more proximal. Heat source thought to be the Mourne mountain granite
	Permian red beds	Thought to be the leached source of elements ²
	Igneous intrusive and water interaction	Key element in the formation of mineralised fluids ²

	Major NE-SW trending faults	Act as conduits to fluid flow
	Intersection of minor NW-SE trending faults	Small scale structural control to mineralised veins
Abbeytown Co. Sligo, ROI Zn-Pb	Carbonate sequence overlying Precambrian meta-sediments	Contrast in age and rheology allows interaction of fluids at interface, with the potential to carrying mineralisation
	Dolomitization of host rocks	Signs of first phase mineralisation
	Permeable sandstone units interbedded	Allows the transfer of fluids through beds and crystallisation of sulphide minerals

Table 1: Key exploration criteria used with their associated mineralised regions. ¹(P.A.J. Lusty, 2009) ²(M.H.Smith, 2003)

The factors described in Table 1 will form the basis of knowledge driven exploration, which is crucial for generating target areas. The principal factor which appears to influence mineralisation in all of these specified cases is the occurrence and orientation of major faults.

3. Tellus Border data analysis

For a full description of the rationale behind the Tellus Border project, details of the sample collection process and types of geochemical analyses employed please see the project website www.tellusborder.eu.

3.1. Analytical approach and statistical methods

Analysis of the top-soil and stream sediment raw data generated by the Tellus Border project formed the initial stage of this work, which involved basic statistical analysis using Excel. To begin with, the complete datasets were analysed to promote an objective approach with no preference shown for certain elements. It should be noted that data for some elements with only trace abundance may be compromised due to the low detection limits of the analytical technique (XRF). The main elements used in exploration were separated and analysed in more detail, with descriptions provided in Table 2 below. An example of the basic statistical analyses employed at the outset is shown in Table 3. Thereafter, the data were compared with crustal abundance for each element in order that anomalies may be recognised.

	Crustal abundance ppm	Sample type with mean values:		Notes :
		Stream sediment (ppm)	Top-soil (ppm)	
Ag	0.075	0.28	0.081	Shows elevated concentration in stream sediments. Used mainly as a pathfinder for Au mineralisation. Strong chemical association with As-Sb. Poor correlation between data sets, most likely due to varying mobilities and sources. However, high end values show some relationship.
As	1.8	15.24	6.49	High values common throughout study area, with strong correlation between data sets with high anomalies. Used as one on the pathfinder elements for Au. Shows moderate relationship with Fe, this is key due to arsenopyrite common occurrence with Au mineralisation
Cd	0.15	0.79	0.41	Very strong correlation across data sets. High average values influenced by high anomalies around mineralisation at Clontibret. May have resulted in lower anomalous values being poorly represented.

				Relationship with Zn and Pb looks strong, with the area around Clontibret proving this. Other high end values appear to have strong lithological control (black shales)
Cu	60	26.86	22.65	Due to its high mobility in water the results show little similarities between the data sets. Top soil data yields better variety and is more consistent with other commonly associated elements like Pb and Zn. Although the top-soil data may have been skewed due to some very high anomalies.
Fe %	~5%*	7.56	1.94	Sources of high Fe values variable, so of limited use in exploration. Anomalous values may be erroneous due to contamination. Can be analysed by comparing with common metallic elements.
Hg	0.085	-	0.1	Only available with top-soil data, despite this strong evidence for chemical associations with Sb-Ag-As. This is consistent with model for the formation of orogenic gold. These high end anomalies appear accurate due to their positive relationship with Sb.
Mn	900	-	461.71	Only available for top-soil data. A large range is shown in the data, with considerable anomalies occurring in isolated areas. Suggested association from literature of Ag and Zn are rarely observed.
MnO%	-	0.51%	-	Data exhibits a large positive skew due to high end values of around 20%. Values appear anomalous, and don't follow any spatial trend.
Mo	1.2	2.12	1.37	Anomalous values show good correlation in top-soil data, potentially due to lithological controls (black shales). Observed in stream sediment data, with generally elevated values compared with crustal abundance. Effect of high values associated with lithologies may hide potential values related

				to mineralisation.
Ni	84	42.79	16.48	High end values spatially correlated, showing strong association. Shows strong positive correlation with Co and Cr across both data-sets. Despite this background levels are considerably low.
Pb	14	30.67	25.83	High Pb values indicate good potential for mineralisation. Pb shows strong associations with other elements such as Zn, Cu, S, As and Cd for both data-sets. Pb levels are consistently high in Co. Monaghan related to Clontibret and Castleblaney mineralisation. The effect of these high values on the data set is considerable. Removal of these data may better reflect Pb levels in other areas. Highest values are from top-soils, where values over 1000 ppm occur.
Sb	0.2	0.82	0.35	Sb shows elevated values across the whole border area, with strong association with high Hg, As, Ag and Mo. This association is consistent with formation of orogenic Au. Due to the high anomalous values > 10 ppm, the data shows a large positive skew. Stream sediment values reach 150 ppm, although this value is isolated. Known Sb mineralisation is found at Clontibret which may elevate average values.
SiO₂%	-	51.07	-	Due to the resistant nature of quartz, SiO ₂ levels will be high. The data can only be used as method to back up theories and models.
Te	0.001	0.23	0.03	Majority of data censored at 0.03 (90%), only upper end values of significance. Mainly used to detect the presence of acid intrusives.
Th	0.85	9.72	2.56	High values common throughout data set, can be used as cross reference, particularly for potential in finding epithermal Au

				deposits.
V	120	90.73	27.1	Very little high end anomalies of interest, general depletion across data-sets
W	1.25	2.25	0.06	Almost all data from top-soil censored (93%), which explains low values. Highly resistant element so will show elevated values in stream sediments. Strong correlation seen with granitic lithologies.
Zn	70	141.36	54.22	Stream sediment average high, most likely elevated due to high end anomalies above 700 ppm. Despite this multiple populations can be seen on histogram for the data. Values around 290-300 ppm depart from trend. Same multiple population occur in top-soil data around, 100-120 ppm. High end values considerable but not isolated. Strong elemental association found mainly with Cd and Mn, and minor associations with As, Mo, Cu and Pb

Table 2: Summary for each element used in exploration process, showing comparison of values with crustal abundance.

Sb ppm			
average grade	0.35	max	10.50
standard deviation	0.36	min	0.03
coefficient of variation	1.02	median	0.27
skewness	10.56	mode	0.23
Crustal abundance*	0.20		

Table 3: Statistics for Sb in top-soils

Following this process, data ranges were assessed for each element in order that they could be displayed effectively using GIS software. Histograms were created for the main pathfinder elements, this is the preferred method for determining specific populations in the data. To create the histograms, cumulative frequency plots were first developed in Excel (Table 4). Thereafter, the histogram was used to determine appropriate ranges for data display (Table 5). The percentile method, shown in Table 5, and the two-standard deviations method were then employed. In each case the method was chosen based on consideration of the elements total average, for example, if the crustal abundance is higher than the 50 percentile the standard deviation method was used. This process avoids giving low values an unrealistic high weighting in GIS.

<i>ppm</i>	<i>Frequency</i>	<i>Cumulative %</i>
0.1	299	8.61%

0.2	879	33.91%
0.3	767	55.99%
0.4	568	72.34%
0.5	338	82.07%
0.6	221	88.43%
0.7	145	92.60%
0.8	70	94.62%
0.9	55	96.20%
1	30	97.06%
1.1	23	97.73%
1.2	21	98.33%
1.3	12	98.68%
1.4	9	98.93%
1.5	3	99.02%
1.6	7	99.22%
1.7	4	99.34%
1.8	4	99.45%
1.9	1	99.48%
2	2	99.54%
10.5	16	100.00%

Table 4: Cumulative frequency plot for Sb, with bins selected at 0.1ppm. Bin ranges selected to best represent the variety in data.

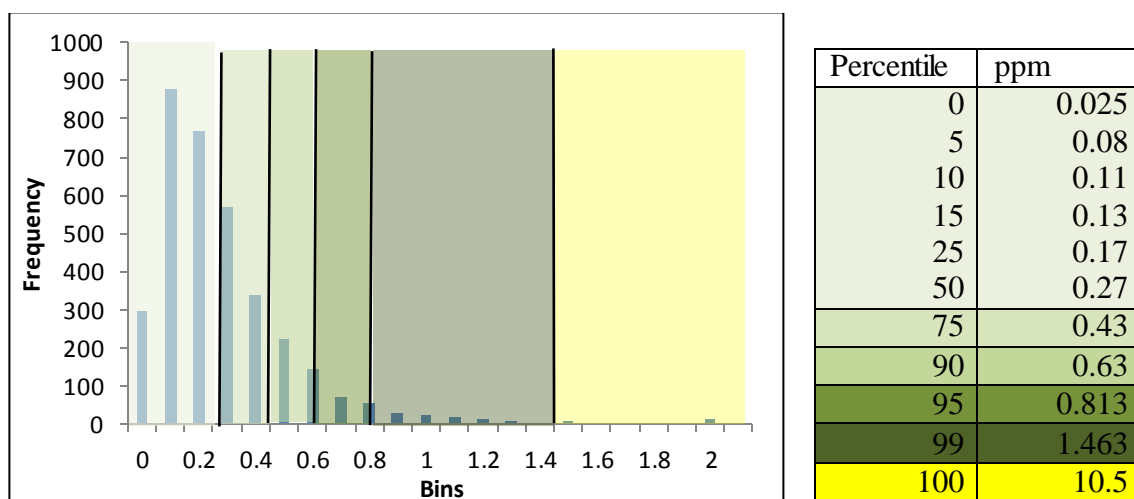


Table 5: Histogram and percentile ranges, colour coded.

3.2. Controls on geochemistry

This stage of analysis integrates background information and genetic models with potential sources of major element concentrations. By interpreting the data in relation to specific theories, such as the orogenic Au model, trends within the data start to become more apparent. This can be done by analysing elements against one another to identify any correlation, to use the orogenic Au example, the theory states that As values should show correlation with Sb and Hg. This will form the foundation for target area designation described in Section 4. Other controls that have been analysed are environmental and geological such as pH and lithology.

3.2.1. Element concentration in relation to pH

It is widely accepted that pH plays a big role in element mobility and concentration. Acidic and oxidising conditions are common throughout Ireland due to the wide covering of bogs, especially in Co. Donegal. Elements such as Zn and Cu are highly mobile in acidic environments and very immobile in a reducing environment (Andrew-Jones, 1968). Element distribution in peat bogs can dramatically vary depending on the height of the water table, with concentrations of Fe, Al, Zn and Pb commonly found at the interface (Damman, 1978). Tables 6 and 7 show how element concentration varies across different pH zones.

	pH > 7			pH 5-7		
	Average	total average	% diff	average	total average	% diff
LOI_%	7.08	35.11	20.16	15.72	35.11	44.78
Al_%	0.43	1.06	40.70	1.49	1.06	140.66
B_mgkg	7.96	5.19	153.56	5.03	5.19	97.09
Ba_mgkg	43.44	72.57	59.86	101.30	72.57	139.59
Ca_%	7.40	0.46	1619.59	0.67	0.46	147.60
Cr_mgkg	8.38	22.20	37.73	34.41	22.20	155.02
Cu_mgkg	8.83	22.66	38.99	30.98	22.66	136.75
Fe_%	0.92	1.94	47.32	2.54	1.94	131.08
K_%	0.10	0.12	84.48	0.16	0.12	133.47
Li_mgkg	5.93	11.49	51.59	16.90	11.49	147.13
Mg_%	0.34	0.31	108.59	0.48	0.31	153.30
Mn_mgkg	296.87	461.72	64.30	658.59	461.72	142.64
Na_%	0.11	0.02	454.92	0.02	0.02	75.82
Ni_mgkg	8.36	16.48	50.77	27.17	16.48	164.93
P_mgkg	398.33	805.40	49.46	1024.33	805.40	127.18
S_%	0.09	0.15	58.48	0.08	0.15	53.25
Sr_mgkg	455.31	29.71	1532.68	27.72	29.71	93.31
Ti_%	0.01	0.01	84.17	0.01	0.01	95.19
V_mgkg	16.88	27.10	62.28	35.93	27.10	132.57
Zn_mgkg	27.48	54.23	50.68	80.66	54.23	148.74
Zr_mgkg	1.41	1.71	82.67	2.36	1.71	137.70
Ag_mgkg	0.04	0.08	46.86	0.09	0.08	114.78
As_mgkg	6.02	6.50	92.61	8.02	6.50	123.46
Be_mgkg	0.25	0.47	52.42	0.67	0.47	142.38
Bi_mgkg	0.06	0.15	41.69	0.16	0.15	106.13
Cd_mgkg	0.19	0.41	45.87	0.52	0.41	127.55
Ce_mgkg	16.91	32.70	51.71	45.63	32.70	139.57
Co_mgkg	2.88	6.76	42.62	9.94	6.76	147.00
Cs_mgkg	0.30	0.64	46.71	0.77	0.64	120.12
Ga_mgkg	1.45	4.14	35.12	5.59	4.14	135.09
Ge_mgkg	0.05	0.05	95.66	0.05	0.05	97.27
Hf_mgkg	0.05	0.05	105.88	0.06	0.05	128.47

Hg_mgkg	0.03	0.10	27.27	0.09	0.10	89.43
In_mgkg	0.01	0.02	70.68	0.02	0.02	119.94
La_mgkg	8.24	14.18	58.10	20.08	14.18	141.64
Lu_mgkg	0.05	0.07	78.09	0.10	0.07	148.91
Mo_mgkg	0.52	1.38	37.77	1.22	1.38	88.44
Nb_mgkg	0.26	0.40	66.67	0.39	0.40	99.51
Pb_mgkg	9.31	25.83	36.04	29.75	25.83	115.19
Rb_mgkg	6.13	12.34	49.64	17.21	12.34	139.51
Sb_mgkg	0.17	0.35	48.66	0.38	0.35	107.78
Sc_mgkg	1.46	2.78	52.52	4.01	2.78	144.33
Se_mgkg	0.56	1.12	49.43	0.74	1.12	65.66
Sn_mgkg	0.31	0.95	33.07	1.16	0.95	122.38
Ta_mgkg	0.04	0.04	110.76	0.03	0.04	84.36
Tb_mgkg	0.18	0.28	65.32	0.40	0.28	146.04
Te_mgkg	0.03	0.03	89.47	0.03	0.03	105.74
Th_mgkg	1.57	2.56	61.30	3.53	2.56	137.73
Tl_mgkg	0.07	0.16	44.32	0.19	0.16	124.04
U_mgkg	0.49	1.29	37.59	1.52	1.29	118.16
W_mgkg	0.06	0.06	104.51	0.05	0.06	93.17
Y_mgkg	5.44	6.79	80.16	10.45	6.79	153.85
Yb_mgkg	0.37	0.47	77.76	0.70	0.47	148.27
	number of samples =		54	number of samples =		870

Table 6: Analysis of element concentrations in relation to pH >7 and 5-7. Colour coding represents the percentage difference between the pH groups average and total data average, with green relating to high difference and red a low difference.

	pH 3-5			pH <3		
	average	total average	% diff	average	total average	% diff
LOI_ %	41.13	35.11	117.14	88.44	35.11	251.91
Al_ %	0.95	1.06	89.25	0.16	1.06	14.97
B_mgkg	5.18	5.19	99.95	5.00	5.19	96.42
Ba_mgkg	64.50	72.57	88.87	20.43	72.57	28.15
Ca_ %	0.24	0.46	52.06	0.15	0.46	33.61
Cr_mgkg	18.75	22.20	84.46	1.90	22.20	8.58
Cu_mgkg	20.52	22.66	90.59	3.98	22.66	17.58
Fe_ %	1.79	1.94	92.42	0.32	1.94	16.61
K_ %	0.11	0.12	90.41	0.04	0.12	30.91
Li_mgkg	9.98	11.49	86.86	1.26	11.49	10.95
Mg_ %	0.26	0.31	82.61	0.14	0.31	43.79
Mn_mgkg	406.62	461.72	88.07	65.83	461.72	14.26
Na_ %	0.02	0.02	100.01	0.03	0.02	128.83
Ni_mgkg	13.26	16.48	80.47	2.92	16.48	17.74
P_mgkg	746.72	805.40	92.71	452.97	805.40	56.24
S_ %	0.18	0.15	114.33	0.33	0.15	213.54
Sr_mgkg	21.24	29.71	71.51	26.46	29.71	89.07

Ti_%	0.01	0.01	102.89	0.01	0.01	66.34
V_mgkg	24.78	27.10	91.42	6.11	27.10	22.54
Zn_mgkg	46.35	54.23	85.48	23.42	54.23	43.19
Zr_mgkg	1.52	1.71	88.72	0.69	1.71	40.31
Ag_mgkg	0.08	0.08	97.04	0.05	0.08	58.92
As_mgkg	6.10	6.50	93.82	1.80	6.50	27.62
Be_mgkg	0.42	0.47	88.43	0.06	0.47	13.53
Bi_mgkg	0.15	0.15	99.44	0.13	0.15	87.58
Cd_mgkg	0.38	0.41	92.27	0.29	0.41	71.62
Ce_mgkg	29.25	32.70	89.45	4.15	32.70	12.70
Co_mgkg	5.89	6.76	87.04	0.89	6.76	13.21
Cs_mgkg	0.62	0.64	96.30	0.10	0.64	15.20
Ga_mgkg	3.77	4.14	91.21	0.80	4.14	19.33
Ge_mgkg	0.05	0.05	100.91	0.06	0.05	105.66
Hf_mgkg	0.04	0.05	90.32	0.04	0.05	84.39
Hg_mgkg	0.11	0.10	104.91	0.12	0.10	114.42
In_mgkg	0.02	0.02	94.49	0.01	0.02	67.70
La_mgkg	12.56	14.18	88.58	1.86	14.18	13.15
Lu_mgkg	0.06	0.07	85.66	0.01	0.07	10.91
Mo_mgkg	1.46	1.38	106.21	0.94	1.38	68.46
Nb_mgkg	0.40	0.40	101.61	0.29	0.40	72.24
Pb_mgkg	24.84	25.83	96.17	24.88	25.83	96.35
Rb_mgkg	11.05	12.34	89.55	1.41	12.34	11.43
Sb_mgkg	0.34	0.35	97.91	0.41	0.35	118.75
Sc_mgkg	2.44	2.78	87.71	0.42	2.78	15.12
Se_mgkg	1.26	1.12	111.82	1.69	1.12	150.15
Sn_mgkg	0.90	0.95	94.43	0.65	0.95	68.78
Ta_mgkg	0.04	0.04	102.50	0.08	0.04	206.31
Tb_mgkg	0.24	0.28	86.94	0.03	0.28	10.85
Te_mgkg	0.03	0.03	98.59	0.03	0.03	85.54
Th_mgkg	2.30	2.56	89.86	0.36	2.56	13.89
Tl_mgkg	0.15	0.16	94.80	0.03	0.16	22.14
U_mgkg	1.25	1.29	97.13	0.22	1.29	17.29
W_mgkg	0.06	0.06	102.11	0.06	0.06	106.88
Y_mgkg	5.70	6.79	83.89	0.73	6.79	10.75
Yb_mgkg	0.41	0.47	85.83	0.06	0.47	13.35
	number of samples =		2487	number of samples =		64

Table 7: Analysis of element concentration in relation to pH 3-5 and <3. Colour coding represent the percentage difference between the pH groups average and total data average, with green relating to high difference and red a low difference.

The data shows strong variation across the different levels of acidity. However, consideration must be given to the number of samples within each pH group, as the groups with more samples are likely to see the least variation. The two end groups of acidic (<3pH) and neutral to alkaline (>7pH) show notable differences. It appears that some elements favour neutral conditions such as Ca, Na and Sr, with the majority of elements showing a

considerable decrease. Between pH 5-7, element concentrations increase and become more consistent with Na% and S% decreasing. The pH group of 3-5 has the highest sample numbers and therefore will have the closest averages, with only Ca% showing a considerable decrease. In the acidic group of <3pH, elemental concentrations reduce and Loss-on-Ignition (LOI) values increase to ~ 80%. Some elements appear to favour the acidic conditions, such as S and Ta with peat and boggy land cover resulting in high LOI values.

3.2.2 Element Concentration in relation to Lithology

The surrounding lithologies play a major role in the geochemical composition of stream sediments and top-soils. The whole border region was broadly divided up based on age and formation of the local bedrock. For example, the meta-sediments of the Southern Highland group were considered one group, but were later divided into its individual formations and units. Each sample location was tagged to the mapped bedrock geology. The lithological groups generated were as follows:

- Argyll group- Quartzites, pelites, Schist, psammities and marble
- Southern highland group- pelites, psammities, schists, and phyllites
- Permo-Triassic- Evaporite, sandstones, mudstones, limestones, turbidite and coal
- Mourne Granite- Granite, granophyre, granodiorite, dolerite
- Upper Carboniferous- Mudstone, sandstone, evaporite and turbidite
- Sliswood Division- Quartz-feldspathic paragenesis
- Lough Eske granite- Granite and granodiorite
- Basic intrusions- dolerite and gabbro
- Donegal granite- granite and granodiorite
- Lower Paleozoic- Turbidite sequence, shales and greywacke

Box and whisker plots were used to display the analyses. As can be seen in Figure 5 for As in top-soils, background levels are consistent across the major formations. Despite this, the effect of high end anomalies can be seen in the error bars, for the Argyll group especially. For most groups the minimum value is generated by the lower limits of detection around 0.25 mg-kg. All elements within each group were compared this way, with several elements showing a strong lithological control, specifically: U, Co, Cr, Ni, Mn, Cu and Zn. Elements such as U and Mn showed a dramatic increase in top-soils surrounding the Lough Eske granite. The lower Palaeozoic group indicated a dramatic increase in Cr, Ni and Co elements. Known geochemical associations exist such as between Mo and black shales, this was also observed in the data where average levels throughout the border region are around 1.5 ppm and average levels within the shale units of the Upper Carboniferous are 5.5 ppm.

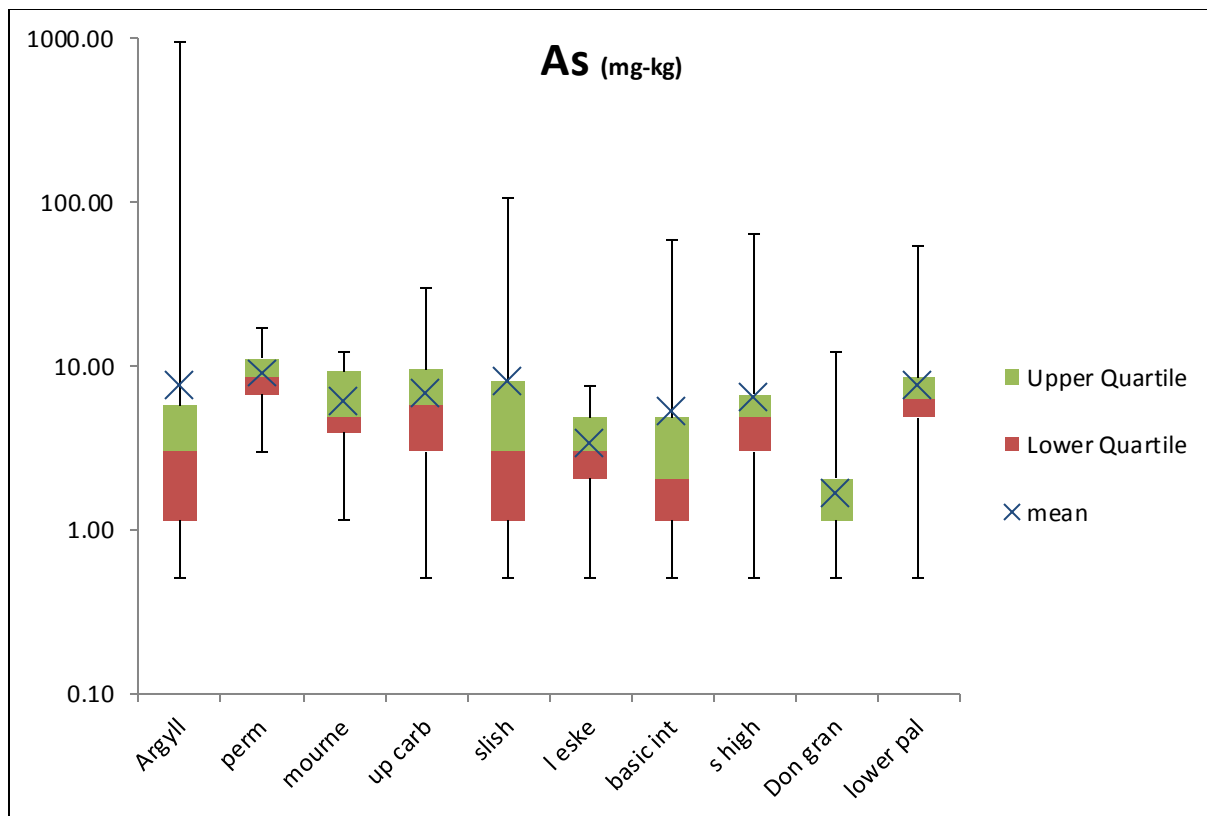


Figure 5: Box and whisker diagram displaying variability of As associated with major bedrock units, with the maximum and minimum values represented by upper and lower error bars respectively.

It should be noted that due to time constraints this test was only carried out for the top-soil data. To summarise, lithological control on the data only appears strong for certain elements such as Mo and U. The biggest contrasts are seen in the upper end anomalies, which are not likely to be related to lithology.

3.2.3. Element concentrations in relation to faulting

One of the main drivers for exploration is the association of mineralisation with major faulting, as mineral rich fluids can penetrate deep seated fracture systems and use these as pathways to the surface (e.g. Table 1). Unlike the lithological analysis, which investigates controls on background levels of elements, the fault analysis scrutinises the high end anomalies and tests a genetic link with faulting. Correlation of background levels is complex with fault analysis due to the unrepresentative small sample size of 720 out of 3475.

The spatial correlation between faulting and geochemical anomalies in the top-soils was examined. Data points falling within a 1 km radius of a mapped fault were tested. Faults were categorised according to their orientation and strike length. For example, all faults trending between 000 to 045 degrees and longer than 50 km were grouped. This method of discrimination examined how fault angle may relate to different styles of mineralisation. Ideally fault groups would be distinguished by their type (ie. normal, reverse or strike-slip), but this data was not available. As can be seen in Figures 6 and 7, As anomalies are higher when associated with particular fault orientations. Major faults orientating to the NE tend to have higher upper end values than elsewhere. The example shown above is only for As

values, other elements analysed did not have the same positive relationship. Table 8 shows the top ten values for each element, and compares values from the whole data set and from all fault analysis data.

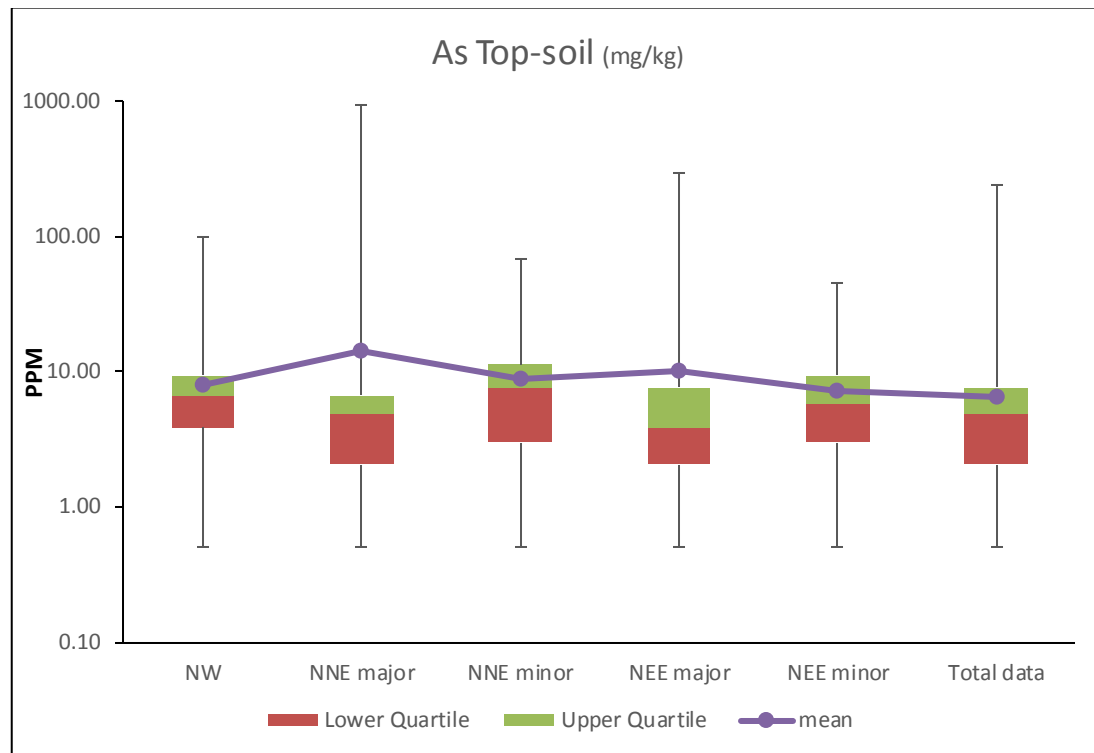


Figure 6: Box and whisker diagram displaying relationship between As levels and fault orientation, with the maximum and minimum values represented by upper and lower error bars respectively

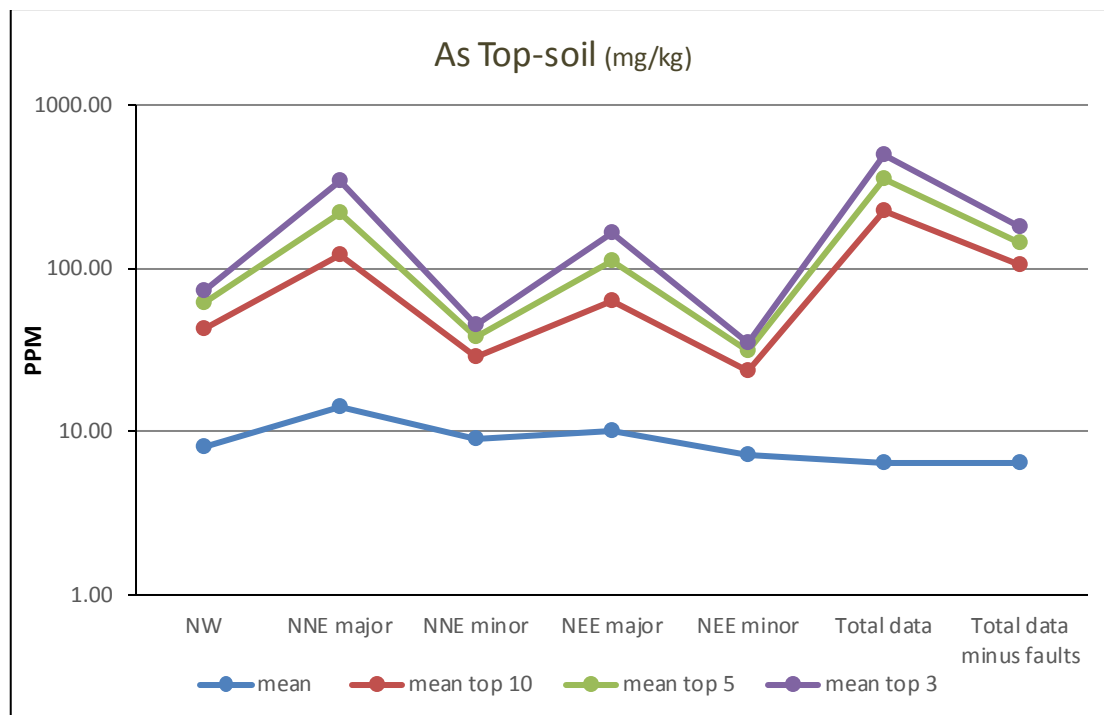


Figure 7: Chart comparing the upper end values of As within each fault group, compared against the total data.

Rank	As fault	As total	Hg fault	Hg total	Pb fault	Pb total
1	960.77	960.77	0.50	1.66	855.61	1116.43
2	299.75	299.75	0.37	1.40	414.84	855.61
3	100.98	236.88	0.36	0.96	309.42	727.47
4	100.98	189.73	0.33	0.64	224.90	553.88
5	90.81	107.45	0.32	0.54	216.72	414.84
6	67.70	100.98	0.30	0.50	194.91	407.57
7	61.23	100.98	0.30	0.44	169.46	332.14
8	59.38	98.21	0.29	0.43	162.19	309.42
9	50.13	90.81	0.29	0.39	154.92	290.33
10	48.28	78.79	0.29	0.38	153.10	255.80
average	184.00	226.44	0.34	0.73	285.61	526.35

Table 8: Data for three elements comparing the top 10 values of the total data set with data from the fault analysis. Colour represents contrasting levels of values.

Of all elements analysed, As showed the highest increase compared with the overall data set. The majority of high As values are around the NE trending faults in Co. Donegal. Anomalies in this region could be lithologically controlled or result from local environmental factors such as boggy ground or high land relief. As shown from the lithological control analysis, the Argyll group does show elevated As values located within Co. Donegal. It is most likely to be a combination of factors, such as lithology and environmental conditions but with this data there remains uncertainty. Other elements which showed a marked increase around faulting include Cu, Cr, Ni and Zn, with elements such as Ca%, Na% and Sr indicating a decrease in average values.

3.3.Evaluation of Geochemical data

A note of caution should be applied in the top-soil dataset for samples with exceedingly high LOI values as they may not be fully representative. All samples were analysed for their variance using ANOVA except for Ag, Cl, In, Ta and Te from the stream sediment dataset. These samples should be treated with caution during interpretation.

When analysing data in GIS, the data ranges for both sample types is critical. The ranges are influenced by areas of high anomalies. These areas include sites of known mineralisation with closed prospecting licences, such as at Clontibret. The high values associated here may have increased overall averages for several elements leading to the concealment of strong values elsewhere. This issue is seen throughout the border region and can be dealt with by having a good understanding of the data ranges for each element affected and appreciating the relative value compared with background concentration.

4. Target Area Generation

During the early stages of this project the main criteria used to identify and isolate the most prospective areas were as follows:

1. Geochemical anomalies identified within the new Tellus Border top-soil and stream sediment datasets and geophysical characteristics
2. The regional and local geology

Preliminary Target Areas (PTAs) were defined using top-soil and stream sediment data independently. Two further targets were included based on geophysical observations. PTAs were determined on elemental association rather than single element anomalies. Consideration was not given at this early stage to logistics, PL area status, urban areas and sources of contamination. Only the Clontibret area was excluded due to its known mineralisation and mining activity.

In order to summarise the geochemical data and highlight broad regions which could be worthy of further investigation, nine pathfinder elements were chosen: Cu, Mn, Zn, Ag, As, Pb, Sb, Ca and Mo. Each sample was ranked according to levels of these nine elements and this ranking system was used for display purposes in GIS. Figures 8 and 9 show the relative prospectivity of areas within the Border region based only on these nine elements in top-soils and stream sediments. The two datasets are combined in Figure 10. It is important to note that this method was only used for display purposes and that several other element associations were considered in conjunction with geophysical criteria when selecting the PTAs.

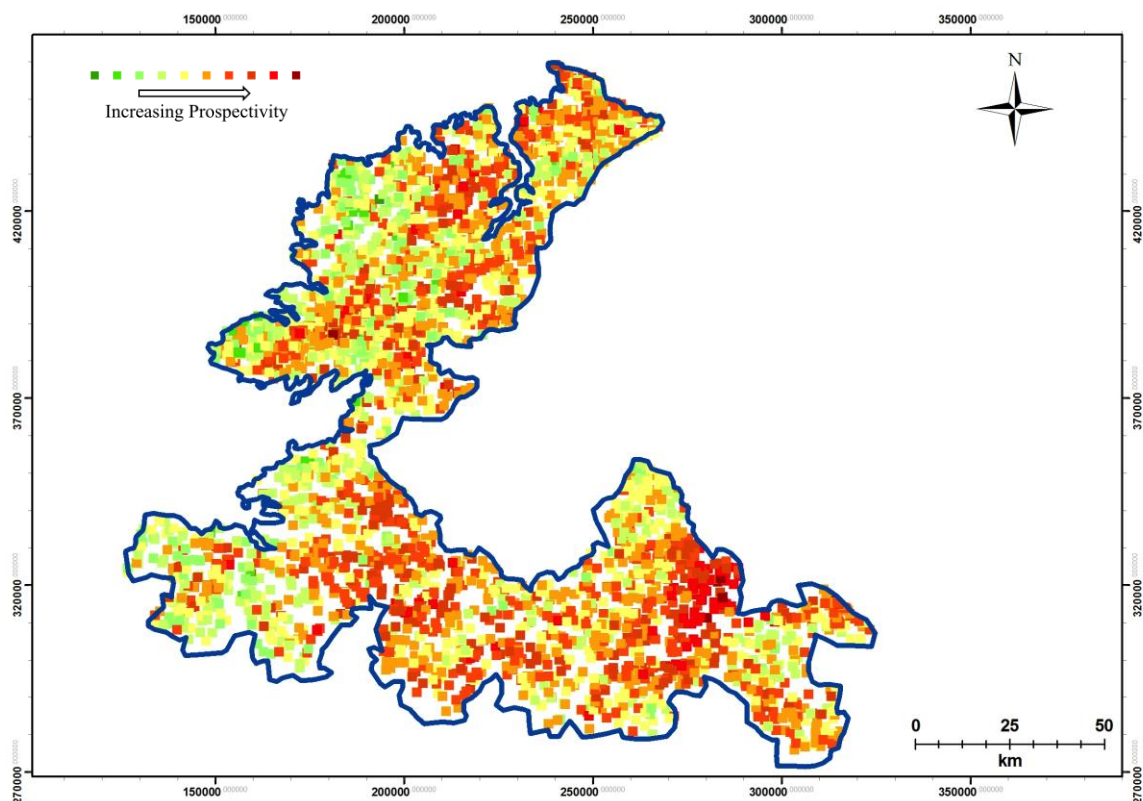


Figure 8: Stream sediment geochemical data analysis using nine selected pathfinder elements.

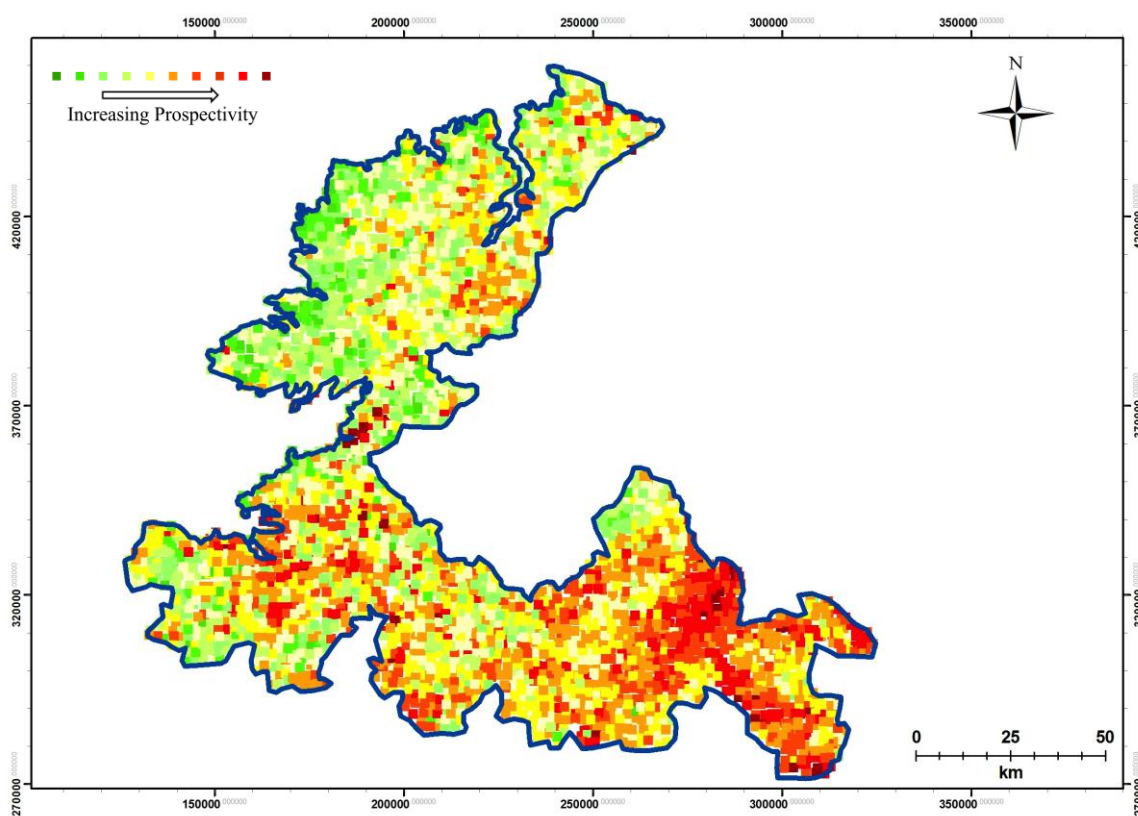


Figure 9: Top-soil geochemical data analysis using nine selected pathfinder elements. Note the apparent low prospectivity values in Co. Donegal, which are likely to be a result of the environmental conditions (see Section 6.4.5)

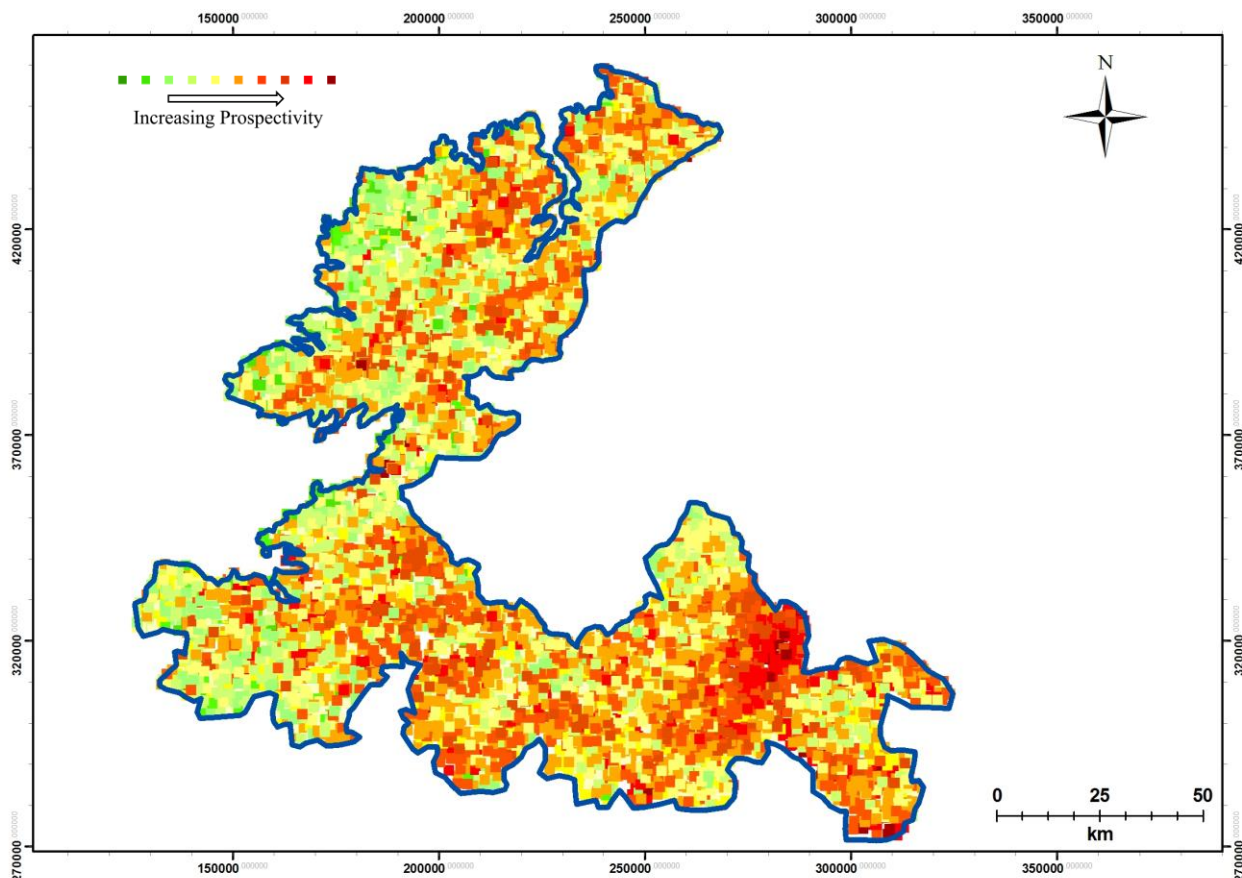


Figure 10: Combined top-soil and stream sediment analysis for major pathfinder elements.

Based on the initial criteria, 19 prospective areas were identified, these PTAs are summarised in Table 9 and highlighted on Figure 11.

Preliminary Target Area (PTA)	Geochemical anomalies	Main Geological and Geophysical Observations
Manorhamilton	TS*: Ag, Hg, Sb, Cu SS*: Sb,	Dalradian metasediments within a faulted block which is bounded by two prominent NE-SW trending faults. High magnetic anomalies associated with faulting within the inlier. On a larger scale a rounded regional high is observed to the west along an E-W fault line.
Ballyshannon	TS: Ag, As, Sb, Hg, Pb, Mn, Cu SS: S	Ballyshannon limestone formation sits between to NE-SW trending faults; directly west of pre-Dalradian Sliswood division psammities.
Pettigoe	TS: As, Ag, Sb	Major fault indicated in the conductivity maps as a contrast between the low values to the west associated with the Sliswood division and the high of the Carboniferous sediments to the east.
Lough Derg	TS: Sb, Hg SS: As	Two small isolated magnetic and conductivity anomalies sit to the SW of the Lough in the Neoproterozoic Sliswood division psammities. Dalradian psammities and pelites to the N and NE. Proximity to the Pettigoe fault.
Glenties	TS: Hg SS: As, Ag, Zn	Dalradian age metasediments and basic volcanics within a heavily faulted zone, close proximity to the Donegal Lineament. NE-SW trending faults.
Millford	TS: Ag, Sb, Hg, Zn, Ba, Cd	Dalradian age metasediments, NE extension of the Glenties faulted zone with prominent NE-SW trending

Preliminary Target Area (PTA)	Geochemical anomalies	Main Geological and Geophysical Observations
	SS: As	faults.
Shercock	TS: Sb, Ag, Cu; SS: Ag	Isolated magnetic highs around the faulted zone, strong correspondence between magnetic and conductivity data. NE and NW trending faults. Lower Palaeozoic turbidite facies.
Lough Allen	TS: Cu, Cd, Mo SS: Cd, Mo, Sb	Dominated by a mix of Carboniferous sediments, with little to no faulting in the region. No anomalous highs featured from the geophysical survey.
Lough Eske	TS: Ag, Th SS: W	Granitic pluton to the north and tertiary dykes clear on the magnetic map. NE-SW trending fault cuts across the Lough, Argyll group Dalradian metasediments to the east and Carboniferous to the west.
Slieve Gamph	TS: Sb, Hg, Cd, Pb SS: As, Ag, S	The Manorhamilton fault controlled inlier is continued SW, with the Slishwood Division giving way to the Argyll group. Magnetic highs and lows cross the map; highs are associated with the Argyll group, lows most likely represent basic intrusions. Granitic pluton is not well defined.
Glengesh	SS: Zn	Dalradian Argyll group quartzite. Large granite pluton to the north. Prominent Glengesh fault trends NE-SW.
Glangevlin	TS: Hg, Sb, Pb, Mo SS: Sb, Mo, Cd, W	The large regional magnetic high is crosscut by intrusions to the north and south. High density of minor faults trending approximately W-E.
Dromod	TS: Pb, Cd, Zn, Hg; SS: Cd, S	Carboniferous lithologies, basic volcanic to SW. NE-SW trending fault.
Dough Mtn.	TS: As, Cd, Mo, Cu SS: Mo, Cd, Sb	Sits directly east of the Manorhamilton target, within a complex faulted zone of Carboniferous lithologies, dominant faults trend NE-SW.
Stranorlar North	TS: Ag, As, Pb SS: As	Series of NE-SW trending faults cut small interior of Southern Highland Group psammites and pelites within larger expanse of Argyll metasediments.
Lurganboy Mtn	TS: Sb, Ag, Hg, Cd, Pb SS: As, Mn	Southern Highland (east) and Argyll Group (west) metasediments; regional faulting NE-SW, cross cutting NW-SE Glentogher Fault.
Balieborough	Ts: Cu, Ag, Sb SS: Ag	Lying southwards of Shercock, Balieborough shares similar lithology and structural geology. NW trending faults dominant structures within host lithologies of Palaeozoic turbidites.
Castleblaney South	TS: Cu	Large magnetic highs in the centre of the region do not appear to be lithologically controlled. Groups of highs have a N-S trend. Potential faulting nearby (unmapped).
Carrickmacross	TS: Zn, As, Sb, Hg, Pb	The magnetics shows low trending features in a NW SE orientation most likely created by the basic igneous dykes. Large isolated lows are spatially related to these dykes. There is a possibility that these lows represent feeder systems suggesting fluid movement from depth which may be associated with mineralisation. However, there is poor correlation with the conductivity which shows little variation.

Table 9: Summary table of each preliminary target area with its associated geochemical anomalies.*SS-stream sediment; TS-topsoil.

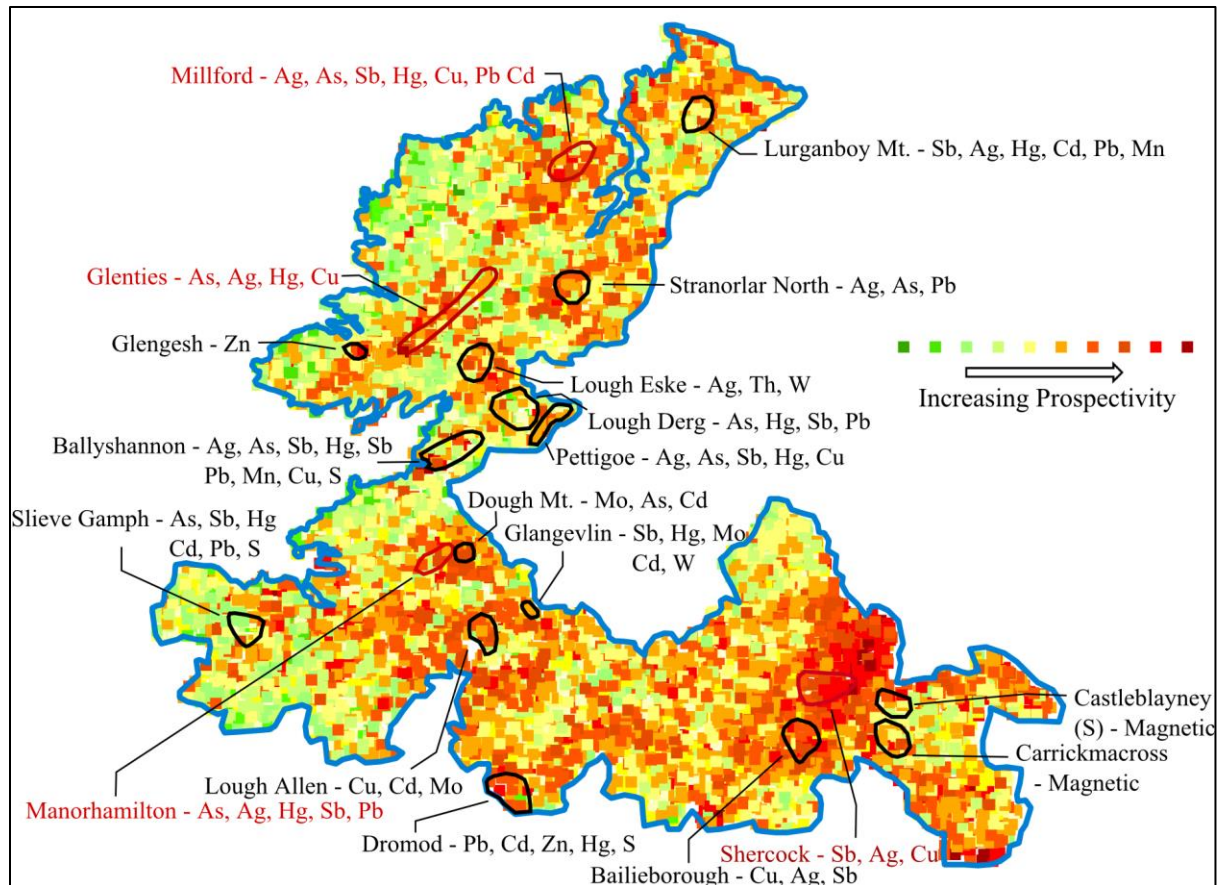


Figure 11: Map showing Preliminary Target Areas.

4.1. Target Area selection

Given the extensive potential for mineralisation in the Tellus Border region as a whole, as demonstrated in Table 9, additional criteria had to be applied in order to derive targets which could be researched within the time frame of the project. With this in mind the following criteria were applied:

1. Status of incorporated Prospecting Licence (PL) areas
2. Access to land / land use
3. Historical data, possible sources of contamination
4. Results of initial field reconnaissance

The main aim of this work is to attract inward investment from exploration and mining companies, for this reason the status of each PL area in the PTAs was considered. Only those PTAs comprised largely of 'open' PL areas were short listed for further work. In addition, sources of contamination such as old adits and waste dumps, forestation and types of land use were looked into for each area (Table 10). All types of mineralisation style were considered, however, orogenic Au and base metal styles appear dominant from analysis of the data. In total, four target areas were designated and are discussed in this document. Each target area was subject to detailed analysis to better understand the geochemical associations.

Criteria	Rationale	Remaining target areas
<i>1. Open Prospecting licence</i>	Only in areas with open prospecting licences will follow up work be completed. This is one of the projects primary objectives	Manorhamilton - Shercock - Balieborough - Castleblaney South - Carrickmacross - Glangevlin - Glengesh - Sleive Gamph - Dough Mt. – Glenties - Millford – Stranorlar North - Lough Eske
<i>2. High Geochemical values</i>	Areas with the highest geochemical values are the most likely to play host to mineralisation	Manorhamilton - Shercock - Glangevlin - Glenties – Millford - Stranorlar North - Lough Eske - Glengesh
<i>3. Strong Geochemical Associations</i>	High values across pathfinder elements is the best signature of mineralisation, and may rule out anthropogenic concentrations	Manorhamilton - Shercock - Glenties - Glangevlin – Millford - Stranorlar North -
<i>4. Geophysical Indicators (exc. Co. Donegal)</i>	Aimed at identifying deep seated structures which may act of fluid pathways or hosts to mineralisation	Manorhamilton - Shercock - Stranorlar North
<i>5. Land Use</i>	Includes proximity to cities and urban areas, also protected sites such as SSIs	Manorhamilton - Shercock - Millford - Glenties
<i>6. Historical Data</i>	Impact of historical workings on the geochemical make up is great, analysed with integration of glacial ice flow maps	Manorhamilton - Millford - Glenties

Table 10: Showing additional criteria for the derivation of final targets.

4.2. Target Area Analysis

Two main methods were applied in the study of each target area, knowledge and data driven exploration, these are an industry standard.

4.2.1. Knowledge Driven Exploration:

This phase involved investigation of geology and geophysical maps to determine local lithologies and important structural features. Mineral database records and possible styles of mineralisation were considered. These factors rely on a strong understanding gained through extensive background reading and experience. When looking at the styles of mineralisation, knowledge of element associations is critical.

4.2.2. Data Driven Exploration:

This part of the process examined key geochemical correlations. For example, high levels of Ag-As indicate the potential for Au type mineralisation. With this in mind, additional Au pathfinder elements, such as Sb-Hg-Mo, are analysed. Other commonly used pathfinder groups are Zn-Pb-Cu-Cd-Mn, which are suitable for base metal exploration.

A polygon was constructed around the best anomalies within a PTA, generating an outline for the target area. Consistency in the selection method was critical. Each sample within the polygon was extracted from the whole dataset in Excel. The first step in the analysis was to compare the average for every selected element within the area, to the whole dataset. From the whole element dataset, the chosen pathfinder elements were separated and analysed independently (Table 11).

Sample_ID	Ag_mgkg	As_mgkg	Hg_mgkg	Sb_mgkg	Mo_mgkg
580467A	0.09	7.60	0.22	0.29	1
580444A	0.33	14.07	0.2	0.33	2.54
580413A	0.12	1.13	0.25	0.41	1.04
580358A	0.25	15.01	0.09	0.23	0.92
580308A	0.25	0.5	0.1	0.17	0.49
580481A	0.2	2.98	0.09	0.13	1.56
580408A	0.18	3.90	0.16	0.59	1.44
580455A	0.03	2.05	0.12	0.32	0.67
580476A	0.07	2.05	0.15	0.63	0.59
580497A	0.12	4.83	0.07	0.23	0.76
580401A	0.27	2.05	0.19	0.96	0.52
580440A	0.13	15.92	0.05	0.37	2.11
580491A	0.37	4.83	0.1	0.21	2.21
580463A	0.11	4.83	0.09	0.14	1.78
580537A	0.71	16.85	0.16	0.26	0.84
580443A	0.11	2.05	0.12	0.23	1.52
580469A	0.1	37.19	0.13	0.11	1.52
580430A	0.31	3.90	0.08	0.21	2.04

Table 11: Example summary table for Au pathfinder elements

At this stage it was possible to identify specific samples which show good consistency across elements. These could be related to mineralisation, and were highlighted for follow up sampling. A correlation matrix was constructed in order to quantify the association between elements (Table 12), the stronger the correlation (closer to 1) the greater the association. However, this method does not take into account possible sources of environmental enrichment and association (Zn and Cd). If element anomalies are formed by contamination (land use, waste dumps etc.), we expect them to demonstrate poor correlation with other elements.

For areas also showing potential for base metal mineralisation a similar process was carried out for the relevant pathfinder elements (Table 13). Thereafter, a correlation matrix for elements showing the highest anomalies for both styles was completed to identify any potential crossovers in element concentrations. This method was only used as a guide, the results are investigated through follow up work in the target areas.

	Ag_mgkg	As_mgkg	Hg_mgkg	Sb_mgkg	Mo_mgkg
Ag_mgkg	1				
As_mgkg	0.208	1.000			
Hg_mgkg	0.007	-0.137	1.000		
Sb_mgkg	-0.059	-0.243	0.447	1.000	
Mo_mgkg	0.212	0.480	-0.241	-0.355	1.000

Table 12: Correlation matrix for Au pathfinder elements in top-soil data from the Millford target area

	Zn_mgkg	Pb_mgkg	Cd_mgkg	Ag_mgkg	As_mgkg
Zn_mgkg	1.000				
Pb_mgkg	0.765	1.000			
Cd_mgkg	0.993	0.755	1.000		
Ag_mgkg	0.808	0.709	0.795	1.000	
As_mgkg	0.273	0.280	0.247	0.160	1.000

Table 13: Correlation matrix for high anomalies from both base metal and Au pathfinder groups, in top-soil data from Millford target area

5. Exploration Methods and Analysis

Four final target areas were selected for closer examination. This follow up work was designed to further understanding about the geological controls on mineralisation in specific parts of the Tellus Border region. In each area broadly similar field methods were used, sample collection was tapered according to local conditions such as the availability of outcrop, topography and geology. During the sampling phase areas of good exposure were marked for mapping. The main objective of mapping was to obtain a greater understanding of the local geology on a smaller scale, such as structure, alteration and deformation.

Each target was assigned the same amount of time in the field to ensure that no bias was awarded to one particular prospective area. Below is a list of the main features of the follow up work:

- A variety of soil, stream sediment, panned concentrates, float and bedrock samples were collected from each area depending on anomalies from Tellus Border survey.
- Mapping of the geology and structural features, where exposure allowed.
- Existing Tellus Border samples specific to the four targets were collected from the GSI archive for own analysis.
- Fire assay and ICP-MS analysis carried out for each sample at ALS laboratories in Co. Galway.
- Identification of possible sources for geochemical anomalies.

5.1. Sample collection strategy

The objective was to enhance the geochemical database provided by Tellus Border by increasing sample density and validating existing areas of high anomalies. With this in mind, the main aspects to sampling were as follows:

- Stream sediment
 - Collect samples upstream and downstream of main faults
 - Collect samples to validate existing data points
 - Complete panning of sediment at each sample site, aiming to identify any signs of mineralisation
 - Sediment sieved at 2 mm size fraction, using wire mesh sieve
 - Collect samples on a bar or bank on inside bend of river, ideally upstream of any source of contaminant (bridge, road, forest etc.)
- Float
 - Collect samples which yield potential source of geochemical anomalies
 - Identify best samples with mineralisation
 - Aim to collect local samples, caution in collecting material which is likely to have distant source
 - Samples within streams and old farm walls ideal float samples
 - Provide detailed description of local environment and location for every sample

- Bedrock
 - Collect bedrock samples at every outcrop, especially in areas of poor exposure
 - Sample bedrock which display any signs of mineralisation, either disseminated or vein hosted
 - Provide detailed field descriptions of exposure, such as structural features including fractures, faults and joints, also depositional features such as bedding, lamination and cleavage.
 - Mark each location of bedrock for field mapping
 - Cross reference field descriptions with mapped lithologies
 - Grab sampling main method
- Soils
 - Selected sample locations were uploaded to a hand held Garmin GPS
 - Samples locations based on 100 m grid centred around high Tellus Border anomalies
 - Samples of top-soil and sub-soil were collected. From depths of 5-20 cm and 50 cm respectively.
 - Target weight for each sample was 1 kg, samples taken from bog land were around three times this weight to account for high organic matter.
 - After extraction of each sample the soil was set onto a plastic sheet where time was allocated for simple descriptions of composition.
 - After description the samples were inserted into zipped plastic freezer bags.
 - Care was taken to thoroughly clean the auger between samples.

5.2. Sample preparation

Samples were weighed, described and photographed before being dispatched to ALS laboratories for analysis. Most whole rock samples were broken down during description, they were weighed before and afterwards. Whole rock descriptions involved grain size and sulphide analysis using a hand lens. Stream sediment was also described in terms of grain size and shape, with brief observations of the minerals present, such as quartz, mica and feldspar.

5.2.1. QA/QC

Measures were taken in the field and back at base to ensure the data was accurate and precise. Methods used during fieldwork include:

- Stream sediment
 - Thorough cleaning of pan and sieve before use at each site
 - Sediment sieved to same size fraction (2mm)
 - Sampling carried out with experienced members of staff
 - Sediment collected into sealed plastic freezer bag
 - Samples double bagged to prevent contamination

- Whole rock samples
 - Grab sample of bedrock taken from single location, no mixing of samples from same outcrop
 - Collect samples into sealed plastic freezer bag
 - Double bag if sample starts to abrade the plastic cover
 - Aim to collect large samples in field and not over fragment with hammer in field
 - Float samples of representative material of area, not taken from aggregate
- Soils
 - Samples taken from sub-surface set onto clean plastic sheet to avoid contamination
 - Sample added to sealed plastic bags
 - Soils auger thoroughly cleaned before and after use
 - Photograph every sample before bagging
 - Storage of each sample in cool, dry environment to stop alteration

Before samples were dispatched, duplicates, blanks and in-house standards were added to each batch at 1 in every 20 samples. The following process was followed in order to derive duplicate samples for the stream sediments:

- Randomly select a sample
- Spread sample over cleaned even surface into circular shape
- When spreading make sure material is well mixed
- Divide sample into four and select upper right and lower left quadrant of sample and bag it, labelling it A; and sample B will be the remaining sediment

Samples were stored in cased plastic boxes to remove any chance of moisture getting to them prior to dispatch.

5.3. Sample analyses

All the samples were dispatched to ALS laboratories in Co. Galway for analysis of precious and base metals. The analytical methods applied to soil, stream sediment and panned concentrate samples collected during this project were: Aqua Regia ICP-MS and ICP-AES for 51 elements (ALS code: ME-MS41); and fire assay / ICP-AES finish for Pt, Pd and Au (ALS code: PGM-ICP23). Float and bedrock samples were analysed via four acid ICP-MS and ICP-AES for 48 elements (ALS code: ME-MS61) including cold vapour/AAS for trace Hg (ALS code: Hg-CV41). They were also subject to fire assay / ICP-AES finish for determination of Pt, Pd and Au.

6. Analysis of Target areas

This section summarises the analyses that were carried out on existing Tellus Border data for the four target areas. For each target there follows a detailed account of recent fieldwork with results of the new data.

6.1. Manorhamilton

6.1.1. Introduction

Manorhamilton is located in NW Leitrim, Republic of Ireland, 15 km East of Sligo town (Figure 12). The N16 main road from Sligo town to Enniskillen passes through Manorhamilton. The border with Northern Ireland is approximately 10 km to the northeast. Reconnaissance work indicated that outcrop in the upland areas was good, with potential for mapping. Outcrop in low lying areas was poor, with streams also yielding few exposures. Streams and rivers are common throughout the area, and are highly silted. The dominant land use is farmland, making access across terrain simple. Woodland cover is little to none, and urban areas are few. Rock piles are a good source of information, as many small quarries are observed in the area.

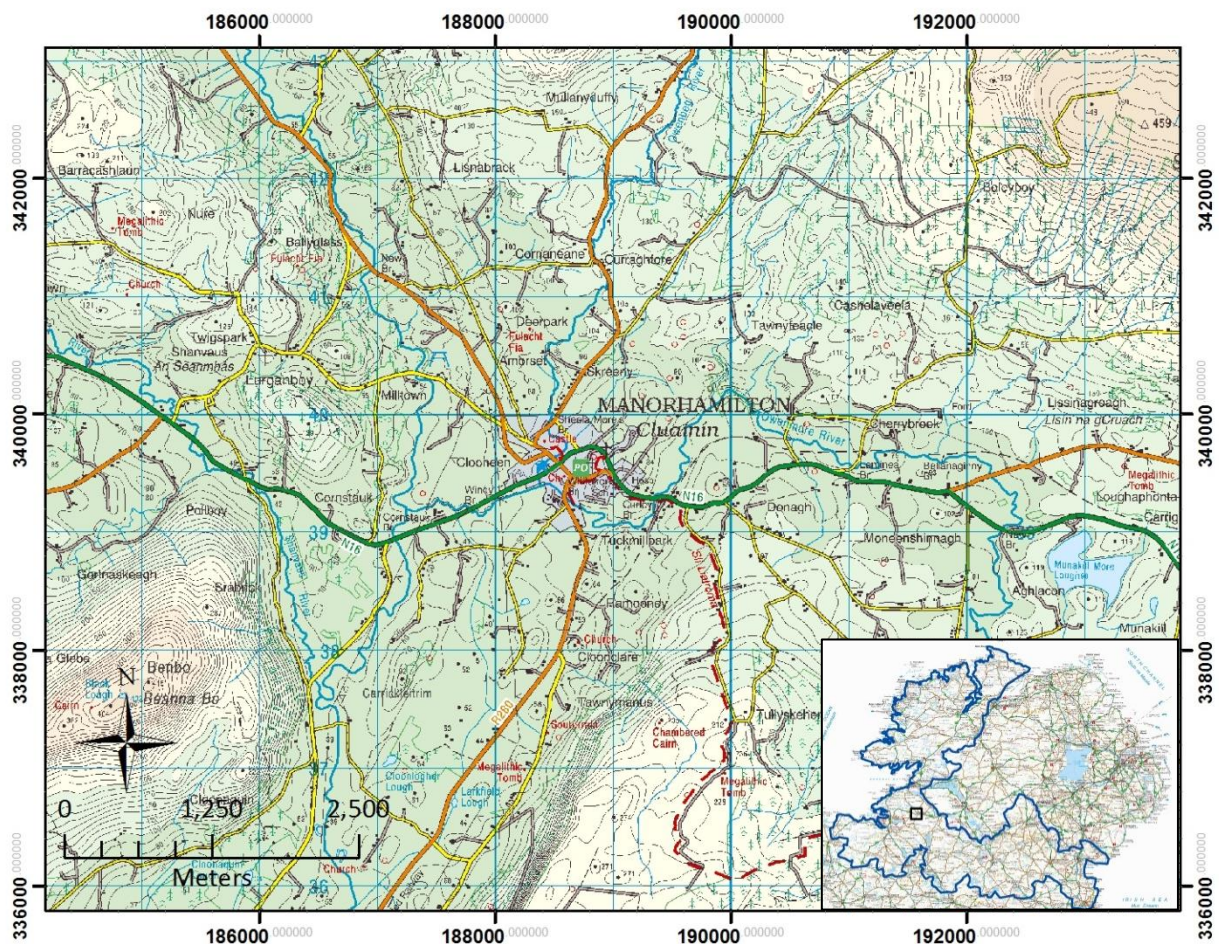
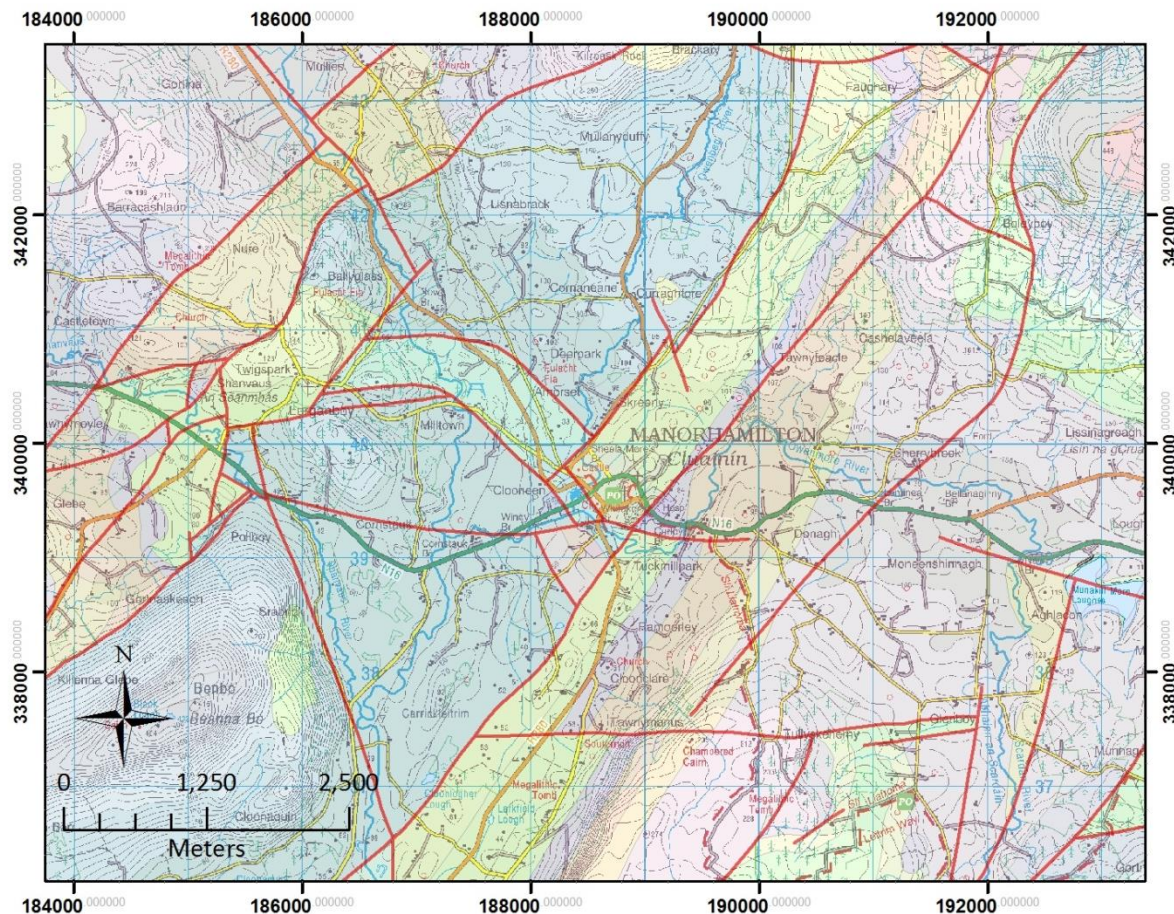


Figure 12: Locality map for the Manorhamilton area, with subset image of its location within the border region.

6.1.2. Local geology

The main geological features to note in this area are the Precambrian meta-sediments which divide Carboniferous carbonates to the west and east. The inlier is made up of the Slishwood division with units from the Dalradian Argyll group, and has a general trend of SW to NE. The Slishwood division are Precambrian psammities, and can be found throughout the NW of Ireland. The surrounding Carboniferous strata are dominantly limestone and calcareous shales, which cover vast parts of western Ireland. A detailed map of the units can be seen in Figure 13.



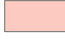





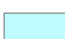




<u>Legend</u>			
<u>Age</u>	<u>Lithology</u>	<u>Symbol</u>	<u>Feature</u>
Carboniferous	 Benbulbin Shale Formation		Fault
	 Ballyshannon Limestone Formation		
	 Bundoran Shale Formation		
	 Glencar Limestone Formation		
	 Mullaghmore Sandstone Formation		
Dalradian	 Meelick Member		
	 Newantrim Member		
	 Leckee Quartzitic Formation		
Precambrian	 Slishwood Division, Psammitic Paragneiss		
	 Metabasite		

Figure 13: Geological base map showing lithology and faulting in the Manorhamilton area.

From the geological map it is apparent that there is a strong structural control at play in the area. The dominant NE trending faults (Figure 13) are common throughout the west of Ireland. The faulting extends southwards for over 100 km. Despite not being able to trace the faults at surface, evidence from the geophysics carried out in the area suggests they continue at depth. When the faults are traced over the border into Northern Ireland they roughly correlate with the orientation of the Omagh Thrust. If there is a correspondence in terms of formation, this has implications for mineral potential in the Manorhamilton area. On a smaller scale, the intensity of faulting is significantly increased to the west of Manorhamilton. Historical records indicate that gold has been found in this area. The faults are likely to be the source of any mineralisation. When adding the geochemical data onto these maps it is apparent that the concentration of element anomalies increases with proximity to the faults, however, there may not be a causal link between the two factors. Figure 14 shows a broad outline for the dominant ice flow paths trending NW-SE, this was taken into consideration when planning the follow up fieldwork.

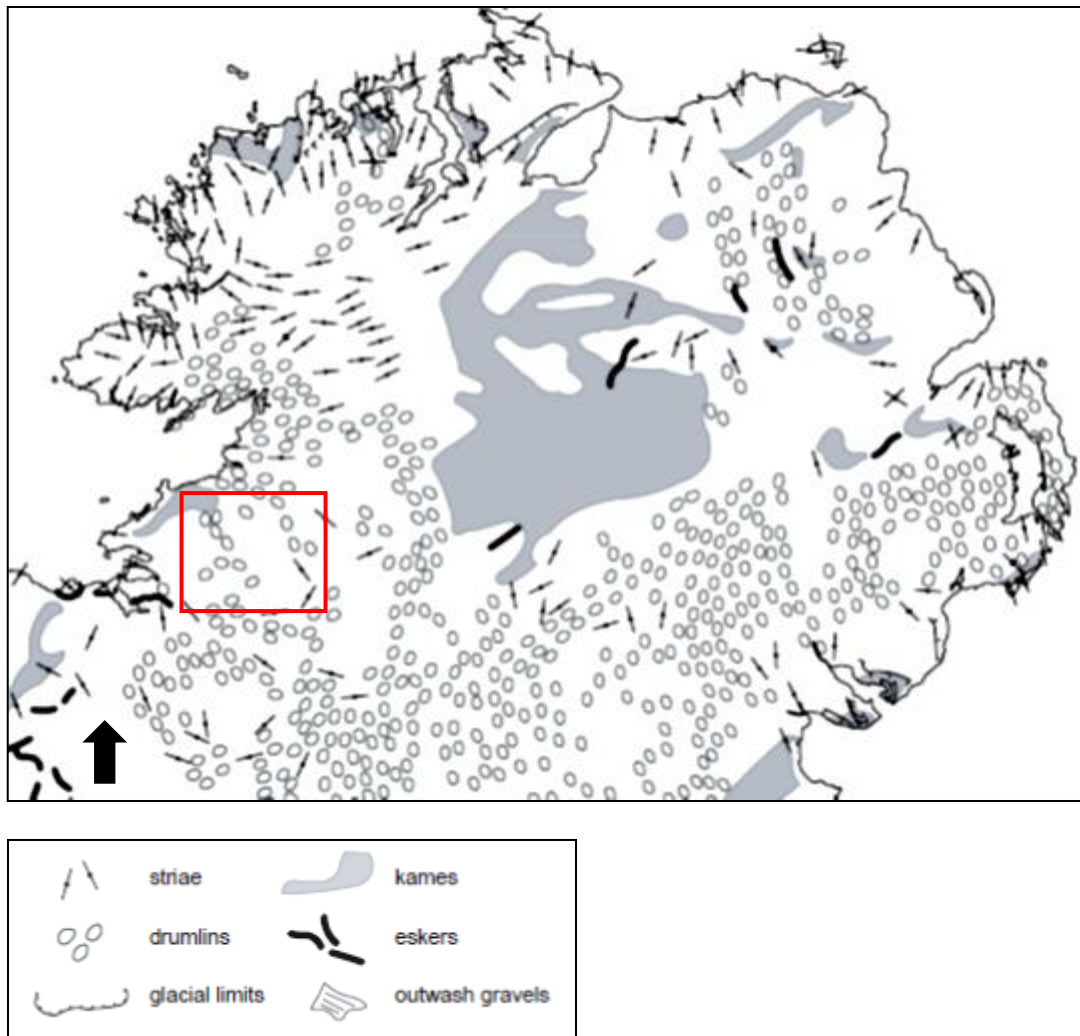


Figure 14: Map for the glacial features in the Manorbhamilton area (red box), the dominant trend is NW-SE orientation. (Clark, 2008)

6.1.3 Existing Data Analysis

6.1.3.1. Knowledge Driven Exploration

Empirical evidence suggests Manorbhamilton is highly prospective based upon mineral associations, structural geology, lithology and historical evidence. From observing geological relationships in the area, similarities can be made with gold mineralisation at Cavanacaw in Northern Ireland. The main attributes are-

- Proximity to NE-SW trending faults
- High concentration of faulting
- Occurrence of Dalradian – Pre-Dalradian meta-sediments
- Inlier structural features
- Geochemical anomalies for Au pathfinder elements

The geochemical anomalies that are associated with typical Au mineralisation are looked at in greater detail for this area, in the next section.

6.1.3.2. Data Driven Exploration

The geochemical data, for both top-soil and stream sediments, in the Manorhamilton area show good potential for Au mineralisation. Before looking specifically at the pathfinder elements, all elements were compared with the whole dataset to identify any other elevated concentrations and also any anomalously low values (Table 14). This is significant as low anomalies may relate to elemental scavenging or depletion due to transport and erosion. The main pathfinder elements that are investigated in greater detail include Ag-As-Hg-Sb-Mo (Table 15). The top-soil dataset was analysed first as it showed the most promise. Figure 15 indicates the sample locations, with the sample identification number. The black outline in Figure 15 was generated around areas with best anomalies and with proximity to faulting in mind. The target area covers 29 km².

Summary of data for Manorhamilton:					
	Element	Overall average (ppm)	Target area average (ppm)	Max	Min
Top soil	Ag	0.08	0.28	2.02	0.04
	As	6.5	10.57	41.81	0.5
	Hg	0.1	0.22	1.4	0.04
	Mo	1.38	1.81	6.23	0.46
	Sb	0.34	0.48	1.71	0.07
	<i>Other selected elements with significant difference</i>	Depleted: Zn, Sr, Ba, Ni, La	Elevated: Cu, Cr, Mn, P, Pb		
Stream sediment	Ag	0.28	0.24	0.4	0.1
	As	15.24	29.98	104.7	3.8
	Mo	2.12	1.16	1.7	0.6
	Sb	0.82	1.96	5.3	0.4
	<i>Other selected elements with significant difference</i>	Depleted: S, Zn, Br, Sr, W, Sm, Ba, Na ₂ O, Al ₂ O ₃ , Fe ₂ O ₃	Enriched: CaO, Ni, Zn, Hf, Cs, SiO ₂		

Table 14: A comparison of Manorhamilton data with the complete Tellus Border geochemical dataset.

From Table 15 it is possible to identify certain locations which demonstrate high values across elements and those that do not. Also, the spatial distribution of anomalies can be studied, in particular, their proximity to faulting as shown in Figure 15. For mineralisation to be present we expect to see raised pathfinder element values across the region. However, due to the wide spacing between sample locations (~4 km) this may not be clear. The best method to test this is with a correlation matrix, but first the results were log₁₀ transformed, due to a positive skew on the data.

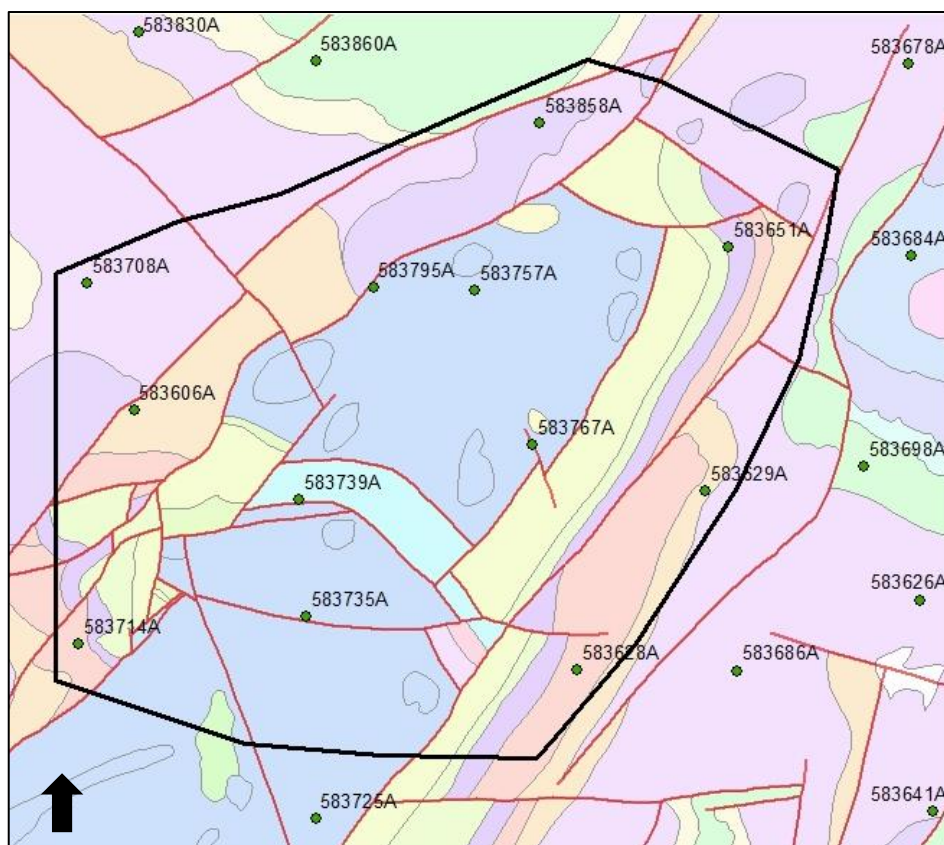


Figure 15: Map of sample locations for top-soil survey of Manorhamilton, outline of target area in black.

Sample_ID	Ag_mgkg	As_mgkg	Hg_mgkg	Mo_mgkg	Sb_mgkg
583757A	0.14	5.76	0.28	0.75	0.50
583767A	0.25	16.85	1.40	1.80	1.33
583739A	2.02	3.91	0.08	0.82	0.28
583735A	0.05	1.14	0.07	0.46	0.13
583751A	0.09	11.30	0.08	6.23	0.19
583758A	0.10	15.00	0.09	1.54	0.14
583795A	0.09	2.06	0.07	1.37	0.15
583714A	0.02	9.46	0.04	0.61	0.57
583708A	0.32	41.81	0.15	4.31	1.71
583629A	0.04	0.50	0.05	0.46	0.07
583628A	0.05	8.53	0.16	1.60	0.21

Table 15: Summary values of Au pathfinder elements from top-soil data in the Manorhamilton target.

	Ag_mgkg	As_mgkg	Hg_mgkg	Mo_mgkg	Sb_mgkg
Ag_mgkg	1				
As_mgkg	0.275	1			
Hg_mgkg	0.360	0.455	1		
Mo_mgkg	0.256	0.725	0.286	1	
Sb_mgkg	0.368	0.757	0.620	0.378	1

Table 16: Correlation matrix for Au pathfinder elements in the Manorhamilton top-soil data.

From the top-soil data it is apparent that the majority of pathfinder elements within the Manorhamilton area have poor correlations, this could be in part a factor of the large sample spacing, however, there is good correlation between As and Mo/Sb (Table 16). Due to the different sampling methods and locations (Figure 16) the results between top-soil and stream sediment datasets (Table 17) may not show a strong relationship. However, where similarities occur they can be a good way of testing the reliability and consistency of high values.

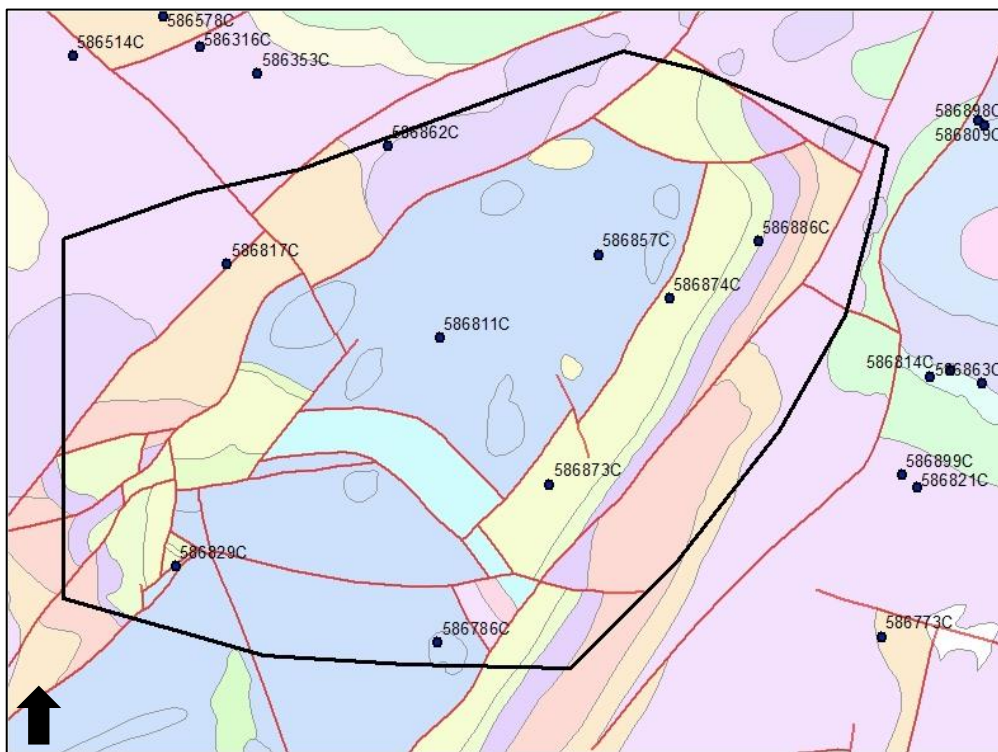


Figure 16: Map indicating the locations of stream sediment samples within the Manorhamilton target.

Sample_ID	As_mgkg	Ag_mgkg	Mo_mgkg	Sb_mgkg
586786C	6.8	0.1	0.6	0.8
586873C	32.4	0.25	1.6	2.9
586874C	43.6	0.25	1.7	5.3
586886C	14.9	0.25	1	0.7
586857C	36.1	0.4	1.4	3.7
586811C	3.8	0.25	1.3	0.9
586829C	104.7	0.25	0.6	1.4
586817C	10.8	0.2	0.6	0.4
586862C	16.7	0.25	1.7	1.5

Table 17: Summary values of Au pathfinders in stream sediments of the Manorhamilton area

	As_mgkg	Ag_mgkg	Mo_mgkg	Sb_mgkg
As_mgkg	1			
Ag_mgkg	0.439	1		
Mo_mgkg	0.073	0.585	1	
Sb_mgkg	0.633	0.457	0.635	1

Table 18: Correlation matrix of Au pathfinder elements in stream sediments at Manorhamilton

The correlation matrix for the stream sediment data shows similar patterns to the top-soil data (Table 18), indicating correlation between Sb - As and Mo. This relationship may be due to the occurrence of particularly high concentrations of certain minerals, for example, tetrahedrite with arsenopyrite, a theory that will be tested in the field. It is clear that this area shows elevated values of key pathfinder elements, however, the data analysis does not confirm that these elements show any naturally occurring correlation.

6.1.4. Fieldwork

Fieldwork in the Manorhamilton area was carried out in two stages, the first involved sample collection followed by three days of mapping. The area was considered for further fieldwork due to raised As, Ag and Sb, with the potential for Au mineralisation. The following objectives were set:

- Obtain comprehensive understanding of present lithology formation and mineralogy.
- Carry out detailed mapping of areas with good exposure.
- Identify possible sources of mineralisation associated with target lithology and regional faulting.
- Pan and collect samples of stream sediments in close proximity to mapped faults, both upstream and downstream of faults.
- Collect float samples which show potential for hosting mineralisation.

The mineralisation which resulted in high anomalous values is likely to have been transported by glacial movement, this was considered in the exploration strategy. The primary targets were good exposures in the streams and rivers, which also yielded ideal size fraction of sediment for panning and collection. Table 19 describes the main lithologies present, also shown on Figure 13.

Lithology	Mapped unit	Description
Meta-basite	Meelick Member	Very fine grained dark mineralogy with thin quartz veins found within. Chloritic alteration with fine grained mica common.
Felsite	Sliswood division	Almost granitic in mineralogy, with abundant feldspar and quartz. Samples distinguished with large muscovite minerals, minor fine biotite. Feldspars can occur >2 cm in diameter giving pegmatic texture in places. Predominantly plagioclase feldspar with minor orthoclase.
Schist	Meelick Member	Rich in quartz and mica, with feldspar less dominant to non-apparent. Little evidence of foliations in bedrock. Grain size is very fine, with coarser quartz bands.
Mudstone	Glencar limestone Formation	Finely laminated mudrock with minor barren veining. Lithology is predominately featureless, can be identified with characteristic desiccation cracks on bedding plane.
Sandstone	Ballyshannon limestone Formation	Well sorted medium grained sandstone with veins of calcite found throughout. Veins appear barren, with pure carbonate composition.
Psammite	Sliswood Division	Fine grained metamorphic sandstone, with dominant quartz mineralogy. May contain fine disseminations of sulphides in certain units.

Table 19: Summary of main lithologies in the Manorhamilton target area.

The Tellus Border sampling locations which yielded anomalous results were used as a guide in order to identify potential sources. The high top-soil Ag anomaly was considered first (583739A), but due to poor outcrop no lithological source could be identified. A thorough investigation of the area suggested that there are no significant sources of anthropogenic contamination such as metal scrap yards or industrial activity. The MinLocs database and historical records detail an Au observation within stream sediments in the SW of the target area, and an old Au-Cu working at Pollboy (Cole, 1922). No evidence for these was found. However, one stream sediment sample (009) shows elevated Au, Cu and Sb in the results of recent fieldwork (Section 6.1.5).

Signs of mineralisation were seldom and minor, with most occurring as disseminated pyrite in meta-sediments. Occasional mineralisation was identified in quartz veins within float material.

6.1.5. Results

The relatively small target area facilitated even sampling throughout the region with stream sediment being the dominant sample type. In addition, all of the main lithologies were sampled from bedrock exposures, but only a selected few were chosen for assay. The results are presented in Table 20 and the sample locations are shown in Figure 17. The results are generally positive with good anomalies of Au backing up original ideas for potential sources and styles of mineralisation. The main pathfinder elements complemented high Au values, all of which were found within stream sediment samples. Certain samples stand out, such as stream sediment OM-13-PS-016 (Table 20), which shows elevated concentrations of Au, Ag, As and Sb. These element associations show potential for orogenic Au style mineralisation. Also, panned concentrates 108 and 109 which contain raised Au, Ag, Sb, Pb and Cu. Sample 016 is situated downstream of a major NE trending fault and meta-sedimentary formation (Figure 17). The values across the stream sediment samples were good, however, fire assay analysis of rock samples failed to yield Au values much above the LLD of 0.001ppm. Nevertheless, sample OM-13-PS-025 of the Sliswood meta-sedimentary formation, shows high values of Ag and Sb, and elevated values of As and Hg (Figure 18).

SAMPLE	Type	Lithology	grams weight	ppm Au	ppm Ag	ppm As	ppm Cu	ppm Hg	ppm Mo	ppm Pb	% S	ppm Sb	ppm Zn
OM-13-PS-006	bedrock	Meta-basite	511	<0.001	0.02	2.5	48.6	0.04	0.26	13.6	0.02	0.97	103
OM-13-PS-017	float	Quartz vein	599	<0.001	0.04	2	4.8	0.04	0.44	7.1	0.11	0.87	9
OM-13-PS-024	float	Quartz vein	87	<0.001	0.04	2.4	7.9	0.02	0.25	83.8	0.08	0.09	8
OM-13-PS-025	bedrock	psammite	76	<0.001	0.5	34.5	23.9	0.44	3	11.5	1.57	15.95	35
OM-13-PS-107	float	psammite	28	0.006	0.19	1.2	11.8	<0.01	0.5	33.4	0.01	0.15	13
OM-13-PS-124	float	meta-basite	636	0.001	0.04	1	39.2	<0.01	0.34	7	0.08	0.15	77
OM-13-PS-125	bedrock	meta-basite	275	<0.001	0.02	0.5	15.4	<0.01	1.32	6	0.05	0.21	66
OM-13-PS-129	float	psammite	148	0.002	0.21	6.2	13.8	0.07	2.68	15.3	0.62	2.02	4

SAMPLE	Type	Grain size	grams weight	ppm Au	ppm Ag	ppm As	ppm Cu	ppm Hg	ppm Mo	ppm Pb	% S	ppm Sb	ppm Zn
OM-13-PS-001A	stream sed	med to coarse	321	<0.001	0.03	12.5	11.8	0.03	0.52	32.5	0.08	0.3	98
OM-13-PS-001B	stream sed	med to coarse	305	<0.001	0.04	10.6	7.4	0.03	0.41	21.9	0.05	0.3	64
OM-13-PS-008	stream sed	coarse	437	<0.001	0.03	17.9	24.6	0.02	0.24	15.1	0.12	0.44	91
OM-13-PS-009	stream sed	coarse	581	0.244	0.09	68.6	61.3	0.04	0.46	35	0.1	1.14	90
OM-13-PS-010	stream sed	very coarse	460	0.006	0.05	19.2	19	0.01	4.19	20	0.04	0.87	83
OM-13-PS-011	stream sed	very fine	312	0.002	0.06	12.4	31.9	0.08	0.53	15.9	0.18	0.27	104
OM-13-PS-012	stream sed	very coarse	403	0.12	0.07	12.8	11.3	0.03	0.4	18.9	0.3	0.55	58
OM-13-PS-016	stream sed	v. coarse - fine	438	0.292	0.24	49.2	22.6	0.06	0.93	27.4	0.11	2.39	51
OM-13-PS-018	stream sed	med to coarse	441	0.1	0.06	19.1	9.9	0.04	1.25	27.8	0.07	0.25	78
OM-13-PS-020	stream sed	coarse	528	<0.001	0.11	13.7	14.6	0.03	1.36	21.8	0.53	0.33	67
OM-13-PS-022	stream sed	med to coarse	486	<0.001	0.09	14	14	0.04	1.07	13.2	0.09	0.79	46
OM-13-PS-023	stream sed	fine to coarse	710	0.016	0.04	16.1	13.6	0.04	0.46	9.9	0.03	0.74	53
OM-13-PS-108	panned conc.	fine	18	1.89	1.46	13.8	59.5	0.26	0.2	62.1	0.09	0.6	30
OM-13-PS-109	panned conc.	fine	11	1.145	0.26	36.2	67.9	0.17	0.29	102.5	0.24	1.22	47
OM-13-PS-110	panned conc.	fine	18	0.723	0.06	15.6	19.6	0.07	0.21	44.6	0.07	0.5	26
OM-13-PS-111	panned conc.	fine	18	0.235	0.03	9.8	11.2	0.05	0.15	31.8	0.04	0.25	21

SAMPLE	Type	Grain size	grams weight	ppm Au	ppm Ag	ppm As	ppm Cu	ppm Hg	ppm Mo	ppm Pb	% S	ppm Sb	ppm Zn
OM-13-PS-112 A	panned conc.	medium	64	0.145	0.01	6.5	2.3	0.04	0.12	9.4	0.01	0.14	15
OM-13-PS-112 B	panned conc.	medium	54	0.215	<0.01	5.2	1.8	0.05	0.1	8.5	0.01	0.09	16
OM-13-PS-113	stream sed	very coarse	376	0.783	0.08	3.4	5.2	0.05	0.12	45.1	0.03	0.81	21
OM-13-PS-114	stream sed	med to coarse	81	0.035	0.01	9	4.2	0.03	0.27	12.6	0.02	0.39	16
OM-13-PS-116	stream sed	med to coarse	267	0.595	0.12	10.3	13.1	0.19	0.43	57.3	0.02	1.55	25
OM-13-PS-117	panned conc.	fine	26	NSS	0.13	2.9	3.9	0.07	0.15	14.3	0.02	0.16	15
OM-13-PS-120	stream sed	med to coarse	212	0.377	0.09	27.2	19.5	0.08	0.85	15.5	0.16	2.49	44
OM-13-PS-121	panned conc.	fine-medium	40	0.084	0.02	25.2	16.6	0.07	0.73	15.8	0.03	2.2	23
OM-13-PS-122	panned conc.	fine	32	0.177	0.02	19.3	16.2	0.08	0.56	16.4	0.02	1.72	19
OM-13-PS-123	stream sed	med to coarse	320	0.317	0.14	70.5	49.4	0.12	1.99	33.7	0.09	4.5	87
OM-13-PS-126	panned conc.	medium to fine	38	0.799	0.01	4.7	4.1	0.04	0.15	12.1	<0.01	0.28	14
OM-13-PS-127	panned conc.	fine	100	0.011	0.01	5.1	5.4	0.01	0.19	7	<0.01	0.43	15
OM-13-PS-128	panned conc.	medium to fine	80	0.312	1.5	5.1	5.6	0.28	0.18	10.6	<0.01	0.44	16

Sample	type	Weight	pH	pH (HCl)	ppm Au	ppm Ag	ppm As	ppm Cu	ppm Hg	ppm Mo	ppm Pb	% S	ppm Sb	ppm Zn
OM-13-PS-213	topsoil	870	4.6	3.98	<0.001	0.14	10.2	11.8	0.1	1.03	15	0.07	0.7	38
OM-13-PS-214 A	subsoil	452	5.15	3.75	0.001	0.07	7.8	28.5	0.1	0.7	7.1	0.04	0.51	48
OM-13-PS-214 B	subsoil	452	5.15	3.75	0.001	0.08	6.8	33.2	0.08	0.6	6.4	0.04	0.43	48
OM-13-PS-215	topsoil	884	4.6	3.9	<0.001	0.2	8.2	11.9	0.16	0.73	27.8	0.07	1.64	30
OM-13-PS-216	subsoil	337	4.72	3.64	<0.001	0.14	14	23.4	0.22	0.89	20.2	0.06	1.65	38
OM-13-PS-217	topsoil	856	4.49	3.72	0.001	0.14	4.5	9.9	0.3	0.74	32.9	0.07	0.43	22
OM-13-PS-218	subsoil	581	4.54	3.6	<0.001	0.05	3.8	12	0.11	0.49	18.8	0.05	0.28	51
OM-13-PS-219	topsoil	613	5.12	3.03	0.002	0.16	8.7	13.1	0.13	1.65	20.2	0.08	0.54	32
OM-13-PS-220	subsoil	515	4.9	4.12	0.001	0.15	9.5	15.1	0.19	1.92	17	0.07	0.63	47
OM-13-PS-221	topsoil	881	3.74	3.41	0.001	0.2	13.2	36.1	0.32	0.81	355	0.22	1.01	16

Sample	type	Weight	pH	pH (HCl)	ppm Au	ppm Ag	ppm As	ppm Cu	ppm Hg	ppm Mo	ppm Pb	% S	ppm Sb	ppm Zn
OM-13-PS-222	subsoil	944	4.33	4.05	<0.001	0.23	11	9.3	0.24	0.53	50	0.09	1.51	10
OM-13-PS-223	topsoil	731	4.59	3.92	0.001	0.31	6.9	13.6	0.16	1.49	50.3	0.09	0.48	31
OM-13-PS-224	subsoil	890	4.54	3.92	0.001	0.23	11.5	31.5	0.27	1.12	58.1	0.06	0.8	54
OM-13-PS-225	topsoil	804	4.79	3.78	0.001	0.11	9.9	19.1	0.2	1.17	25.8	0.07	0.61	38
OM-13-PS-226	subsoil	1063	4.77	4.05	0.001	0.06	10.9	34.9	0.19	0.77	21.3	0.05	0.75	53
OM-13-PS-227	topsoil	730	4.32	3.71	0.002	0.22	7.4	14.2	0.16	1.7	38	0.07	0.52	32
OM-13-PS-228	subsoil	402	4.68	3.87	0.001	0.38	6	9.9	0.2	1.58	26	0.06	0.29	31
OM-13-PS-229	topsoil	720	4.67	4.21	0.001	0.15	5	20.5	0.17	0.42	30.4	0.35	0.56	14
OM-13-PS-230	subsoil	896	4.79	4.33	0.002	0.13	4.1	19	0.17	0.37	14.2	0.48	0.41	10
OM-13-PS-231	topsoil	694	3.71	3.18	<0.001	0.19	1.1	4.9	0.18	0.5	11.2	0.18	0.1	3
OM-13-PS-232	subsoil	861	4.6	3.62	<0.001	0.06	2.3	10	0.08	0.13	14.1	0.05	<0.05	18

Total number of samples = 55
soil samples = 20
sediment samples = 27
whole rock samples = 8

Table 20: The key results for new samples collected in the Manorhamilton target.

Figure 17: Map displaying the location of sample sites in the Manorhamilton target

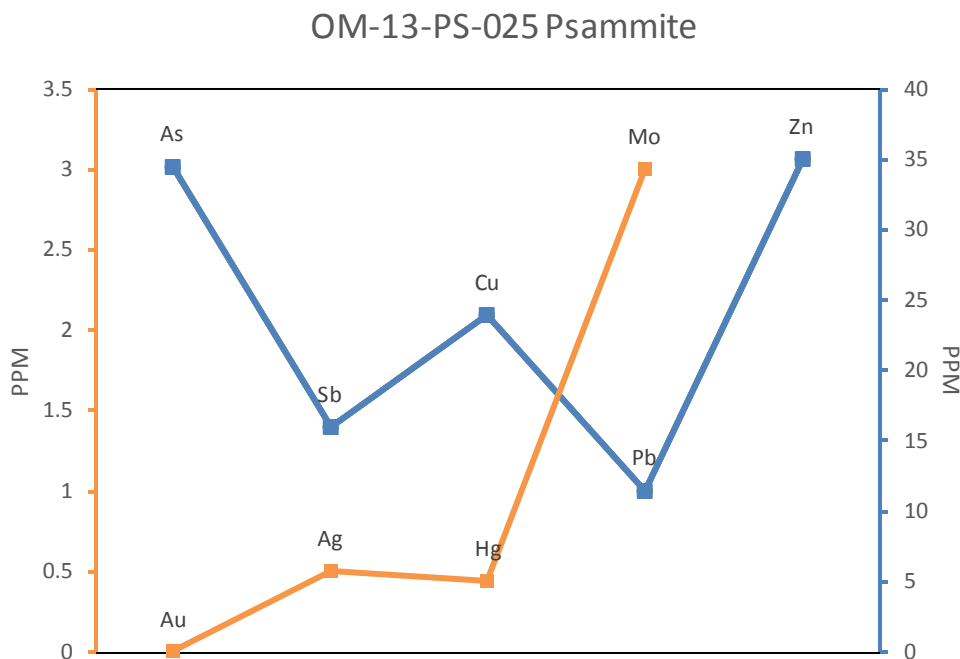


Figure 18: Graph representing main pathfinder anomalies for bedrock sample 025, with line colour relating to axis

The float samples were observed to contain fine disseminations of pyrite. Due to the size and coverage of the formation within the target area, this may be the genetic link between local lithology and high background levels of pathfinder elements. If this can be proved to be true, it would lower the potential for a major source of mineralisation. To test the association, a greater number of sample analyses are required.

Two soil sample grids were developed, one centred in the west of the target area where raised Sb and Au were identified in bedrock and stream sediments, respectively; the other grid centred on a high Ag Tellus border sample of 2 ppm (table 21). Twenty samples were collected, ten top-soils and ten sub-soils at 100 m spacing. Contrasting colour and composition between sub-soils and top-soils was observed, showing ideal variation with depth. Neither the top-or sub- soils display above background levels of Au. However, Au pathfinder elements indicate strong values above background, with Ag and Hg the most concentrated. The soils taken closest to the Tellus Border sample point tend to show the highest values, this is most likely due to the type of ground chosen by the survey which is flat grassland in contrast with the usual boggy ground. The western grid (samples 213-222) backs up original prospectivity with strong values of Sb and average values nearly double that of the other grid. Similar differences can be seen in elements Pb, Sn, Co and Cr. This may reflect a lithological control from nearby basic intrusions, and with close proximity to minor NW trending fault possibly a source for base metals. The Tellus Border based grid is located on top of a hill, with a higher elevation the ground conditions are predominately boggy, and this may explain the lower values. Due to the contrasting environments of the two grids a study of their pH is useful. The results show that the western grid has a weak negative correlation of element values and increasing pH and the southern grid has a weak positive correlation of element values and increasing pH. This highlights the significance of

environment when analysing soils, as ground conditions play a large role in determining element concentrations.

Eight existing Tellus Border samples for the Manorhamilton target areas, which hadn't previously been analysed, were selected from GSI for analysis and inclusion in this project (Table 21). The four sub-soil samples revealed negligible pathfinder concentrations, with the exception of sample 583767 which indicates slightly raised Pb and Zn. This is surprising given that the top-soil values from the same sample locations yielded high anomalous results.

Sample type	ID	Au	Ag	As	Hg	Sb	Cu	Mo	Pb	Zn
Sub-soil	583757 -S	0.001	0.06	1.8	0.06	0.34	23.4	0.23	11	12
	583767a	0.001	0.01	1.7	0.01	0.1	4.8	0.12	3.3	30
	583767 -S	0.003	0.15	8.5	0.81	0.82	36.1	1.43	93.2	145
	583739 -S	0.001	0.34	5.8	0.1	0.46	24.4	0.92	26.8	52
Panned Conc.	586829	NA	0.01	12	<0.01	0.24	4.2	0.22	5.5	64
	586874	NA	0.17	82.3	0.28	7.03	105.5	2.68	50.5	43
	586857	0.013	0.03	10.6	<0.01	1.22	5	0.27	7.7	15
	586873	<0.001	0.06	22.5	0.04	4.26	127	0.54	8.1	23
top-soil	583757A	NA	0.14	5.76	0.28	0.50	198.21	0.75	29.23	20.00
	583767A	NA	0.25	16.85	1.40	1.33	38.84	1.80	727.47	175.00
	583739A	NA	2.02	3.91	0.08	0.28	16.74	0.82	38.50	42.00
stream sediment	586873C	NA	0.25	32.4	NA	2.9	62.8	1.6	36.4	92.7
	586874C	NA	0.25	43.6	NA	5.3	38.5	1.7	40	88.9
	586857C	NA	0.4	36.1	NA	3.7	36.1	1.4	33.1	103.2
	586829C	NA	0.25	104.7	NA	1.4	48.3	0.6	25	119

Table 21: Comparison of selected sub-soil and panned concentrate samples with associated top-soils and stream sediment samples in Manorhamilton

Two of the four panned concentrate samples indicate high Cu and Sb with sample 586874a also containing raised concentrations of As and Mo. A series of panned concentrate samples were collected from locations based on proximity to the major NE trending faults, high stream sediment values from the Tellus Border survey and also our data from initial sampling. The results show high values for base and precious metals, and also high values in metals such as Cr, W and Sn (See Appendix). The precious metal results are also well correlated with values of pathfinder elements (Figure 19), which display a gradual increase in values downstream from sample 111 to 108. The area is closely related to the Pollboy working discussed previously in this chapter. The gradual increase in values may reflect the catchment after the join of rivers, with decreases in elevation resulting in greater deposition of material. The High Cr and W values could indicate high background levels controlled by local lithology, as meta-basite pods have known high Cr values and the granitic type psammities may show higher concentrations in W and Sn.

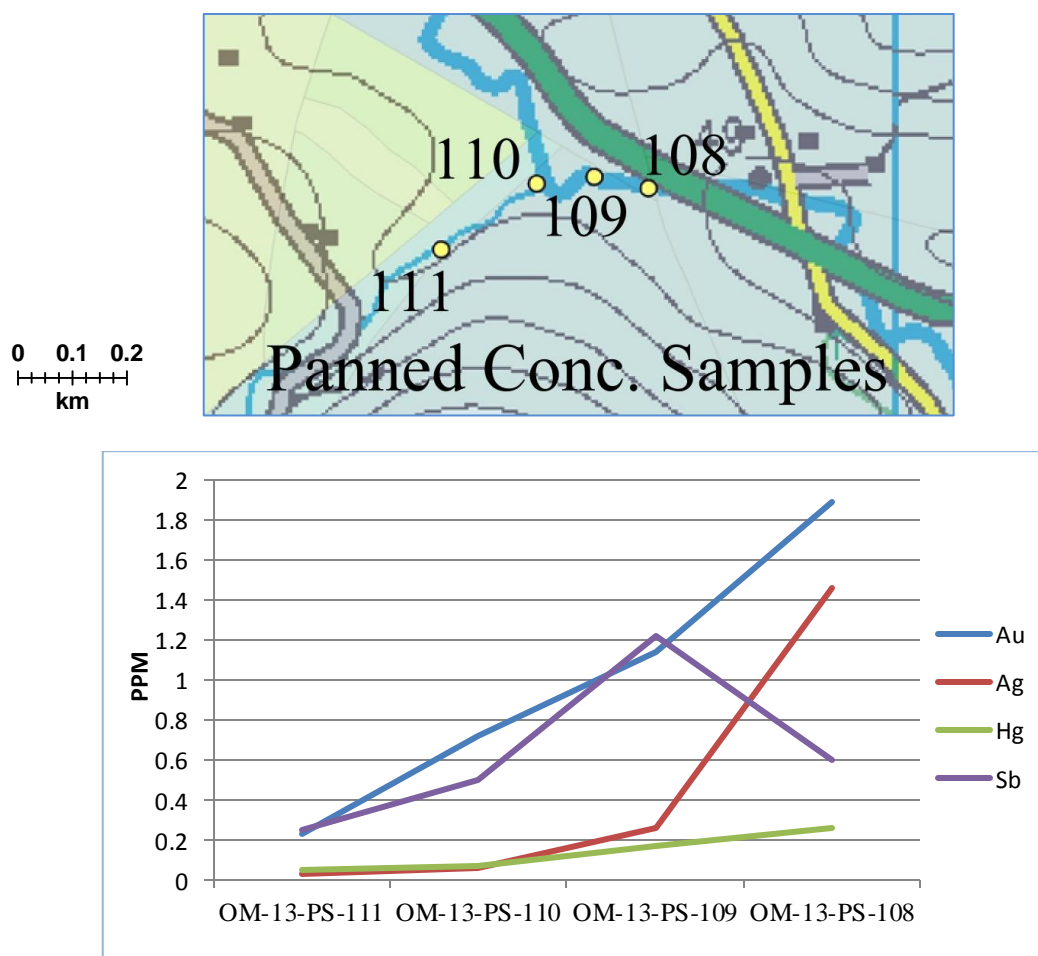


Figure 19: Map showing the location of panned concentrate samples (above) and their relative levels of Au, Ag, Hg and Sb (below).

Certain areas within the Manorhamilton target remain prospective for Au mineralisation. Increased sampling density and mapping are required to find the source. The abundant streams could provide ideal targets for stream sediment and panned concentrate sampling. Faulting as the source remains the theory that should form the basis of further exploration, with areas where streams cross cut the NE trending faults being most prospective.

6.2. Glenties

6.2.1. Introduction

The town of Glenties is situated to the south-west of the target area (Figure 20). Glenties is one of the main towns in western Donegal, and is approximately 25 km from both Ballybofey and Donegal town. The area is sparsely populated with farmland and peat bogs dominating the landscape. The topography is a mix of steep sided hills to low lying valleys, where small loughs are common. To the east lie the Bluestack Mountains, which are the most prominent feature in the landscape and a major control on the drainage system. Outcrop in the area is plentiful, with upland areas showing good exposure and lowland areas displaying outcrop in rivers and streams. The region contains many inactive and disused quarries which are ideal

for mapping. In one area, a quarry has exposed quartz veining with sulphide mineralisation adjacent to a fault.

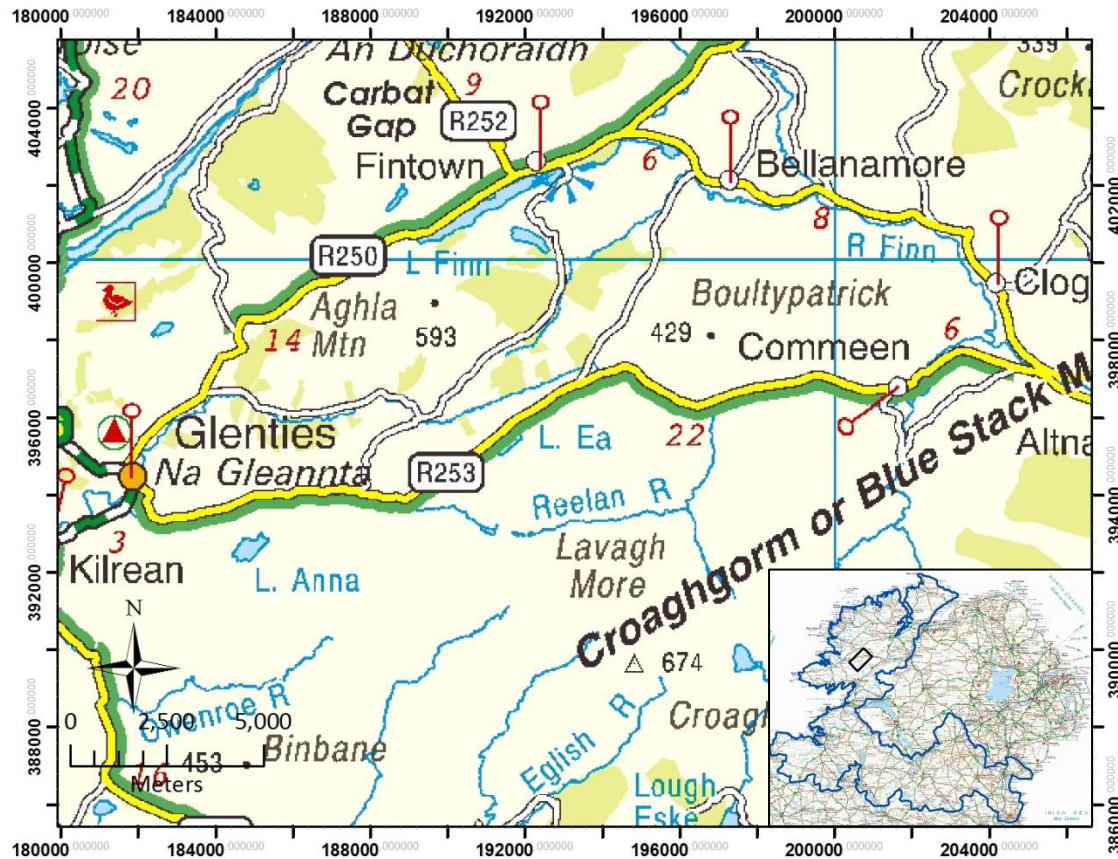


Figure 20: Locality map for the Glenties area, with a sub-set of its location in the border region

6.2.2. Local Geology

The area is dominated by heavily deformed meta-sediments of Dalradian age, which are typical throughout Co. Donegal. The main lithological formations form long thin bands in the landscape due to the strong structural control in the area (Figure 21). The meta-sediments are made up of pelites and psammities, metamorphosed to schistose type facies. Two main volcanic features are found in the shape of the Donegal Appinite suite and meta-dolerite. The Appinite suite has a composition from ultramafic basalt to silica poor andesite, with trace element concentration similar to many basaltic rocks. Typical element associations include enrichment in Ni, Co and Cr. The meta-dolerite is common throughout both areas, whereas the Appinite suite is only found in target area A. Tectonic schist is mylonitic, showing the strong structural deformation in the surrounding lithologies.

The structural complexity of the area is easily observed with a high density of faulting displayed in Figure 21. The dominant trend is NE-SW, along the main Donegal Lineament. In close proximity to the main fault are a series of NW-SE trending minor faults, which show a variety of orientations. This main fault runs through the Millford target area, and appears to show a strong association with geochemical anomalies along strike. Mineralisation is

recorded in the MinLocs database and in some historic documents. Sulphide mineralisation is found in both meta-sediments and the Appinite suite, mainly in the form of pyrite and chalcopyrite within narrow quartz veins with a thickness of ~5 cm. Other mineral occurrences include galena in float samples, pyrite with molybdenum and minor sphalerite.

The undulating nature of the landscape and topography makes delineating origin of potential float material relatively straight forward. The principle direction of glacial movement is NE-SW as indicated by drumlin trends in the area (Figure 22). Despite this, the distance travelled of any float material may be hard to determine, especially for stream sediments due to fast flow throughout both target areas.

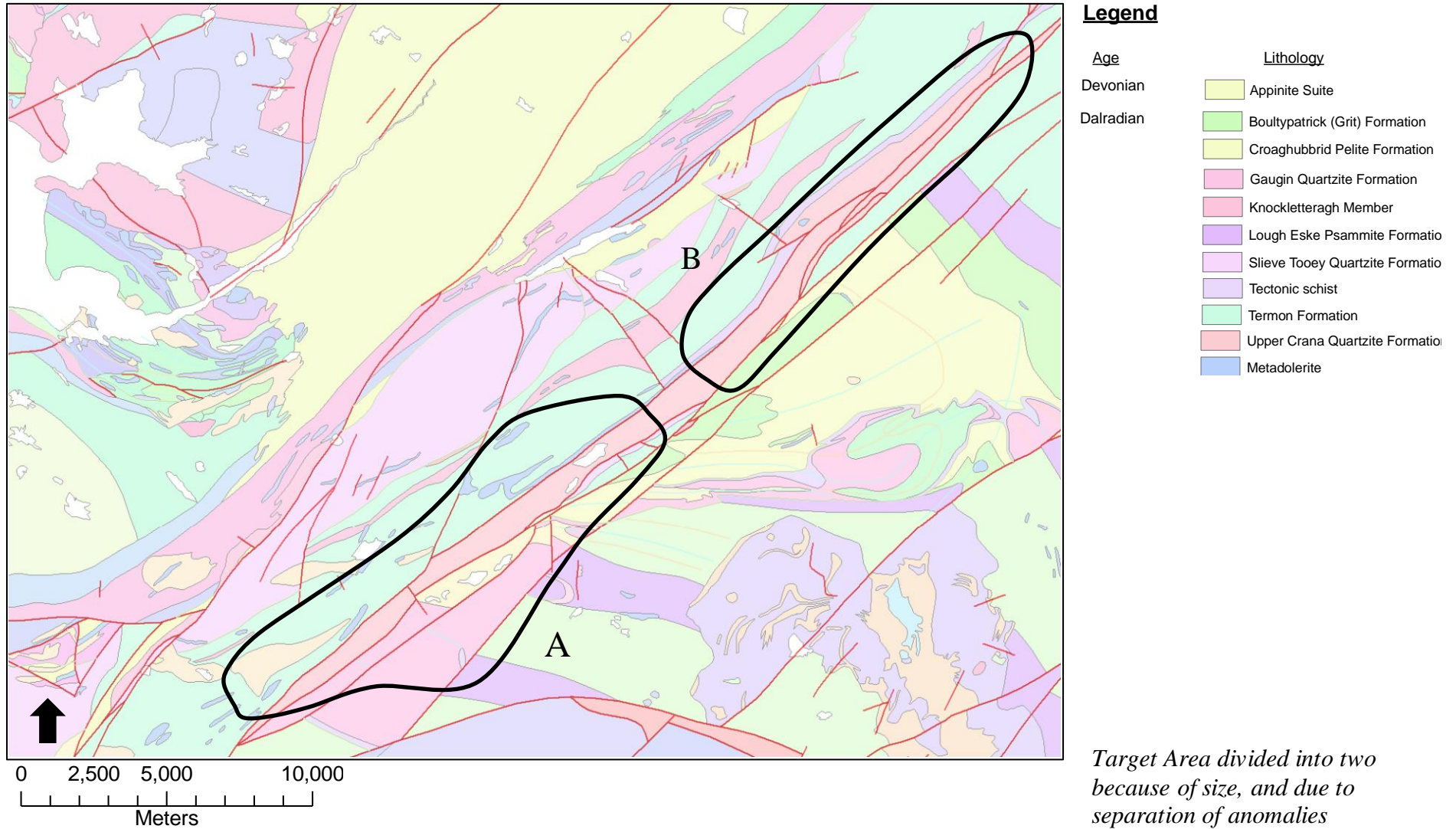


Figure 21: Detailed geological map of Glenties target areas A and B.

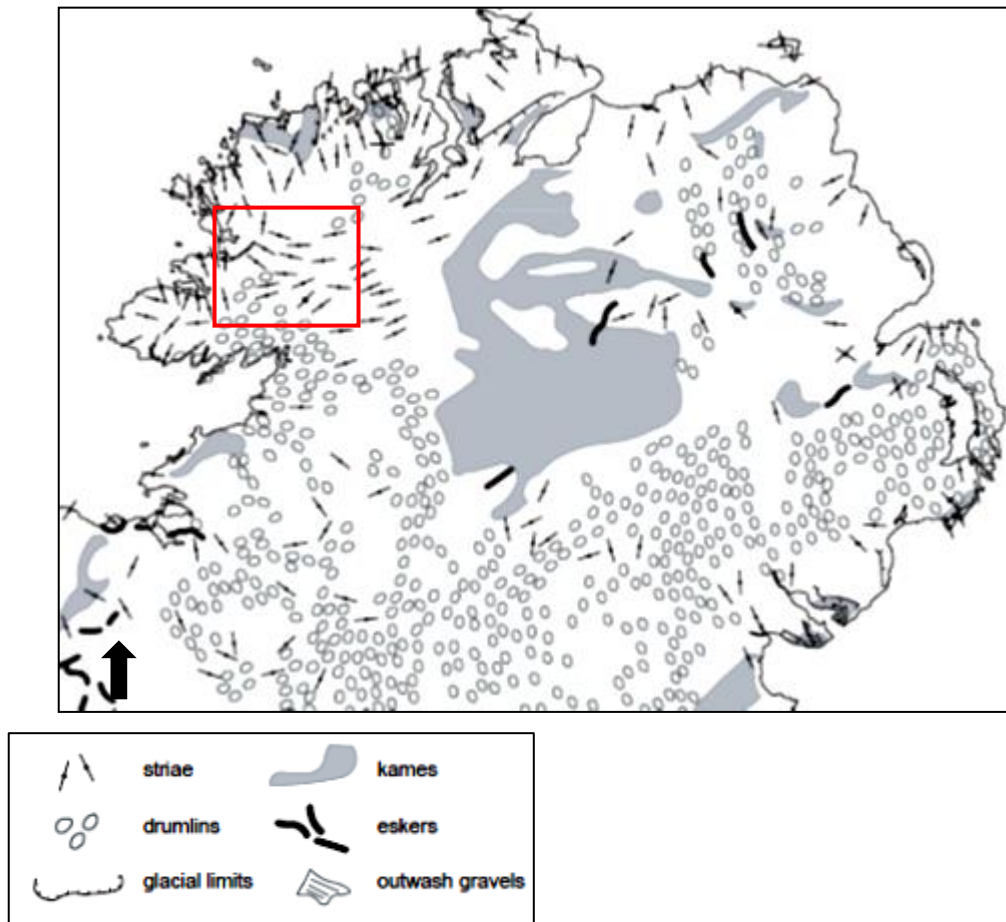


Figure 22: Map displaying the trend of glacial movements in the Glenties target, with the dominant orientation being E-W using evidence from striae and NE-SW using drumlin evidence. (Clark, 2008)

6.2.3. Existing Data Analysis

6.2.3.1. Knowledge Driven Exploration

The Glenties area is highly prospective both in terms of the age of host rocks and the orientation of dominant fault trends. A deep seated lineament has long been considered as a potential source for mineral rich fluids. The main features of the Glenties area include:

- Major NE-SW trending faults
- Minor faulting associated in NW-SE orientation
- Dalradian age meta-sediments
- Known sulphide mineralisation
- Extensive quartz veining in both meta-sediments and Appinite suite

These factors show a strong similarity with other target areas, such as Manorhamilton and Millford. For the next phase of analysis the Glenties target area will be split into two, mainly due to its size and also the potential for separate sources of geochemical anomalies.

6.2.3.2. Data Driven Exploration

Geochemical anomalies have been observed throughout the whole 102 km² region within top-soil and stream sediment data (Table 22). Due to the widespread nature of high values, the anomalies adjacent to the major fault lines were considered for further investigation. Area A was investigated first, followed by B. The two target areas are compared to test for any cross over in multi-element relationships.

The similarities and differences between datasets and target sub-areas are evident from summary Table 22. The biggest contrast is seen in elevated As and Mo values for top-soils in target B, with As values across all data appearing the most elevated. The high values tend to cluster, this may be related to a local source of contamination or the underlying bedrock.

Summary of Glenties target area:					
		Area average	Total Data Average	Max	Min
Top-soil- A	Ag	0.060	0.081	0.150	0.005
	As	3.095	6.500	9.456	0.500
	Hg	0.105	0.102	0.220	0.020
	Mo	0.906	1.376	3.510	0.380
	Sb	0.320	0.349	0.840	0.025
	<i>Other selected elements with notable difference:</i>	Elevated: Se, Ba	Depleted: Cr, Cu, Li, Mn, Ni, P, Sr, V, Zn, Ce, Co, La, Pb, Y		
Top-soil- B	Ag	0.061	0.081	0.110	0.030
	As	18.804	6.500	100.981	2.060
	Hg	0.167	0.102	0.260	0.090
	Mo	2.490	1.376	14.400	0.580
	Sb	0.383	0.349	0.630	0.120
	<i>Other selected elements with notable difference:</i>	Elevated: Ba, Fe%, Mn, S%, Co, Se	Depleted: Y, U, Th, Sc, Rb, Ga, Ce, Be, Zn, Cu, Ni, Li, Cr, V		
Stream sediment: A	As	45.671	15.244	242.900	2.900
	Mo	1.751	2.120	7.600	0.500
	Ag	0.456	0.282	1.000	0.100
	Sb	0.734	0.817	4.400	0.100
	<i>Other selected elements with notable difference:</i>	Elevated: MnO%, Fe ₂ O%, Cl, Cu, Br, Rb, Y, Nd, Sm, Sn, I, Ba, La, Ce,	Depleted: CaO%, SiO ₂ , Cd, Sr, Zr, Cr, Ni		
Stream Sediment: B	As	49.350	15.244	83.900	2.200
	Mo	1.456	2.120	3.300	0.500
	Ag	0.269	0.282	0.800	0.100
	Sb	0.503	0.817	0.900	0.100
	<i>Other selected elements with notable difference:</i>	Elevated: CaO%, Cl, V, Cr, Ni, Zn, Sr, Zr, Sm, Hf, Pb, U, Cd, Sb, Te, I, SiO ₂ %	Depleted: Ba, W, Yb		

Table 22: Summary table for Tellus Border geochemical data for the Glenties target area.

6.2.3.3. Target A

Stream sediment data show the expected elevated averages for As-Ag (Table 23). Only one sample shows good correlation between the high end values (587389C), with two samples in close proximity displaying elevated Ag (587441C and 587449C). Levels of Mo and Sb are anomalously low throughout the area, this could be a regional feature and could be tested through comparison with the Millford target. However, elevated Mo and Sb are found in a single sample, 587871C. The relationship between As- Ag is important to consider, as these two elements are ideal pathfinders for Au mineralisation. However, stream sediment data can be misleading due to the contrasting mobility of certain elements. Also, the target area size and sample density (Figure 23) complicate correlation of the high end anomalies to a single source. It should be noted that area has shown little potential for base metal mineralisation, and so will not be included in the analysis of the Tellus Border results.

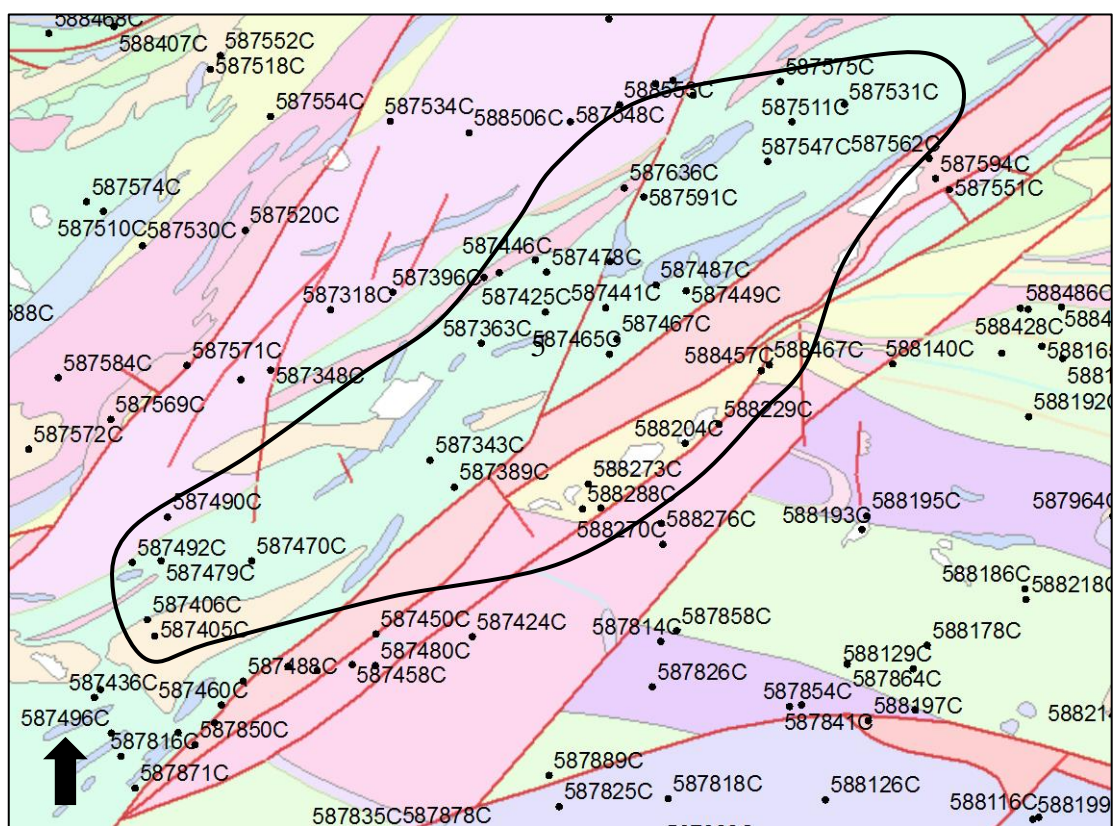


Figure 23: Summary map of stream sediment sample locations in the Glenties A target.

Sample_ID	As_mgkg	Mo_mgkg	Ag_mgkg	Sb_mgkg
587446C	16.9	1	0.9	0.8
587449C	16.4	1.6	1	0.5
587461C	35.7	2.3	0.5	1
587467C	12.9	0.6	0.8	0.7
587478C	11.7	1.3	0.6	0.5
587487C	20.1	1.7	0.7	0.8
587547C	50.7	1.5	0.25	0.4
587562C	13.8	1.2	0.5	0.4
587591C	120.3	3.4	0.4	0.9

587636C	9.5	0.6	0.3	0.9
587759C	13.8	1.3	0.25	1.6
587343C	119.1	1.4	0.3	0.9
587389C	242.9	1.8	0.9	1.1
587441C	48.5	1.5	1	1.1
587451C	2.9	4.7	0.25	0.1
587465C	58.8	1.5	0.25	2.1
588204C	29.5	0.9	0.4	0.1
588229C	8.8	0.5	0.25	0.1
588270C	23.5	1	0.2	0.2
588273C	23.2	1.3	0.3	0.25
588288C	46.2	2.9	0.4	0.1
587426C	9.6	0.5	0.25	0.3
587450C	14	0.5	0.4	0.2
587458C	17.3	0.5	0.1	0.4
587460C	15.2	0.6	0.3	0.8
587480C	17.5	0.9	0.5	0.6
587488C	113.7	1.5	0.3	0.7
587850C	35.5	1.8	0.3	0.5
587871C	30.9	5.1	0.4	4.4
587405C	75.8	1.7	0.8	0.5
587406C	146.5	2	0.6	0.7
587436C	7.3	1.8	0.7	0.25
587470C	103.7	1.3	0.5	0.8
587496C	62	7.6	0.25	0.2
587816C	24.3	1.5	0.1	0.8
588229C	8.8	0.5	0.25	0.1
588270C	23.5	1	0.2	0.2
588273C	23.2	1.3	0.3	0.25
588288C	46.2	2.9	0.4	0.1
588457C	15.5	1	0.3	0.25
588467C	10.9	0.9	0.25	0.25

Table 23: Summary table for Au pathfinder elements in stream sediment analyses for Glenties A

The correlation matrix (Table 24) shows consistently weak relationships between all elements, with As-Mo and As-Sb showing the strongest correlation. The correlation of As-Ag is lower than expected, but this may be a reflection of differing levels of element transport and mobility in the fluvial system.

	<i>As_mgkg</i>	<i>Mo_mgkg</i>	<i>Ag_mgkg</i>	<i>Sb_mgkg</i>
As_mgkg	1.000			
Mo_mgkg	0.400	1.000		
Ag_mgkg	0.199	0.169	1.000	
Sb_mgkg	0.371	0.146	0.243	1.000

Table 24: Correlation matrix for stream sediment Au pathfinder data in Glenties A.

The top-soil data for this target shows less potential when compared with the stream sediments, the reduced number of samples of this type is a limiting factor (Figure 24). Only Hg indicates any anomalously high values, with As demonstrating the most significant decrease (Table 25). The uneven nature of the stream sediment sampling locations could incur bias, less so with the top-soil sample locations.

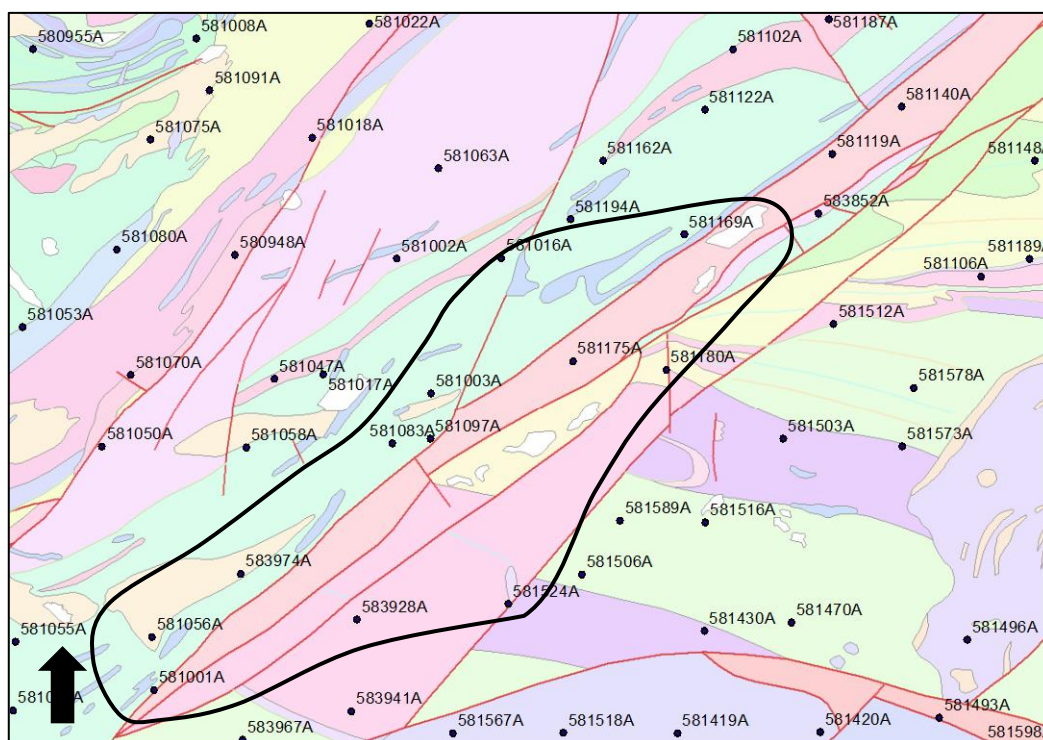


Figure 24: Summary map for top-soil samples within Glenties target A.

Sample_ID	Ag_mgkg	As_mgkg	Hg_mgkg	Mo_mgkg	Sb_mgkg
581001A	0.05	1.13	0.15	0.56	0.46
581003A	0.02	9.45	0.02	0.51	0.06
581056A	0.005	0.5	0.03	0.38	0.025
581083A	0.04	2.05	0.11	0.5	0.41
581097A	0.03	2.05	0.07	0.42	0.4
583974A	0.05	2.98	0.12	0.52	0.84
581016A	0.14	5.75	0.22	1.14	0.25
581169A	0.04	4.83	0.12	0.65	0.2
581175A	0.1	1.13	0.15	1.24	0.35
581180A	0.15	2.98	0.08	3.51	0.14
581194A	0.04	1.13	0.08	0.54	0.39
583928A	0.07	10.38	0.17	0.71	0.33
581524A	0.17	3.90	0.06	0.64	0.14

Table 25: Summary table for Au pathfinder elements in Glenties A top-soil data.

The majority of results show a moderate to strong correlation in Table 26, especially Ag with other elements. Hg demonstrates good correlation with Sb and Ag, however, the values are generally low and inherently less variable, therefore, apparent correlations should be treated with caution. When comparing the matrices for the sample types, Ag appears the dominant correlation for most elements within the top-soils and As appears stronger in the stream sediments. This contrast is likely to be directly related to the surficial environment.

	<i>Ag_mgkg</i>	<i>As_mgkg</i>	<i>Hg_mgkg</i>	<i>Mo_mgkg</i>	<i>Sb_mgkg</i>
<i>Ag_mgkg</i>	1.000				
<i>As_mgkg</i>	0.408	1.000			
<i>Hg_mgkg</i>	0.613	0.103	1.000		
<i>Mo_mgkg</i>	0.688	0.192	0.327	1.000	
<i>Sb_mgkg</i>	0.482	0.068	0.753	0.025	1.000

Table 26: Correlation matrix for Au pathfinder elements in Glenties A top-soils

6.2.3.4. Target B

Despite being closely linked with Target A, the geochemical anomalies for this area (Figure 25) appear significantly different. This could result from a different source of mineralisation or be related to a different expression of the same source.

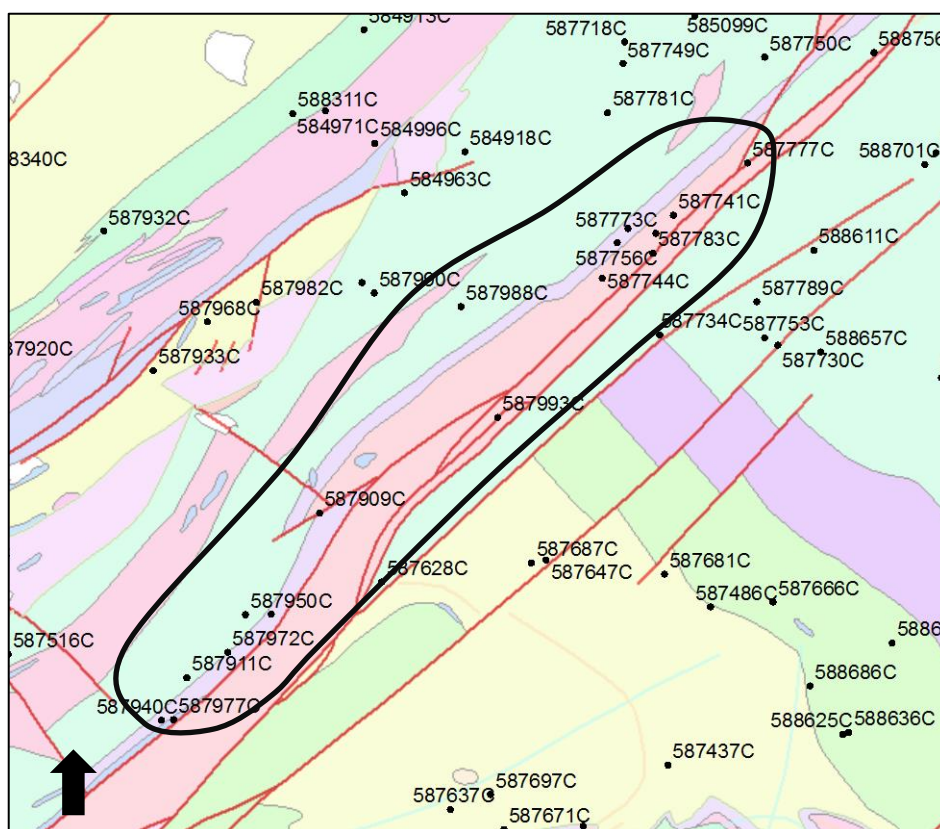


Figure 25: Map of stream sediment sample locations in Glenties target area B.

Sample_ID	<i>As_mgkg</i>	<i>Mo_mgkg</i>	<i>Ag_mgkg</i>	<i>Sb_mgkg</i>
587909C	49.6	0.9	0.1	0.25
587911C	73.2	1.8	0.1	0.5
587928C	2.2	0.5	0.25	0.3
587940C	78.6	2.2	0.3	0.7
587950C	50.6	1.2	0.2	0.7
587972C	83.9	0.9	0.25	0.2
587977C	73.8	0.7	0.1	0.6
587988C	76.4	1.8	0.25	0.4
587993C	25.7	1.1	0.25	0.7
587734C	19.3	0.9	0.25	0.5
587741C	16.1	1.8	0.25	0.4
587744C	57.6	1.8	0.5	0.6

587756C	52.2	2.2	0.25	0.9
587773C	83.3	3.3	0.8	0.7
587777C	19.8	0.9	0.25	0.5
587783C	27.3	1.3	0.2	0.1
area average	49.350	1.456	0.269	0.503

Table 27: Summary table for stream sediment Au pathfinder elements in Glenties area B

The stream sediment results indicate elevated As levels and low values for the other elements (Table 27), similar to target A. Despite the similarities, Ag values appear considerably lower in area B. When using stream sediment data to compare different areas within a region it is important to have an awareness of the drainage basin and different catchments. This will play a large role in determining movement of material, which is specifically important when attempting to trace anomalies to source. A weak correlation between each element is displayed in the correlation matrix (Table 28).

	As_mgkg	Mo_mgkg	Ag_mgkg	Sb_mgkg
As_mgkg	1.000			
Mo_mgkg	0.568	1.000		
Ag_mgkg	-0.016	0.502	1.000	
Sb_mgkg	0.239	0.374	0.257	1.000

Table 28: Correlation matrix for stream sediment Au pathfinder elements in Glenties area B

The location and results for top-soil samples are shown in Figure 26 and Table 29. High concentrations of As are found in some of these samples, specifically in sample 581143A. The same sample demonstrates significantly raised Mo.

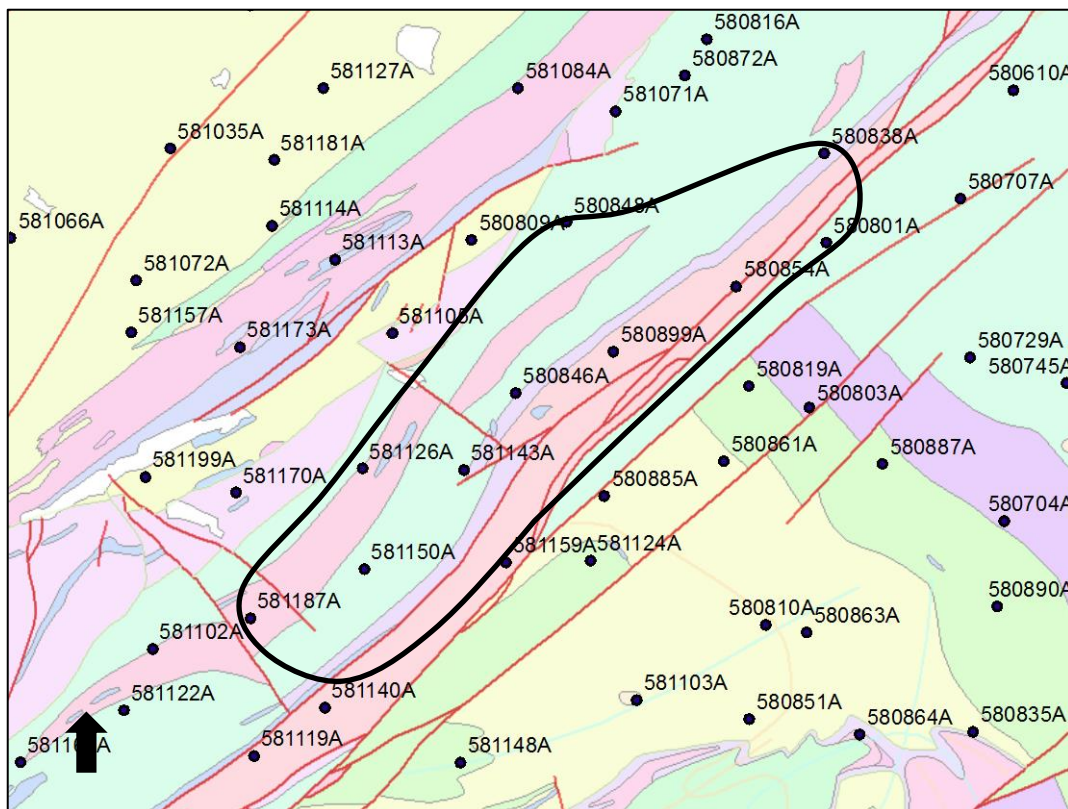


Figure 26: Summary map for top-soil data in Glenties area B.

Sample_ID	Ag_mgkg	As_mgkg	Hg_mgkg	Mo_mgkg	Sb_mgkg
580801A	0.04	2.060	0.16	0.79	0.49
580838A	0.06	23.323	0.09	2.26	0.12
580846A	0.07	15.003	0.19	1.07	0.33
580885A	0.06	11.305	0.15	0.9	0.39
580889A	0.08	2.060	0.15	0.76	0.63
581126A	0.04	5.758	0.17	0.86	0.4
581143A	0.11	100.981	0.24	14.4	0.41
581150A	0.03	5.758	0.09	0.58	0.12
581159A	0.06	2.984	0.26	0.79	0.56

Table 29: Summary table for Au pathfinder elements in top-soil samples for Glenties B

The correlation matrix (Table 30) shows strong to moderate associations for many elements, however, the actual element values are relatively small. Only if the average values greatly exceed the total dataset average would any correlation be of significance.

Considering the proximity of the target areas and their association with the main structural lineament, targets A and B can be compared and entered into a correlation matrix to identify any new potential elemental associations (Tables 31 and 32).

	<i>Ag_mgkg</i>	<i>As_mgkg</i>	<i>Hg_mgkg</i>	<i>Mo_mgkg</i>	<i>Sb_mgkg</i>
Ag_mgkg	1.000				
As_mgkg	0.536	1.000			
Hg_mgkg	0.526	0.074	1.000		
Mo_mgkg	0.694	0.867	0.297	1.000	
Sb_mgkg	0.404	-0.343	0.807	-0.034	1.000

Table 30: Correlation matrix for Au pathfinder elements in top-soils for the Glenties B region

	<i>As_mgkg</i>	<i>Mo_mgkg</i>	<i>Ag_mgkg</i>	<i>Sb_mgkg</i>
As_mgkg	1.000			
Mo_mgkg	0.386	1.000		
Ag_mgkg	0.042	0.209	1.000	
Sb_mgkg	0.316	0.166	0.213	1.000

Table 31: Correlation matrix for Au pathfinder elements in stream sediment data for Glenties A and B

	<i>Ag_mgkg</i>	<i>As_mgkg</i>	<i>Hg_mgkg</i>	<i>Mo_mgkg</i>	<i>Sb_mgkg</i>
Ag_mgkg	1.000				
As_mgkg	0.395	1.000			
Hg_mgkg	0.703	0.271	1.000		
Mo_mgkg	0.640	0.691	0.396	1.000	
Sb_mgkg	0.570	0.034	0.759	0.075	1.000

Table 32: Correlation matrix for top-soil Au pathfinder elements for Glenties areas A and B

Both sample types show considerable differences in element correlations when the two areas are combined together. The stream sediment data displays a moderate decrease in the correlation strengths. The top-soil analyses indicate a strengthening of correlations, especially for Ag-Hg and Ag-Sb. The impacts of large anomalies become less significant as more data is added to the analysis. By splitting the data it is easier to test the relationships between high end anomalies. The main reason for choosing this area was based upon good anomalies for Au pathfinder elements in the Tellus Border datasets, however, the existing data does not show clear correlation across these elements.

6.2.4. Fieldwork

The Glenties target areas were selected for further fieldwork due largely to high anomalies of As and Ag within the stream sediments. The target was divided into two for analysis purposes but fieldwork was carried out as one. The field area extended over 30 km north to south, to the east of Glenties town. The rough orientation correlates with major NE-SW faults of the region. The main objectives for fieldwork were as follows:

- Target major NE trending faults as potential source of mineralisation
- Collect stream sediments proximal to major faults
- Due to good exposure in places, detailed mapping of structural geology and veining
- Collect data of joint and fracture patterns where possible and relate to major faults
- Collect stream sediment samples in areas of high anomalies from Tellus data
- Source possible reasons of poor relationship between stream sediment and top-soil data from the Tellus Border survey

The majority of samples collected were float and stream sediments, with bedrock samples examined for lithological analysis and recognition. The initial stages of exploration were centred on streams flowing perpendicular to the major NE trending faults. Stream sediment collection facilitated panning of material and analysis for any potential sulphides. However, this was complicated by the high concentration of fine mica which is hard to distinguish from sulphides with any degree of certainty. Surrounding float material exhibited fine disseminations of pyrite. All rocks showing signs of mineralisation were sampled and sent for analysis. The majority of float material was made up of quartz, both from quartzite formations and veins hosted in the surrounding lithology. The quality of exposure was variable, as the majority of outcrop was highly weathered. Despite this, the topography provided a good indication of the underlying geology. The quartzite formations tend to form distinctive ridges in the landscape due their hardness, whereas schists and pelites are less evident. The target area has frequent small disused quarries, mainly within the schists and dolerites, and these localities were a priority focus for mapping and sampling. A full summary of all observed lithologies is provided in Table 33, along with field maps (see Appendix).

Formation	Lithology	Description
Upper Crana Quartzite Form.	Banded pelites and psammities	Varied from fine laminations associated with pelite layer (2cm) to thicker beds (20cm) of psammitic units. Quartz veins common and mineralised in places with minor pyrite. Mineralised veins roughly parallel to bedding, which is heavily folded.
	Quartzite	Appears white in colour due to near pure quartz mineralogy. Minor dissemination observed, but very rare. Vuggy quartz veins common and barren. Tend to form distinctive ridges in landscape.
	Psammite	Greater thickness than pelites, but of similar composition. Mineralogy predominately quartz with minor biotite and feldspar.
Termon Form.	Pelite	Very finely laminated, with gentle folding. Quartz veins common throughout, often oblique to bedding or parallel along fragmented platy layers in pelite. Sulphide mineralisation found throughout formations, predominately as disseminations.
	Psammite	Thicker bedding units to pelite, and coarser more granular texture. Finely laminated in places with minor disseminations of pyrite and

		arsenopyrite.
	Schist	Highly variable texture and grain size. Finely laminated but coarser than pelitic unit. Small lens of quartz common feature.
Slieve Tooley Quartzite Form.	Quartzite	Almost pure quartz composition, making unit highly resistant to erosion. Quartz veins occur in multiple orientations and barren.
	Psammite	More variable composition, with higher feldspar mineralogy. Quartz veins mineralised at contact with dolerite pods.
Meta-dolerite	Basalt	Very fine grained and featureless. May appear chloritised on surface. When formed as minor dykes and sills can have characteristic onion skin weathering and chilled margin
	Dolerite	Found mainly as large pods within meta-sediments with variable grain size and mineralogy. Coarser samples contain greater concentration of feldspars. Vein mineralisation massive in places, with mix of pyrite, chalcopyrite and pyrrhotite.
Glencolumbkille Pelite Formation	Pelitic schist	Dark in colour with very fine grained texture. Large quartz veins crosscut laminations, appear barren but heavily hematized in places.
Boultypatrick (Grit) Formation	Psammite	Poorly sorted with minor clasts of quartz material. Shows minor disseminations of arsenopyrite and pyrite.
Gaugin Quartzite Formation	Quartzite	Pale quartzite with thick bedding and consistent mineralogy.
	Psammite and pelite schist	Grading in grain size forming coarser psammite to finer pelite units. Composition variable with feldspar and biotite content. Large quartz veins commonly barren but with possible minor arsenopyrite.

Table 33: Summary of mapped units within the Glenties area.

Vein hosted and disseminated sulphides were found throughout the field area, with certain formations being more prospective than others. The best example of vein host mineralisation was identified in a small disused quarry within a pod of dolerite to the south of the area. The mineralisation here, like with most examples, consists predominately of pyrite with minor amounts of chalcopyrite and arsenopyrite. In certain places the associated blue to green copper staining can be seen where the sulphide hosted copper has been oxidised Figure 27. The pyrite is found both massive and fine, with the most common occurrence being at the outer edges or contact of the vein with the host rock. The samples show weak magnetisation which may indicate minor pyrrhotite in places. When veining is irregular and fragmented, narrow stringers of host material are commonly included and it's there that fine crystals of pyrite can be found. Disseminations are the most frequent occurrence of mineralisation, and are found predominately within pelitic and psammitic schist formations such as the Termon formation and Upper Crana Quartzite formation. The light metallic colour indicates arsenopyrite, an observation which supports the high As values from the stream sediment survey. Interestingly, As anomalies are not evidenced in the top-soils.



Figure 27: photographs displaying the two forms of mineralisation in the Glenties region, with the top showing vein host sulphides and bottom showing disseminations. Both photos taken from dolerite quarry to the south of the area.

The low As levels found in the top-soils may relate to the local environment being predominately thick peat, with composition not fully reflecting the underlying lithology. There are no signs of major sources of contamination, with bog and farm land the main features in the landscape. The relationship between vein hosted mineralisation within the dolerite and meta-sediments is important as it may represent a significant phase of veining with associated mineralisation. If a genetic link can be found it may lead to identification of a major episode of mineralisation. A method of determination is to compare the orientation and potential controls on veining through the use of stereonet and detailed structural mapping (Figure 28). Structural analysis was carried out within the dolerite quarry to the south of the target area, as it provided the best exposure. The results show dominant sets of joints have a correlation with quartz veining, however the joints may have formed due to a period of deformation or during cooling. The major faults in the area trend to the NE and SW which is well correlated with sets of joints and veins, which may imply a genetic link between the veining and large scale deformation.

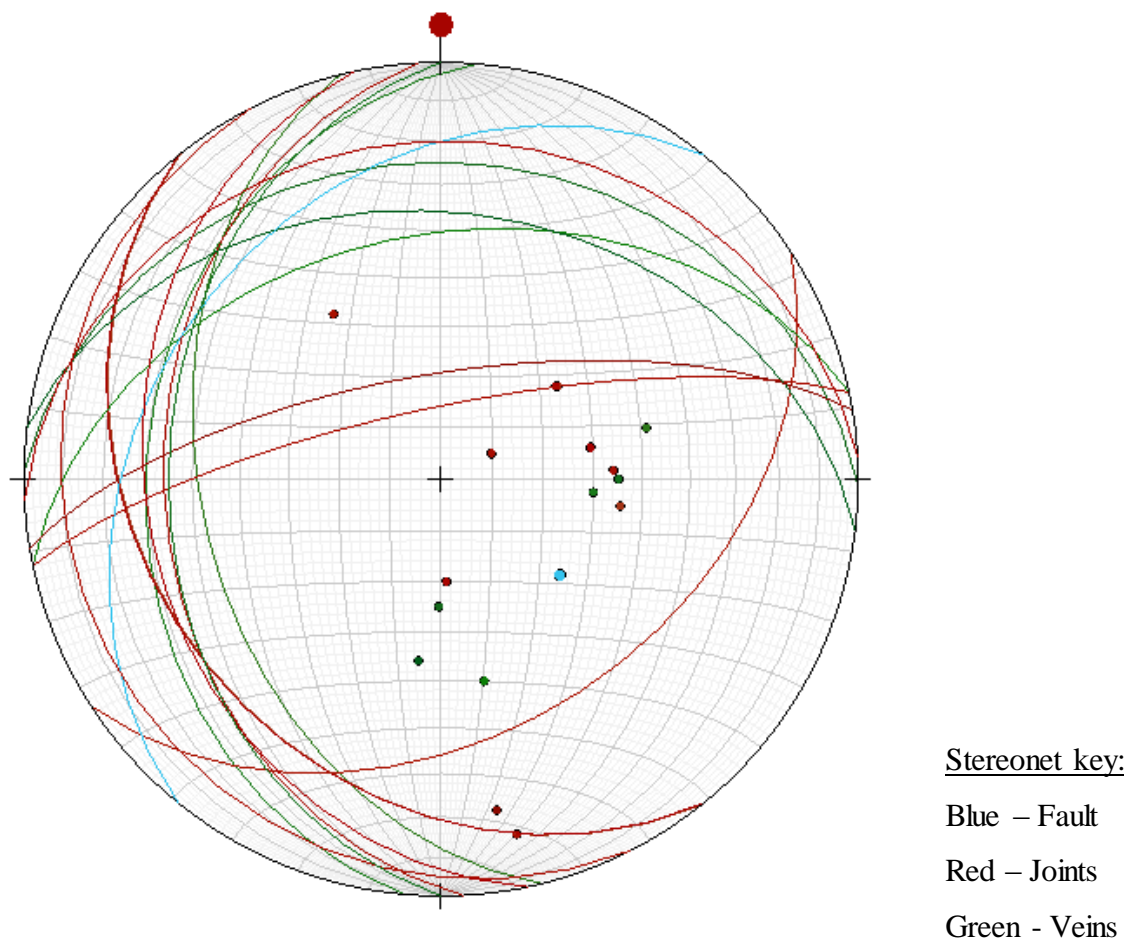


Figure 28: Stereonet of the main structural features within pod of dolerite within the Glenties target.

6.2.5. Results

The collected samples were spread over the target area with specific areas designated from reconnaissance trips and based on theoretical sources of mineralisation. Due to the good outcrop, bedrock samples were common, but it should be noted that exposure was variable depending on lithology, leading to potential preferential sampling of more resistant lithologies. The results of analysis were highly promising with a good range of anomalies in target elements such as Au and Ag, in both stream sediment and whole rock samples (Table 34, Figures 29 and 30). The majority of initial stream sediment results were positive (samples 028-055, Table 34), with samples exhibiting Au values of between 1 and 10 ppm, where <10ppm is the upper limit of detection. The high Au values are complemented by strong data for Ag, Pb, As and Sb. The wide variety in geochemical anomalies is encouraging and suggests provenance in mineralisation. The upper end anomalies for Pb suggest the presence of galena, which may be associated with high Ag values in the data. From the whole rock dataset, two samples stand out and for contrasting styles of mineralisation. The first, sample OM-13-PS-032, is significant as it has the highest Au values of any whole rock sample in each of the four target areas, with 2.43 ppm Au. The sample was taken from a large boulder of vein material within a narrow mountainous stream, which suggests low distance from source. The boulder is composed of large quartz vein, with surface alteration of predominately hematization. Field observations at the time noted a fine grey mineral interstitial within the quartz, originally thought to be magnetite but later disproved with lack of response to a magnet. Other possible minerals included galena due to its relatively high density. This theory can now be supported with high Pb values of >2000 ppm, however, other potential minerals include tetrahedrite with impurities of Ag, Pb and Au which could explain the higher than average values of Cu. Other questions posed during fieldwork included the composition of fine disseminations within pelite and schist units, at the time arsenopyrite was suggested and can be loosely backed up with the data as schist units mainly from float material show elevated concentrations of As but not in the upper end category of anomalies. This may be due to the fine grained and disperse nature of the disseminations.

SAMPLE	Type	Lithology	grams weight	ppm Au	ppm Ag	ppm As	ppm Cu	ppm Hg	ppm Mo	ppm Pb	% S	ppm Sb	ppm Zn
OM-13-PS-027	Bedrock	quartz	343	<0.001	0.43	0.7	119	0.03	1.13	47.1	0.15	0.14	61
OM-13-PS-029	Float	grano-diorite	375	<0.001	0.03	1	9.4	0.02	1.71	18.8	0.22	<0.05	48
OM-13-PS-031	Float	quartz	109	<0.001	0.05	9.5	5.2	0.02	0.33	2.6	0.29	0.1	7
OM-13-PS-032	Float	quartz	17	2.43	67.8	27.8	144	0.38	0.4	2090	0.23	<0.05	8
OM-13-PS-034	Float	pelite	460	<0.001	0.22	5.6	24.8	0.03	0.46	26.4	0.2	0.11	54
OM-13-PS-038	Bedrock	quartz	1223	0.068	0.13	59.3	26.2	0.01	0.21	6	0.27	0.21	36
OM-13-PS-040	Bedrock	quartz vein	166	0.02	0.05	<5	14.8	0.01	0.11	5.3	0.02	0.31	9
OM-13-PS-041	Float	meta basite	292	0.097	2.33	25.7	5440	0.06	0.24	5.3	0.76	<0.05	117
OM-13-PS-043	Float	schist	921	0.016	0.43	116.5	12	0.05	0.87	56.4	3.68	5.6	70
OM-13-PS-045	Bedrock	schist	412	0.007	0.1	3.2	80.1	0.07	0.78	6.6	2.06	0.18	99
OM-13-PS-047	Float	schist	454	0.013	0.09	83.5	380	0.09	0.41	6.4	0.83	5.17	121
OM-13-PS-048	Float	psammite	35	<0.001	0.07	8.3	35.4	0.06	0.26	8.9	0.11	0.08	51
OM-13-PS-050	Bedrock	gritstone	308	0.001	0.07	8.4	14.1	0.04	1.97	10.9	0.68	0.13	24
OM-13-PS-056	Bedrock	quartzite	1140	0.002	0.11	33.1	7.9	0.04	0.33	10.6	0.64	0.09	14
OM-13-PS-033	Float	quartz	501	0.008	0.24	33.3	107	0.06	0.39	12.7	1.07	0.93	45
OM-13-PS-130	bedrock	quartz	24	0.011	0.04	0.3	21.4	<0.01	0.49	3.4	0.01	0.29	15
OM-13-PS-131	bedrock	quartz	126	0.003	<0.01	1	6	<0.01	0.31	1.9	0.01	0.39	4
OM-13-PS-132	bedrock	quartz	297	0.001	0.36	13.8	4.6	0.01	0.31	22.5	0.11	0.64	42
OM-13-PS-133	bedrock	quartz	528	0.001	0.37	6.1	36.3	<0.01	0.21	12.6	0.08	0.48	58
OM-13-PS-137	bedrock	quartz vein	111	0.002	0.04	1.3	109	<0.01	0.43	1.7	0.03	0.2	10
OM-13-PS-143	bedrock	schist with q vein	158	0.001	0.03	0.9	11.9	<0.01	0.2	15.4	0.02	0.2	17
OM-13-PS-144	float	quartz vein	268	0.04	0.12	4990	16.4	0.01	0.41	29.3	0.58	1.74	18
OM-13-PS-146	bedrock	coarse schist	42	0.003	0.08	10.6	22.6	<0.01	0.58	10.5	0.39	0.17	71
OM-13-PS-147	bedrock	quartz vein	117	0.786	7.34	20.7	>10000	0.03	0.45	5.9	3.67	0.26	73
OM-13-PS-148	bedrock	vein with dolerite	133	0.086	0.1	4.7	219	<0.01	0.31	0.9	0.03	0.4	34
OM-13-PS-149	bedrock	quartz vein	116	0.001	0.01	1.9	5.5	<0.01	0.23	<0.5	0.02	0.07	<2
OM-13-PS-150	bedrock	psammite/pelite	165	0.002	0.04	1.8	21.2	<0.01	0.8	6.2	0.9	0.67	143

SAMPLE	Type	Lithology	grams weight	ppm Au	ppm Ag	ppm As	ppm Cu	ppm Hg	ppm Mo	ppm Pb	% S	ppm Sb	ppm Zn
OM-13-PS-151	bedrock	psammite	127	0.001	<0.01	5.2	5.6	<0.01	0.18	1	0.04	0.12	5
OM-13-PS-152	float	psammite	286	0.003	0.15	8	211	<0.01	0.2	14.8	0.77	0.14	75
OM-13-PS-153	bedrock	quartz vein	20	0.007	0.09	15.2	47.4	<0.01	0.61	112	0.6	0.76	38
OM-13-PS-182	float	psammite	274	0.001	0.05	1.7	8.1	<0.01	0.19	26.8	0.21	0.31	62
OM-13-PS-185	bedrock	quartz vein	50	0.008	0.12	21.5	24.1	<0.01	0.63	3.5	1.41	1.37	16
OM-13-PS-188	float	quartz vein	256	0.004	0.62	17.7	26.5	<0.01	0.34	13	0.97	1.15	17
OM-13-PS-192	float	quartz vein	211	<0.001	0.01	1.4	1.1	<0.01	0.18	<0.5	0.04	0.4	2
OM-13-PS-200	float	quartz vein	148	0.002	0.04	5.3	11.7	<0.01	0.31	<0.5	0.16	0.37	6
OM-13-PS-204	float	quartz vein	103	0.712	50.1	65.9	71.6	0.08	0.36	3420	2.79	0.67	5

SAMPLE	Type	Grain size	grams weight	ppm Au	ppm Ag	ppm As	ppm Cu	ppm Hg	ppm Mo	ppm Pb	% S	ppm Sb	ppm Zn
OM-13-PS-028	stream sed	fine-coarse	107	0.8	0.14	35.7	23.8	0.02	0.56	126.5	0.06	1.63	227
OM-13-PS-030	stream sed	fine-med	380	>10.0	1.03	82.6	26.3	0.04	0.81	301	0.07	0.54	216
OM-13-PS-035	stream sed	med-coarse	258	8.07	1.19	118.5	63.2	0.15	1.27	696	0.2	1.73	383
OM-13-PS-036A	stream sed	med-coarse	201	>10.0	3	113.5	67.3	0.21	0.44	875	0.17	2.94	163
OM-13-PS-036B	stream sed	coarse	177	>10.0	1.28	111	40.9	0.08	0.32	470	0.17	1.13	150
OM-13-PS-037	stream sed	fine-med	195	>10.0	9.46	143.5	85.6	0.26	0.95	1050	0.1	1.97	252
OM-13-PS-042	stream sed	medium	393	>10.0	6.43	180.5	116	0.4	0.63	1590	0.16	3.22	187
OM-13-PS-044	stream sed	coarse	420	>10.0	2.31	38.2	104	6.88	0.43	1100	0.1	1.68	145
OM-13-PS-046A	stream sed	fine-med	473	2.62	0.96	39.5	41.6	0.15	0.4	315	0.06	0.48	105
OM-13-PS-046B	stream sed	med-coarse	420	3.84	0.58	53.6	49.9	0.07	0.49	365	0.08	1.39	177
OM-13-PS-053	stream sed	fine-med	700	2	0.26	17.2	20.3	0.02	0.96	55.3	0.02	0.15	73
OM-13-PS-054	stream sed	med-coarse	520	1.39	0.1	27.6	24.7	0.02	0.81	84.3	0.04	0.12	94
OM-13-PS-055	stream sed	med-coarse	332	4.83	0.32	45.7	23.9	0.05	0.66	214	0.03	0.52	124
OM-13-PS-183	stream sed	fine to coarse	127	1.325	0.26	7.3	14.8	0.05	0.26	65.5	0.09	0.34	95
OM-13-PS-184 A	stream sed	fine to coarse	129	0.209	0.2	2.2	16	0.06	0.19	15.9	0.1	0.25	142

SAMPLE	Type	Grain size	grams weight	ppm Au	ppm Ag	ppm As	ppm Cu	ppm Hg	ppm Mo	ppm Pb	% S	ppm Sb	ppm Zn
OM-13-PS-184	B stream sed	fine to coarse	173	0.531	0.04	2.1	19.2	0.01	0.18	13.8	0.11	0.39	144
OM-13-PS-186	stream sed	fine to coarse	124	4.59	0.32	16.9	18.3	0.05	0.46	146	0.07	0.38	136
OM-13-PS-187	stream sed	fine to coarse	122	4.06	1.53	29.6	18.3	0.13	0.66	226	0.1	0.55	147
OM-13-PS-189	stream sed	fine to coarse	213	2.76	2	20.1	12.6	0.35	0.55	75.6	0.06	0.71	139
OM-13-PS-190	stream sed	fine to coarse	134	0.588	0.09	10.8	13.4	0.03	0.37	54.5	0.04	0.32	78
OM-13-PS-191	stream sed	fine to coarse	123	3.7	2.23	26.8	18.7	0.08	0.91	243	0.1	0.26	305
OM-13-PS-194	stream sed	medium-coarse	280	1.145	0.71	13.4	14.4	0.04	0.54	80.6	0.06	0.33	151
OM-13-PS-195	stream sed	medium-coarse	254	2.58	0.97	14.6	15.2	0.03	0.49	168.5	0.04	0.3	150
OM-13-PS-196	stream sed	medium-coarse	362	1.52	0.25	28.5	12.6	0.03	0.53	117.5	0.08	0.31	157
OM-13-PS-197	stream sed	fine to coarse	326	0.089	0.04	18.3	13.8	0.01	0.52	23.7	0.05	0.25	144
OM-13-PS-198	stream sed	fine	284	0.14	0.29	12.4	8.9	<0.01	0.37	26	0.08	0.23	86
OM-13-PS-199	stream sed	fine to coarse	258	0.271	0.97	16.7	15.9	0.04	0.68	53.1	0.04	0.45	147
OM-13-PS-201	stream sed	fine to coarse	246	3.07	0.05	23.5	13.2	0.02	0.56	45.9	0.03	0.35	159
OM-13-PS-202	stream sed	fine to coarse	229	0.745	0.05	12.2	9.3	0.02	0.38	28.4	0.02	0.18	88
OM-13-PS-203	stream sed	fine to coarse	265	0.479	0.15	23	6.7	0.02	0.45	41.1	0.03	0.55	82
OM-13-PS-205	stream sed	coarse t med	152	1.23	0.05	28.2	13.3	0.03	0.77	46.9	0.05	0.8	145
OM-13-PS-206	stream sed	fine to coarse	343	0.095	0.06	16.4	59.5	0.03	0.85	16.4	0.03	0.19	130
OM-13-PS-207	stream sed	coarse t med	271	0.122	0.04	17.2	10.4	0.06	0.77	25.2	0.01	0.16	116
OM-13-PS-208	stream sed	fine to coarse	187	2.21	0.21	31.5	23.2	0.03	1.59	130.5	0.02	0.57	141
OM-13-PS-209	pan conc.	fine to coarse	51	2.89	1.45	52.3	24.5	0.11	0.4	267	0.03	0.52	129
OM-13-PS-210	pan conc.	fine to medium	107	0.759	0.04	17.9	7.5	0.05	0.37	44.7	<0.01	0.14	83
OM-13-PS-211	stream sed	fine to medium	445	1.655	0.17	14.2	14.2	0.02	0.74	58.9	0.02	0.2	117
OM-13-PS-212	stream sed	coarse to medium	177	0.277	0.03	14.4	10.8	0.01	0.62	32.7	0.02	0.19	121
Total number of samples = 71													
soil samples = 0													
sediment samples = 35													
whole rock samples = 36													

Table 34: The results of analyses for new samples collected within the Glenties targets.

Figure 29: Map showing location of new samples taken in the Glenties target

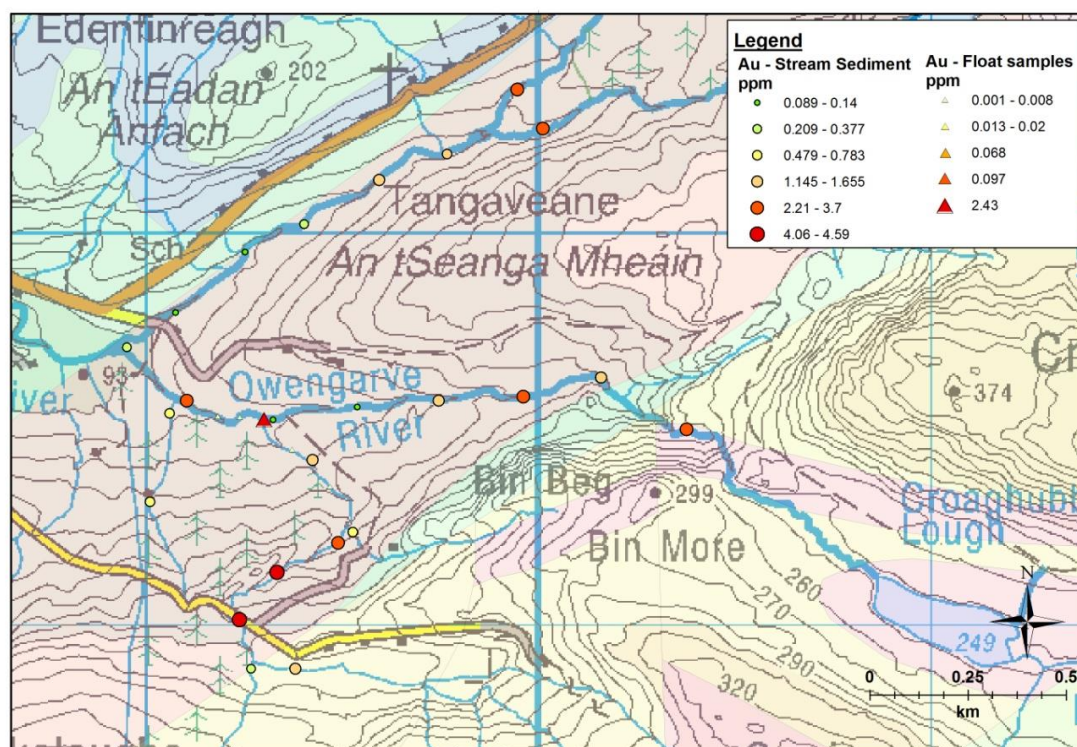


Figure 30: Map displaying location of significant Au anomalies in the Glenties target

Follow up fieldwork involved a high resolution stream sediment sampling profile to develop further understanding of the spatial distribution of anomalies and provide statistical validity to any results. The secondary focus was to follow up on Au bearing boulder (032) defined during the initial sampling, including boulder mapping and greater description aimed at delineating a source. The stream sediment grids were developed for two main rivers and several tributaries, to the NW of Silver hill. Sample spacing was set at 200 m, and a total of 24 samples were collected (183-212, Table 34). The streams were at a much higher level during the second phase of fieldwork, making access to material more difficult. The procedures used during collection were the same as with the first sampling phase.

The results as shown above (Figure 30) further the areas potential for Au mineralisation with strong values seen throughout the area. The relationship between Au, Ag and Pb appears strong in the data, with this relationship also noted in float samples showing galena occurring with pyrite (Figure 31). This relationship may indicate the presence of argentiferous galena, with minor gold occurring within pyrite. However, high levels of Te may have originated from minor gold tellurides which can be commonly found in many Au deposits. Au tellurides have the potential to host Ag and Pb, in minerals such as petzite or sylvanite. XRD analysis is required to confirm the mineralogy.

Other results of interest show the potential for a completely different style of mineralisation. The quartz veins occurring within dolerite pods contain significant Cu with values in excess



Figure 31: Quartz vein sample OM-13-PS-032 containing pyrite with minor galena

of 5000 ppm (OM-13-PS-041) and >10000 ppm (OM-13-PS-147). Field observations noted abundant sulphide mineralisation with high surface tarnishing, with the resulting iridescence colour being attributed to bornite. Other elements concentrated in sample 147 include Ag and Au with values of 7.8 and 0.7 respectively, with elements such as Se, Te, Pd and In also showing elevated concentrations.

The new data indicates that the two areas have great prospectivity. Float mapping and boulder tracing in the vicinity of sample 032 should be a starting point for any future exploration. Further stream sediment sample analysis would benefit from the collection of a finer fraction, as the coarse nature of samples collected thus far may mean that the material is more representative of till than local geology. The continuity of Cu mineralisation associated with dolerite pods in the SW should be tested.

6.3. Millford

6.3.1. Introduction

The Millford target area is located adjacent to the town of Millford in NW Donegal (Figure 32). The town is approximately 15 km north of Letterkenny. The main road between Millford and Letterkenny is the R245. Mulroy bay is located directly to the north.

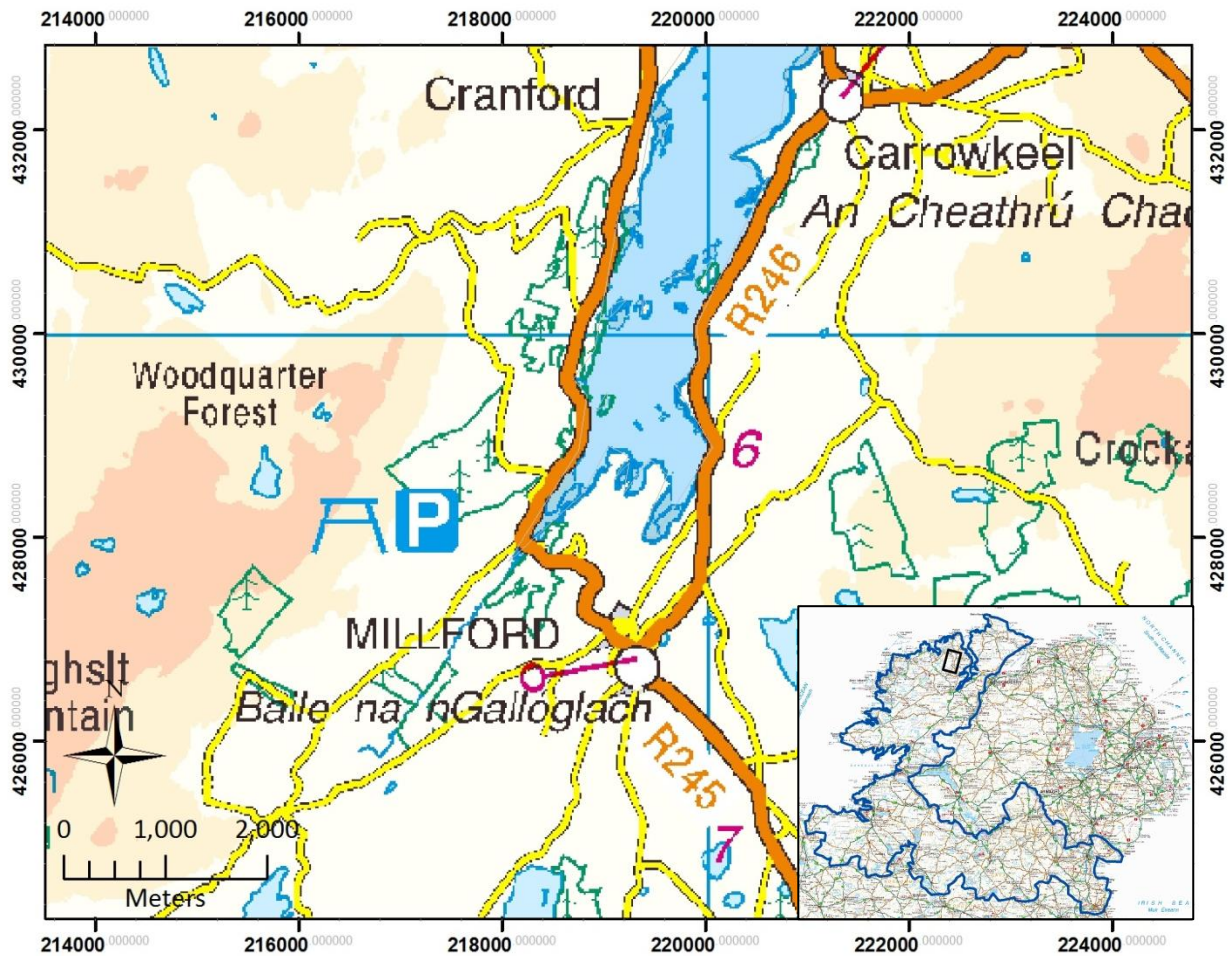


Figure 32: Locality map of the Millford target area, with a sub-set of its location within the border region

6.3.2. Local geology

The geology is dominated by Dalradian meta-sediments, the majority of which are associated with the Argyll group. The meta-sediments are intruded by linear meta-dolerites and meta-gabbros, altered to hornblende type facies. The meta-sediments are made up of several formations, including banded semi-pelitic and psammitic schist of the Termon Formation, and quartzite with pebbly beds associated with the Slieve Tooley Quartzite formation (Figure 33). Minor formations occur with slight variations in grain size and composition. Quartz veins are noted throughout the meta-sediments, commonly containing traces of pyrite and chalcopyrite. The structural geology is dominated by the NE-SW faults that run through western Donegal. These features show a variety of trends, with several sets of faulting evident. Similar to other target areas, the faulting is the most likely conduit for the flow of mineral rich fluids. The lack of geophysical data for the region means that any evidence for a deep seated structure is based on published work.

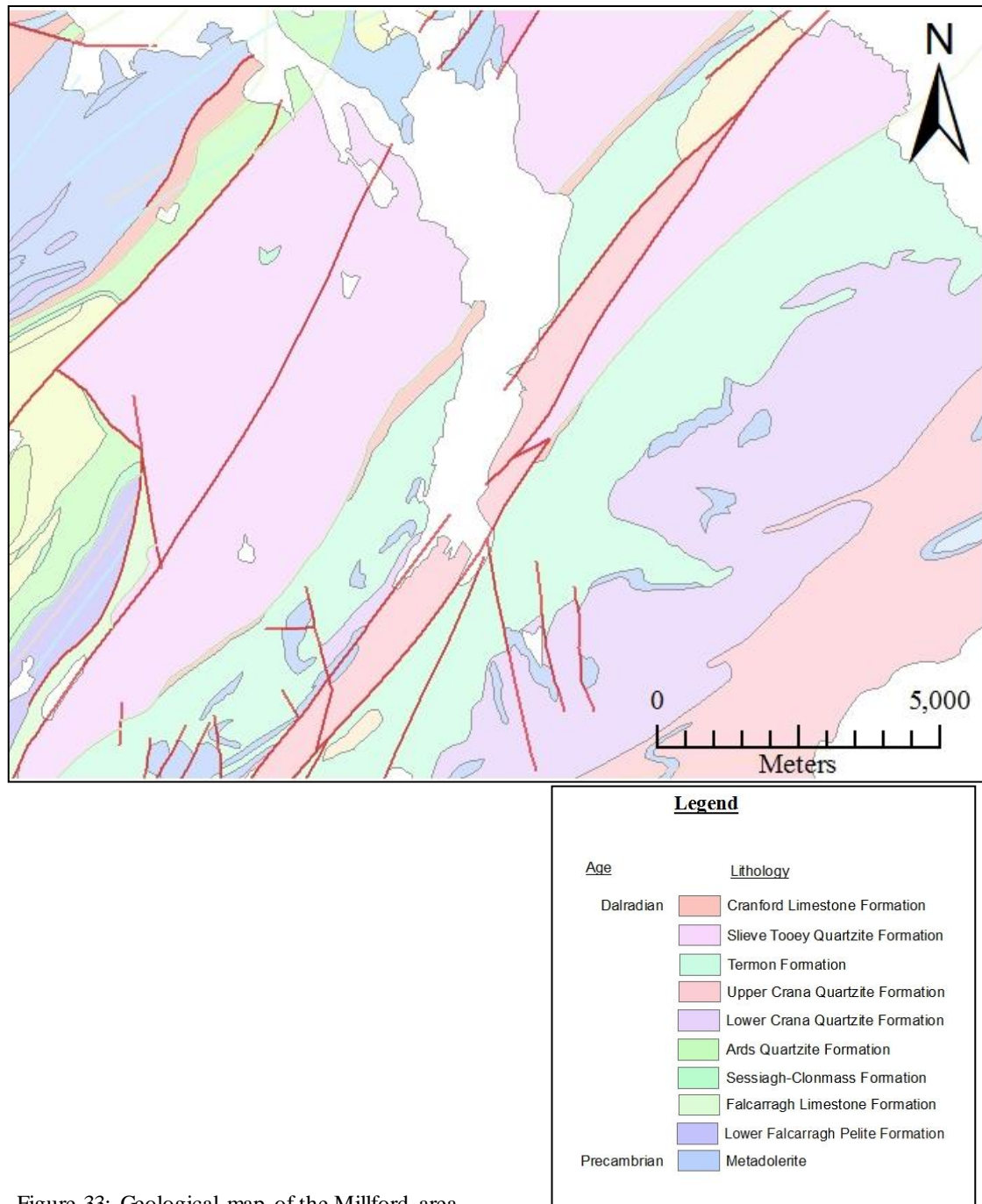


Figure 33: Geological map of the Millford area

As represented in Figure 34, the dominant orientation for glacially derived material is north-south. From the map there appears to be a switch in glacial movement, this was taken into account when planning the follow up work.

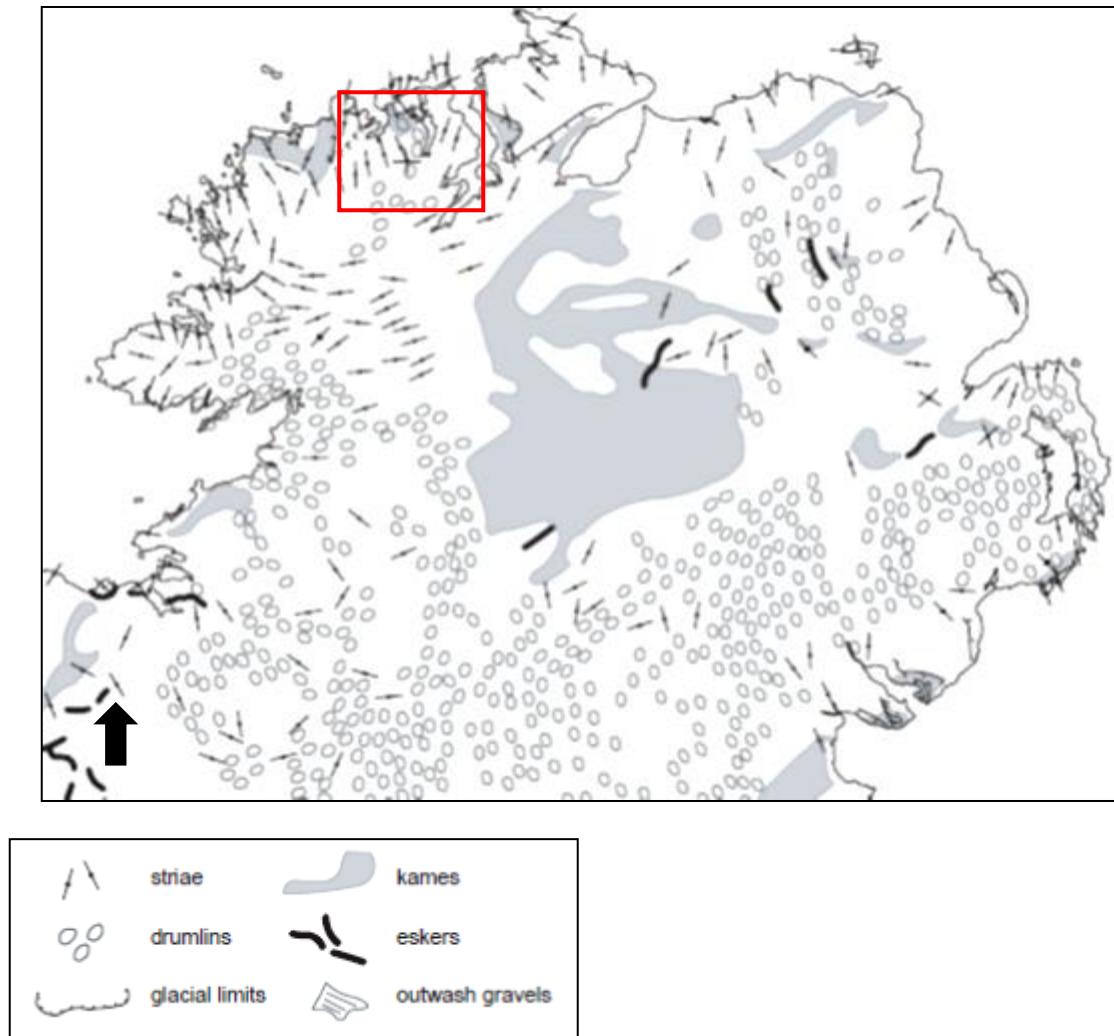


Figure 34: Map displaying the trend of glacial movements in Millford, with the dominant orientation being NNW-SSE and NNE-SSW, shown by drumlins and Striae. (Clark, 2008)

6.3.3. Existing data analysis

6.3.3.1. Knowledge driven Exploration

The Millford area appears highly prospective based on the empirical evidence. The large NE-SW trending faults are the main feature, with comparable structures and geology here as in known gold producing regions. The evidence suggests this locality is ideal for Au exploration. The main factors include:

- Large NE-SW trend faults
- Cross cutting of smaller oblique trending faults in NNW-SSE orientation
- Dalradian age lithologies
- Known occurrences of quartz veining and sulphide mineralisation

6.3.3.1. Data Driven Exploration

When analysing the whole dataset in GIS the area stands out due to its high anomalies for base metals and Au pathfinder elements within top-soils. The values, while raised, are not exceptional for any individual element, but the consistency of high values is what is rare about this target area. The typical Au pathfinder elements are strong, with base metals such as Cu-Zn-Pb also yielding good results (Table 35). Therefore, when analysing the data for this locality, both Au pathfinder elements and base metals were looked at separately. The main reason for this is that the different element groups will most likely have had separate genesis, however, at this point a relationship between these two groups of elements should not be ruled out.

Summary of Millford target area:					
	Element	Overall average (ppm)	Target area average (ppm)	Max	Min
Top-soil	As	6.50	7.88	37.19	0.03
	Ag	0.08	0.21	0.71	0.5
	Hg	0.10	0.13	0.25	0.05
	Sb	0.35	0.32	0.96	0.11
	Mo	1.38	1.31	2.54	0.49
	Zn	54.23	95.00	978.00	13.00
	Pb	25.83	44.04	207.63	11.79
	Cu	22.66	22.18	70.68	2.55
	MnO	461.72	382.76	1266.52	51.35
	Cd	0.41	1.07	14.80	0.11
	<i>Other selected elements with significant difference.*</i>	Elevated: Ba, Ce, La, Th,	Depleted: Sr, Be, Rb, Ni		
Stream Sediment	As	15.24	23.73	60.20	4.50
	Mo	2.12	1.64	2.50	0.90
	Ag	0.28	0.24	0.50	0.10
	Sb	0.82	0.91	2.50	0.20
	Cu	26.86	35.42	179.30	12.70
	Zn	141.37	195.05	491.90	65.30
	Pb	30.67	36.95	165.80	15.50
	Cd	0.79	0.63	2.80	0.10
	MnO%	0.51	1.39	3.85	0.36
	<i>Other selected elements with significant difference.*</i>	Elevated: Fe ₂ O ₃ %, Co, Nd, Sn, I, Be, Ce	Depleted: Zr, Br, Cr, Cl, S		

Table 35: Summary table of Tellus Border geochemical data for the Millford target area

The top-soil data indicate the most positive results and will be reviewed first. The sample locations are evenly spaced, typically 4 km² (Figure 35). The outline for the target area encompasses 33 km² and was generated to include all significant anomalies for both stream sediments and top-soil data.

As is evident from Table 36, the anomalies present are significant, especially when compared with the averages for the total dataset. A couple of samples should be highlighted for their high multi-element values, such as 580537A and 580444A, both lie on the margins of the Termon Formation. The former shows the greatest potential, good correlation exists between

Ag and As, this is typical of many Au bearing deposits found in Tyrone, Northern Ireland. A correlation matrix will indicate if this relationship is pervasive throughout the area.

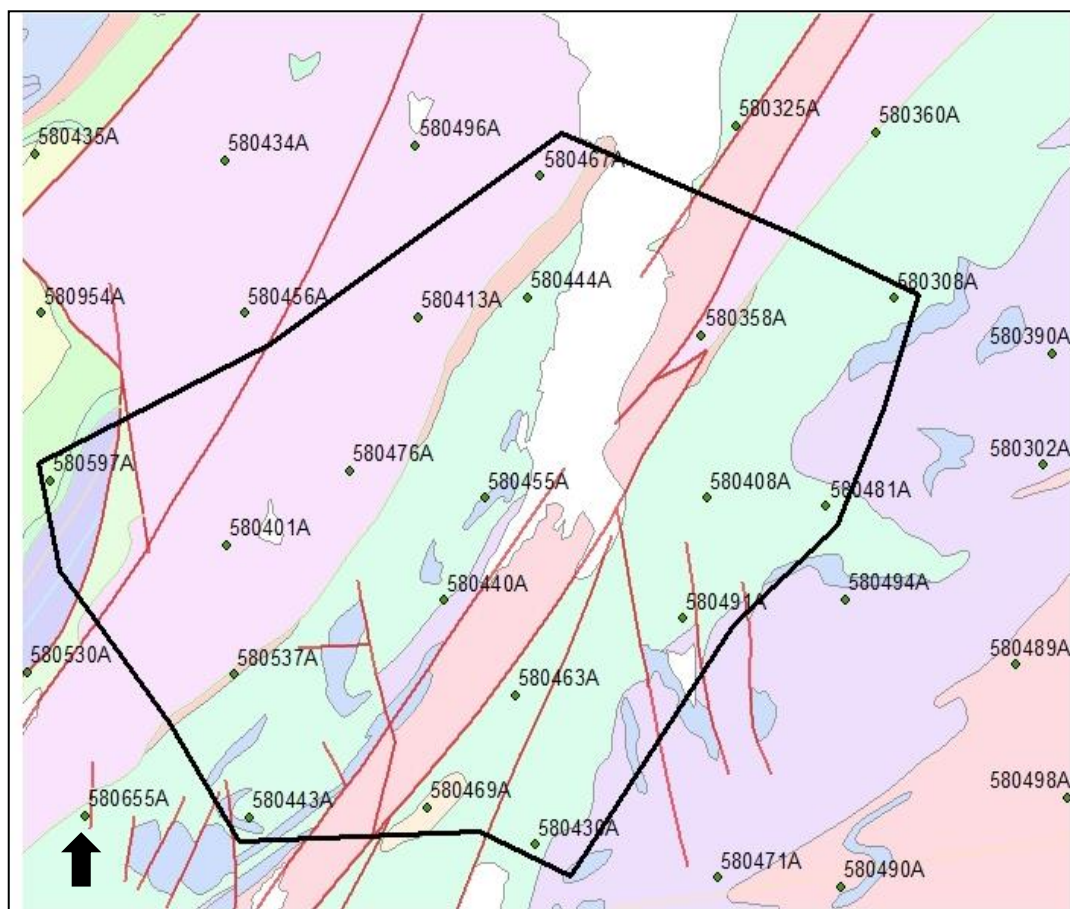


Figure 35: Location map of top-soil samples in the Millford target area.

Sample_ID	Ag_mgkg	As_mgkg	Hg_mgkg	Sb_mgkg	Mo_mgkg
580467A	0.09	7.6068	0.22	0.29	1
580444A	0.33	14.0783	0.2	0.33	2.54
580413A	0.12	1.1353	0.25	0.41	1.04
580358A	0.25	15.0028	0.09	0.23	0.92
580308A	0.25	0.5	0.1	0.17	0.49
580481A	0.2	2.9843	0.09	0.13	1.56
580408A	0.18	3.9088	0.16	0.59	1.44
580455A	0.03	2.0598	0.12	0.32	0.67
580476A	0.07	2.0598	0.15	0.63	0.59
580497A	0.12	4.8333	0.07	0.23	0.76
580401A	0.27	2.0598	0.19	0.96	0.52
580440A	0.13	15.9273	0.05	0.37	2.11
580491A	0.37	4.8333	0.1	0.21	2.21
580463A	0.11	4.8333	0.09	0.14	1.78
580537A	0.71	16.8518	0.16	0.26	0.84
580443A	0.11	2.0598	0.12	0.23	1.52
580469A	0.1	37.1908	0.13	0.11	1.52
580430A	0.31	3.9088	0.08	0.21	2.04

Table 36: Summary table of Au pathfinder elements in top-soils for the Millford target area.

	<i>Ag_mgkg</i>	<i>As_mgkg</i>	<i>Hg_mgkg</i>	<i>Sb_mgkg</i>	<i>Mo_mgkg</i>
<i>Ag_mgkg</i>	1				
<i>As_mgkg</i>	0.208	1.000			
<i>Hg_mgkg</i>	0.007	-0.137	1.000		
<i>Sb_mgkg</i>	-0.059	-0.243	0.447	1.000	
<i>Mo_mgkg</i>	0.212	0.480	-0.241	-0.355	1.000

Table 37: Correlation matrix for Au pathfinder elements in the Millford top-soils

The correlation matrix yields a mixture of positive and negative associations (Table 37). The relationship highlighted above, between As-Ag, shows a weak positive correlation, with the best correlations noted for Mo-As and Hg-Sb. The negative correlations appear to reveal a divide in the data between Hg-Sb and As-Ag-Mo. This suggests that sources for these anomalies are separate and may be related to differing styles of mineralisation.

The same process of analysis was carried out for the main base metal pathfinder elements, they are Cu-Zn-Pb-Cd-Mn. Table 38 shows the summary for each sample location. A potential point of interest is to look at the similarity in anomalous values for the two highlighted sample points (580537A and 580444A) across base metal and Au pathfinder elements.

Sample_ID	Zn_mgkg	Pb_mgkg	Cu_mgkg	Mn_mgkg	Cd_mgkg
580467A	15.00	19.69	26.47	116.13	0.28
580444A	48.00	43.77	70.68	263.15	0.61
580413A	17.00	51.14	9.14	273.12	0.19
580358A	61.00	169.46	29.01	194.21	0.18
580308A	13.00	11.79	4.27	66.30	0.16
580481A	64.00	16.51	19.58	435.92	0.21
580408A	21.00	27.69	9.64	111.98	0.30
580455A	22.00	18.15	4.88	51.35	0.21
580476A	28.00	25.78	2.55	51.35	0.39
580497A	45.00	15.06	19.17	518.98	0.11
580401A	37.00	39.14	19.88	54.67	0.55
580440A	99.00	24.05	55.67	672.64	0.29
580491A	78.00	33.87	22.32	1117.01	0.16
580463A	74.00	27.87	34.99	1266.52	0.22
580537A	978.00	207.63	10.15	225.77	14.80
580443A	14.00	22.60	5.29	77.10	0.17
580469A	38.00	13.06	12.99	459.17	0.21
580430A	58.00	25.42	42.59	934.28	0.28

Table 38: Summary of base metal pathfinder elements from top-soil data for the Millford target area

Similar to the Au pathfinder elements, it is easy to spot good correlation of high values across multiple elements. Sample 580537A again shows the highest values for a number of elements, however, Cu appears anomalously low which may be a reflection of its mobility, or the style of mineralisation. The anomalously high Cd levels could be linked to high Zn, the two elements have a known geochemical relationship in the surface environment. The relationship between pathfinder elements is largely positive (Table 39). Specifically, Zn-Cd shows the strongest correlation, with Zn showing strongly positive correlations with all other elements, particularly Pb. These relationships will be analysed through further sampling. In terms of potential styles of mineralisation, the base metals and gold could be

contemporaneous which has implications when analysing the other target areas. This applies specifically for Glenties as it sits on the same structural lineament.

	<i>Zn_mgkg</i>	<i>Pb_mgkg</i>	<i>Cu_mgkg</i>	<i>Mn_mgkg</i>	<i>Cd_mgkg</i>
<i>Zn_mgkg</i>	1.000				
<i>Pb_mgkg</i>	0.609	1.000			
<i>Cu_mgkg</i>	0.359	0.179	1.000		
<i>Mn_mgkg</i>	0.475	0.021	0.681	1.000	
<i>Cd_mgkg</i>	0.727	0.635	0.000	-0.111	1.000

Table 39: Correlation matrix for base metal pathfinder element for the Millford target area.

The stream sediments do not yield comparable anomalies, but could provide vital clues as to the spatial distribution and validity of the data previously discussed. The stream sediment sample locations differ in area and spacing from the top-soil survey (Figure 36). The total number of samples located within the target area is larger than the top-soil survey, and there is sample clustering in places. Sample 584691C is located closest to sample 580537A (Figure 35). This sample does show elevated concentrations of certain elements, but not to the same degree as in the top-soil (Table 40). No other samples stand out, however, the area shows raised concentrations of all the major elements except for Ag which rarely registers above total data average.

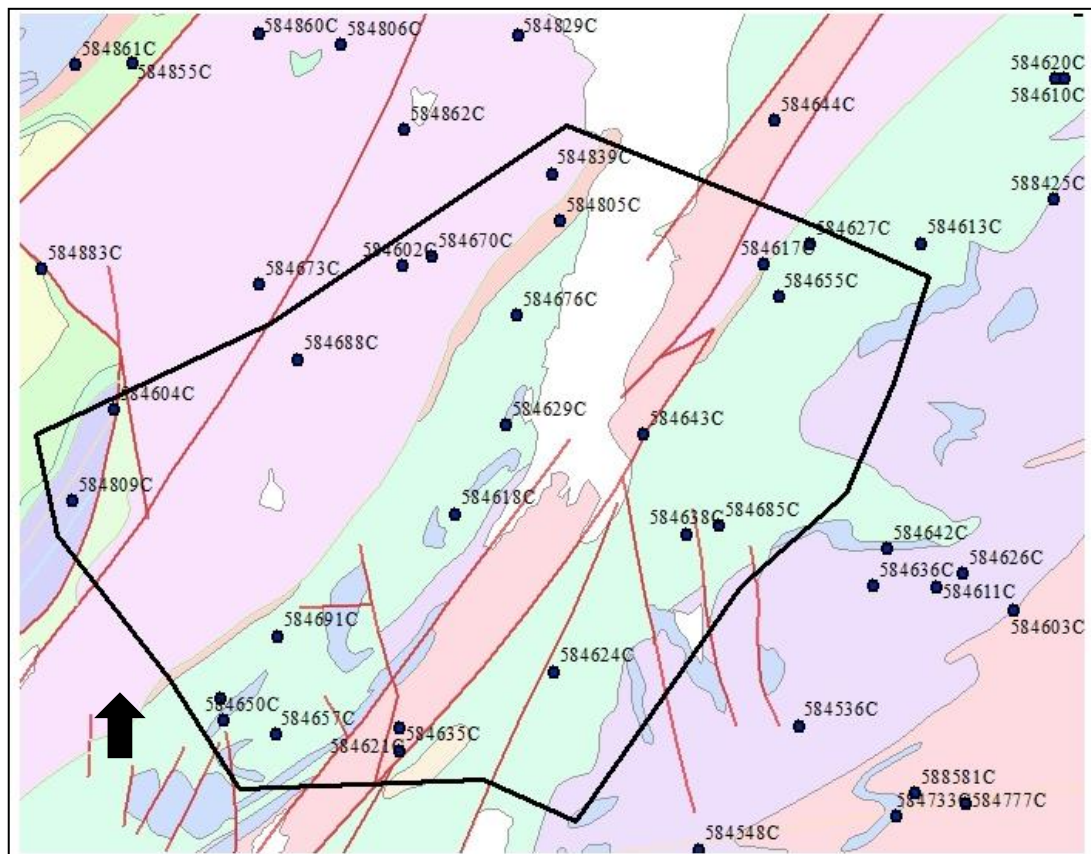


Figure 36: Location map of stream sediment sample points for the Millford target area

Sample_ID	As_mgkg	Mo_mgkg	Ag_mgkg	Sb_mgkg
584602C	18.4	1.4	0.1	0.8
584617C	36	1.8	0.25	0.5
584627C	12	1.7	0.25	0.7

584655C	17.9	2	0.25	0.9
584670C	25.9	1.9	0.25	0.9
584805C	27.5	1.6	0.25	1.2
584839C	11.8	1.3	0.1	0.5
584604C	6.5	1.5	0.3	0.5
584618C	31.9	1.5	0.25	1.2
584621C	60.2	2.4	0.25	1.4
584624C	4.5	1.4	0.25	2.5
584629C	17.5	1.2	0.25	0.8
584635C	35.9	2.5	0.25	0.5
584638C	21.9	1.2	0.25	0.5
584643C	14.2	0.9	0.1	0.2
584650C	31.4	1.8	0.5	0.7
584657C	48.8	2.1	0.25	0.8
584676C	13.8	2	0.25	1.7
584685C	5.5	1.6	0.25	0.8
584688C	45.3	1.8	0.25	0.5
584691C	27.7	1.2	0.25	1.8
584809C	7.4	1.2	0.2	0.6

Table 40: Summary table of base metal pathfinder elements from stream sediment data in the Millford target.

The correlation matrix (Table 41) displays different element relationships when compared with the top-soil data. The strongest correlations observed in the stream sediment data are Mo-Ag and Mo-As. This could be as a result of the solubility and mobility of each element being similar. Elemental mobility is the biggest determining factor in each elements concentration.

	As_mgkg	Mo_mgkg	Ag_mgkg	Sb_mgkg
As_mgkg	1.000			
Mo_mgkg	0.473	1.000		
Ag_mgkg	0.195	0.484	1.000	
Sb_mgkg	-0.026	0.277	0.355	1.000

Table 41: Correlation matrix of Au pathfinder elements in stream sediments for the Millford area.

The stream sediment base metal data show similarities with the top-soils (Table 42). Pb and Zn remain the highest anomalies. The strong consistency across many metals will be researched further to test for contamination.

Sample_ID	Cu_mgkg	Zn_mgkg	Pb_mgkg	Cd_mgkg	MnO_ %
584602C	19.1	92.2	19.5	0.2	0.435
584617C	28.6	197.5	35.1	0.25	1.447
584627C	38.8	178.5	23.6	0.8	1.055
584655C	29	150.9	21.2	0.1	1.085
584670C	12.7	146.9	24.1	0.5	3.088
584805C	18.6	162	37.7	0.2	0.417
584839C	14.9	73.6	15.8	0.3	0.362
584604C	29.1	491.9	68.9	1.4	1.436
584618C	24.5	216.1	22	1.3	1.926
584621C	23.9	224.2	26.5	0.5	2.66
584624C	97	211.6	165.8	0.2	0.562
584629C	20.7	198.3	31	0.7	1.495
584635C	23	248.4	20	1.1	2.054

584638C	34	245.6	26.5	1.1	1.775
584643C	26.3	123.1	25	0.5	0.591
584650C	179.3	173.6	15.5	0.1	0.722
584657C	36.5	188.9	23.1	0.3	1.205
584676C	26.5	348.9	27.1	2.8	3.845
584685C	23.2	169.7	22.5	0.7	2.446
584688C	12.9	65.3	35.3	0.1	0.672
584691C	31.2	241.5	103.2	0.5	0.84

Table 42: Summary table of base metal pathfinder elements for Millford

The expected base metal associations are observed in the correlation matrices, e.g. Pb-Zn-Cd (Tables 43 and 44). Several positive correlations exist, with Zn-Ag and Zn-Cd being the main ones. The high Zn levels are consistent throughout the area, making this target prospective for base metals such as Zn and Pb, with additional potential for Ag-Au mineralisation.

	<i>Cu_mgkg</i>	<i>Zn_mgkg</i>	<i>Pb_mgkg</i>	<i>Cd_mgkg</i>	<i>MnO_%</i>
<i>Cu_mgkg</i>	1.000				
<i>Zn_mgkg</i>	0.335	1.000			
<i>Pb_mgkg</i>	0.221	0.377	1.000		
<i>Cd_mgkg</i>	-0.197	0.660	0.021	1.000	
<i>MnO_%</i>	-0.132	0.591	-0.107	0.657	1.000

Table 43: Correlation matrix of base metal pathfinder elements in stream sediments for Millford

	<i>Zn_mgkg</i>	<i>Pb_mgkg</i>	<i>Cd_mgkg</i>	<i>Ag_mgkg</i>	<i>As_mgkg</i>
<i>Zn_mgkg</i>	1.000				
<i>Pb_mgkg</i>	0.293	1.000			
<i>Cd_mgkg</i>	0.698	-0.083	1.000		
<i>Ag_mgkg</i>	0.367	0.077	0.056	1.000	
<i>As_mgkg</i>	-0.133	-0.249	0.197	0.235	1.000

Table 44: Correlation matrix combining Au and base metal pathfinder groups in stream sediments for Millford.

The Tellus Border data for the Millford target make this a top locality in terms of prospectivity. There appears to be a good spatial correlation between base metal style and Au-Ag style mineralisation. This relationship was investigated through further fieldwork (Section 6.3.4). Key observations include:

- Relationship between Zn and other base metals + Ag
- Role of Mn in possible concentration of base metals
- Possible environmental source of enrichment of Zn and Cd

6.3.4. Fieldwork

The target area was originally selected on potential for Au and base metal mineralisation from predominately top-soil data. The area is the northern extension of the geological trend found in the Glenties target area. As with Glenties, the main NE trending faults are of greatest interest and formed the primary targets during further exploration. The main fieldwork objectives were:

- Further sampling and mapping in areas which yielded high anomalies, to aid geological interpretations
- In areas of good exposure complete detailed geological assessments and collect bedrock samples
- Carry out stream sediment sampling in areas of high geochemical anomalies
- Identify possible association of high geochemical anomalies with local bedrock, with greater attention to the potential for base metal mineralisation
- Compare and assess connection with Glenties target area in terms of structure and lithology

The initial objectives followed in the field where to target the high top-soil anomalies to identify either outcrop or signs of contamination. The location of sample 580537a was revisited but due to limited outcrop the bedrock source of the anomalies was not possible to confirm, however, there were no obvious signs of contamination. The surrounding area is dominated by vegetation and boggy ground, with dilapidated forest nearby. In order to counteract the poor exposure, stream sediments became the main method of exploration with samples taken from a nearby stream at intervals of around 100 m. The sampling was carried out alongside mapping, lithologies were found to vary perpendicular to the flow of the stream, ideal when targeting faults as a source of mineralisation. With time spent in the area the relationship between geology and landscape became clear, with steep mountain sides being controlled by the major NE trending faults.

The geology of the area has been previously described, but the fieldwork phase provided an opportunity to compare units along strike and investigate structural deformation. The similarity in formations made field identification more straight forward during the mapping phase of fieldwork. Table 45 provides a summary of the observed lithologies, and these are marked on the field map (see Appendix).

Mapped formation	lithology	Description
Termon formation	pelite	Fine grained unit with low grade metamorphism, easily identified with crenulation cleavage and abundant coarse cubes of pyrite along cleavage planes. Vein of quartz with minor pyrite, also associated with narrow veins rich in fluorite. Minor occurrences of calcite overprint quartz veins.
Slieve Tooey quartzite formation	quartzite	White colour and highly resistant nature make identification in the field straightforward. Commonly found as distinct ridges in the landscape. Minor black material along bedding planes exhibit abundant pyrite.
Meta-dolerite	Dolerite	Featureless fine grained dolerite, commonly found as pods within the Termon formation. Lithology rarely observed in outcrop, but commonly found as aggregate material on roadside.
Cranford limestone formation	Quartzite breccia	Thin units found associated with Slieve Tooey quartzites. Distinguished by fine clasts of predominately shale and feldspar in white quartzite. Pluck marks of surface relate to weathering out of less resistant clasts.
Lower Crana Quartzite formation	Mudstone	Fine grained with large bedding, shows no signs of mineralisation.

Table 45: Summary table of mapped lithologies in the Millford area.

Float samples were taken throughout the area, mainly from the roadside and stream beds. The samples of most interest were collected at a roadside location, with predominately quartz rich material containing abundant pyrite (Sample 095). The provenance of the samples is hard to delineate so sample results should be treated with caution. Mineralisation was commonly found throughout the area in both float and bedrock samples. Bedrock associated with the Termon Formation displays abundant pyrite, however the coarse cubic nature of the sulphide may indicate lack of key element concentrations. Other units showing the potential to host mineralisation include the Slieve Tooley quartzite which contains fine stringers of pyrite, having a strong similarity to stringer veins of known Au host lithologies found in Co. Tyrone. There was little evidence of vein hosted mineralisation, with minor occurrences within quartz lenses associated with schist and pelites units in the Termon Formation. Pyrite is the dominant sulphide but traces of chalcopyrite and arsenopyrite have been observed.

6.3.5. Results

The results show Millford to be highly prospective in relation to Au style mineralisation, with the majority of stream sediment values occurring above 10 ppm Au (Table 46; Figure 37). The highest values are all found within a single stream in the SW (Figure 38), which flows perpendicular to the NE faults, and over the dominant formations of the area: Slieve Tooley and the Termon. The Au values are supported by high values in pathfinder elements such as As (>200 ppm), Ag (<20 ppm), Hg (~3 ppm), Sb (~2 ppm) and above background concentrations of base metals, especially Pb. In many examples the Au values have reached the upper limits of detection at >10 ppm. However, semi-quantitative analysis carried out revealed Au levels up to 32 ppm. High levels of Pb indicate the presence of galena which is often associated with elevated Ag. Another potential host mineral includes arsenopyrite which is commonly found carrying Au. A further stream to the NE of the target area also yields raised Au and Pb in two panned concentrate and one stream sediment sample, this stream transects a similar geology to that in the SW (Figure 37). A similar relationship between Au and Pb was identified in the Glenties area which lies on the same structural trend. In order to validate the high values within stream sediment samples, evidence of source is needed within bedrock samples. However, no bedrock was collected proximal to the key stream sediment samples due to bad levels of exposure. Of the bedrock samples assayed, only one (158) indicates raised Au.

Two float samples indicate significant Cu values, 082 and 095, these are separated by over 5 km; one sample (082) was collected from the stream containing sediments with raised Au in the west of the target area (Figure 37).

SAMPLE	Type	Lithology	grams	ppm	ppm	ppm	ppm	ppm	ppm	ppm	%	ppm	ppm
			weight	Au	Ag	As	Cu	Hg	Mo	Pb	S	Sb	Zn
OM-13-PS-078	float	quartz vein	252	<0.001	0.03	2.3	5.1	0.01	0.63	11.6	0.02	0.26	11
OM-13-PS-082	float	pelite	42	0.01	0.18	5.5	444	0.04	0.37	4.3	3.29	0.4	85
OM-13-PS-085	float	dolerite	95	0.009	0.1	7	14.3	0.01	0.24	3.3	3.72	0.35	23
OM-13-PS-088	float	quartz vein	55	<0.001	0.04	0.5	16.5	0.01	0.27	11.3	0.22	<0.05	37
OM-13-PS-090	float	quartz vein	374	<0.001	0.04	0.9	25.7	0.01	0.22	20.2	0.75	<0.05	44
OM-13-PS-095	float	schist	852	0.012	0.25	10.6	861	0.03	0.49	13.1	4.06	0.21	56
OM-13-PS-097	Bedrock	schist	852	0.008	0.52	4.7	137.5	0.03	0.33	60.2	0.33	0.42	137
OM-13-PS-098	Bedrock	quartz lens	45	<0.001	0.03	2	55.9	0.02	0.38	4.6	0.06	<0.05	48
OM-13-PS-099	Bedrock	schist	88	0.005	0.22	0.2	54.6	0.02	5.09	21.6	0.16	0.36	95
OM-13-PS-100	Bedrock	schist	51	0.008	0.15	9.9	64.9	0.02	0.2	24.2	1.14	0.34	126
OM-13-PS-101	Bedrock	psammite	52	0.004	0.2	1.9	105	0.02	0.64	43.3	0.02	0.56	125
OM-13-PS-102	Bedrock	quartz vein	189	0.001	0.07	2.5	94.4	0.04	1.12	24.8	0.16	0.24	77
OM-13-PS-103	Bedrock	psammite	1557	0.002	0.34	8.6	382	0.05	0.4	32.4	0.63	0.61	165
OM-13-PS-105	Float	quartz vein	774	0.001	0.19	2.6	26.4	0.01	0.4	7.2	0.16	0.26	26
OM-13-PS-157	bedrock	schist	22	0.005	0.52	33	52.2	<0.01	4.48	29.9	1.28	0.26	90
OM-13-PS-158	bedrock	quartz vein	83	0.06	0.43	69.4	71.4	<0.01	4.01	24.1	1.99	0.64	102
OM-13-PS-159	bedrock	meta-basite	46	0.005	0.08	28.3	92.6	0.02	0.35	4.8	0.2	0.65	102
OM-13-PS-160	float	quartzite	427	0.001	0.04	<5	7.2	<0.01	0.15	6	0.59	0.66	28

SAMPLE	Type	Grain size	grams	ppm	ppm	ppm	ppm	ppm	ppm	ppm	%	ppm	ppm
			weight	Au	Ag	As	Cu	Hg	Mo	Pb	S	Sb	Zn
OM-13-PS-080	Stream sed	med to coarse	535	>10.0	37.2	456	46.1	4.65	1.38	1380	0.2	3.89	107
OM-13-PS-081A	Stream sed		286	>10.0	21	129.5	79.6	0.95	1.1	455	0.11	0.63	80
OM-13-PS-081B	Stream sed		237	>10.0	23.3	152.5	93.1	3.23	0.96	540	0.13	0.67	83
OM-13-PS-083	Stream sed		280	>10.0	35.8	214	71.5	5.37	0.67	865	0.15	1.61	76

SAMPLE	Type	Grain size	grams weight	ppm Au	ppm Ag	ppm As	ppm Cu	ppm Hg	ppm Mo	ppm Pb	% S	ppm Sb	ppm Zn
OM-13-PS-084	Stream sed		333	8.93	4.18	95.1	38.1	0.42	0.95	503	0.2	0.72	164
OM-13-PS-086	Stream sed	fine to med	424	3.44	1.06	64	19	0.1	1.67	63.1	0.04	0.23	108
OM-13-PS-087	Stream sed		351	2.48	1.01	71.8	17	0.11	1.49	82	0.04	0.26	163
OM-13-PS-089	Stream sed		494	1.095	0.13	50.9	31.1	0.05	1.55	49.3	0.02	0.34	149
OM-13-PS-091	Stream sed		401	2.27	0.1	36.8	57.6	0.06	0.97	94.6	0.03	0.15	210
OM-13-PS-093	Stream sed		449	0.548	0.14	13.3	63.4	0.85	1.81	524	0.05	7.11	278
OM-13-PS-096	Stream sed		335	0.177	0.15	12.4	20.2	0.08	1.11	29.9	0.01	<0.05	88
OM-13-PS-104	Stream sed		587	0.934	0.12	21.3	30.4	0.03	1.42	56.1	0.02	0.15	128
OM-13-PS-155	panned conc.	fine to med	32	5.12	0.17	15.5	26.2	0.06	0.68	114.5	0.06	0.37	93
OM-13-PS-156	panned conc.	fine to med	40	0.37	0.14	15.5	28.1	0.04	0.75	70.9	0.1	0.43	100

Sample ID	type	Weight	pH	pH (HCl)	ppm Au	ppm Ag	ppm As	ppm Cu	ppm Hg	ppm Mo	ppm Pb	% S	ppm Sb	ppm Zn
OM-13-PS-161	topsoil	1108	4.35	3.47	0.002	0.36	13.8	21.1	0.07	0.28	186	0.08	0.57	32
OM-13-PS-162	subsoil	801	4.82	3.8	<0.001	0.72	11.5	8.8	0.05	0.61	116.5	0.07	0.33	23
OM-13-PS-163	topsoil	803	4.83	4.43	0.004	0.18	47.7	12.1	0.21	0.77	88	0.4	0.49	41
OM-13-PS-164	subsoil	418	4.28	3.89	0.002	0.19	20.5	17	0.08	0.45	100.5	0.19	0.48	41
OM-13-PS-165 A	topsoil	380	4.71	4.29	0.002	0.58	19.9	14.5	0.28	1.13	101.5	0.5	0.46	114
OM-13-PS-165 B	topsoil	380	4.71	4.29	0.007	0.56	19.9	15	0.24	1.17	97.4	0.47	0.52	106
OM-13-PS-166	subsoil	534	4.3	4.01	0.001	0.49	17.2	12.7	0.21	0.76	60.1	0.53	0.4	179
OM-13-PS-167	topsoil	705	3.91	3.38	0.001	0.12	4.5	11	0.07	0.59	61.4	0.18	0.41	10
OM-13-PS-168	topsoil	980	5.73	5.94	0.003	1.65	123	43.5	0.37	1.02	2340	0.13	5.95	1330
OM-13-PS-169	subsoil	1160	6	5.26	0.002	0.83	138	56.3	0.25	1	1560	0.05	5.88	1280
OM-13-PS-170	topsoil	853	4.67	4.32	0.005	0.38	10.5	41.1	0.17	2.36	41.4	0.24	0.27	75
OM-13-PS-171	subsoil	604	4.79	4.45	0.005	0.35	12.4	40.3	0.19	2.07	41.1	0.3	0.4	76

Sample ID	type	Weight	pH	pH (HCl)	ppm Au	ppm Ag	ppm As	ppm Cu	ppm Hg	ppm Mo	ppm Pb	% S	ppm Sb	ppm Zn
OM-13-PS-172	topsoil	746	4.7	4.1	0.002	0.26	7.8	32.8	0.26	0.87	25	0.49	0.2	29
OM-13-PS-173	subsoil	681	5.14	4.65	0.001	0.25	4.8	40	0.27	0.81	19.3	0.68	0.18	29
OM-13-PS-174	topsoil	828	4.52	4.17	0.002	0.15	11.2	50.7	0.18	0.92	42.3	0.25	0.38	24
OM-13-PS-175	subsoil	720	4.6	4.18	0.003	0.13	11.7	47.8	0.17	0.66	41.2	0.3	0.36	22
OM-13-PS-176	topsoil	1213	4.89	4.33	0.003	0.29	18.4	92.5	0.22	2.7	31.3	0.27	0.44	47
OM-13-PS-177	subsoil	620	4.88	4.62	0.003	0.33	16.3	91.1	0.26	2.59	28	0.33	0.48	51
OM-13-PS-178	topsoil	804	4.54	4.2	0.004	0.61	27.9	90.8	0.24	3.54	42.2	0.31	0.61	42
OM-13-PS-179	subsoil	742	4.6	4.18	0.004	0.6	25.7	80.2	0.15	2.94	36.2	0.33	0.55	28
OM-13-PS-180	topsoil	605	4.4	3.88	0.003	0.15	12.3	24	0.09	1.99	25.2	0.07	0.28	26
OM-13-PS-181	subsoil	304	4.68	4.16	0.006	0.11	21.5	14.2	0.06	3.93	49.6	0.04	0.47	22

Total number of samples = 52
soil samples = 21
sediment samples = 13
whole rock samples = 18

Table 46: Results of analyses on samples collected in the Millford target area.

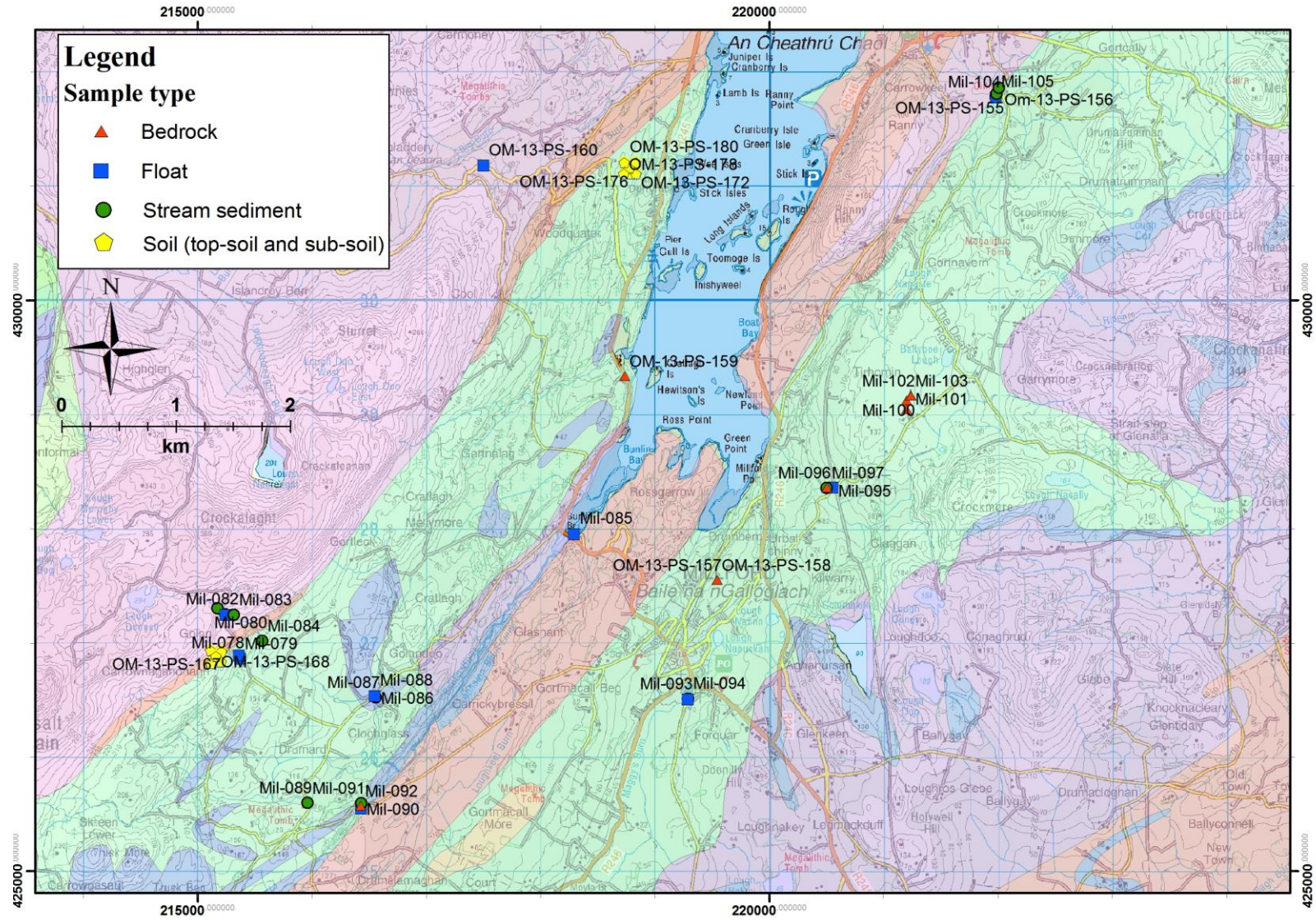


Figure 37: Map showing the location of new sample sites within Millford.

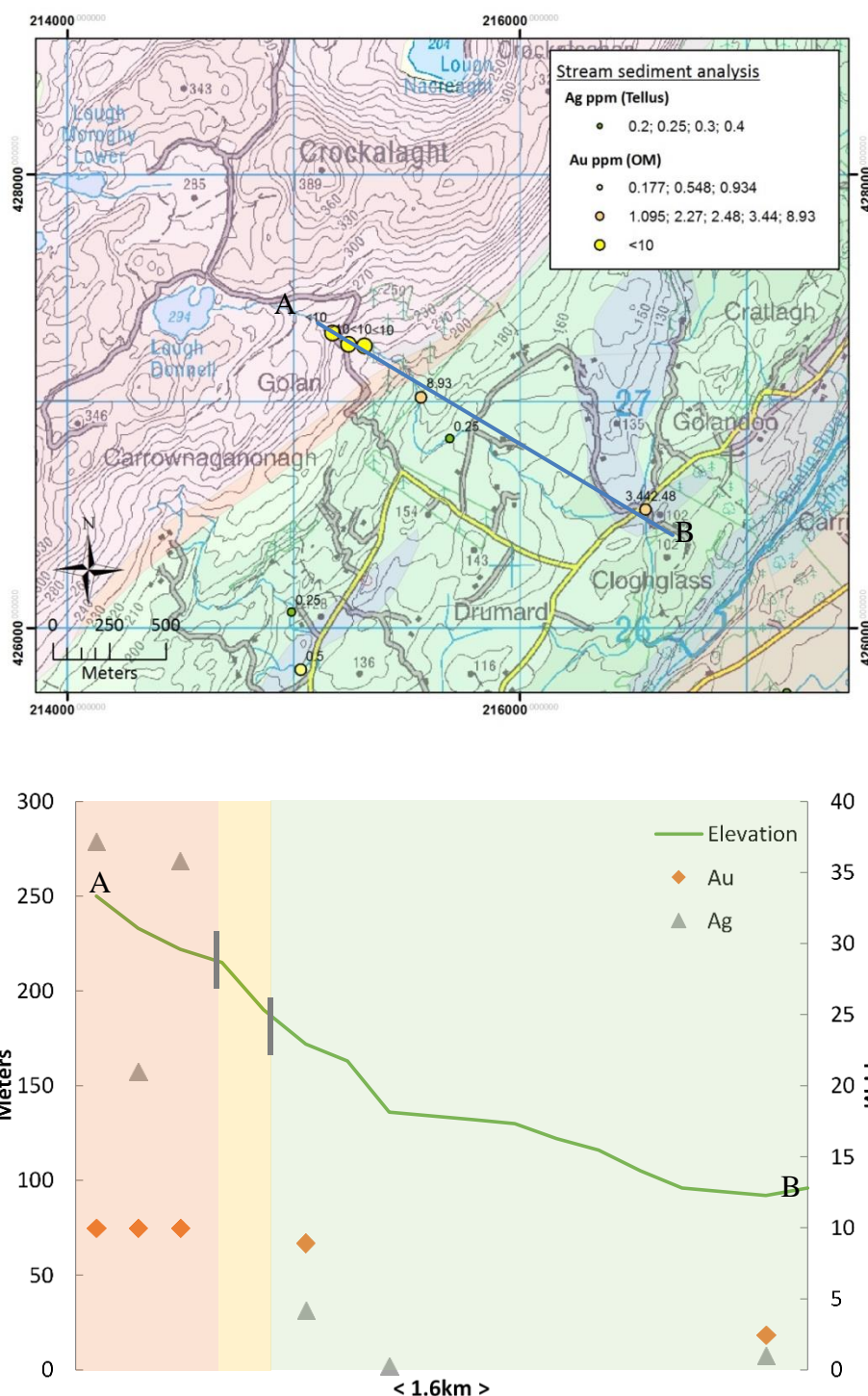


Figure 38: Sample locations of high stream sediment anomalies (top), with graphical representation of the data showing the overprint of topography and mapped lithology (bottom) .(<10 should read >10)

The main bedrock sample assayed was the Termon Formation, with the characteristic large cubes of quartz. The results show the pyrite to be largely barren (sample OM-13-PS-100), except for elevated values of Cu and Zn. Other float samples of the schist and pelite units reveal higher concentration of Cu with values >400 ppm, indicating the presence of chalcopyrite. The roadside aggregate material shows the highest values of Cu, upwards of 800 ppm, but as the origin is questionable no further investigation was carried out.

Two soil grids were developed on a 100 m spacing centred on high top-soil anomalies from the Tellus Border data, samples 580537 and 580444, which showed elevated concentrations of Ag, Sb, Ag and base metals Pb, Zn and Cu. At each sample location a top-soil and sub-soil sample was collected, with top-soil derived from 5-20 cm and sub-soil samples from 50 cm. In total, 21 samples were collected, with samples from each corner of a 100 m grid and also samples from the location of the highlighted Tellus samples. The ground conditions were predominately bog land, recent wet weather resulted in a high water table. An increased risk of side wall contamination due to wet conditions was noted during sample collection. The organic nature of the samples necessitated increased sample sizes to counteract weight loss during analysis. Acknowledging these factors, results for sub-soils should be interpreted with caution. A soil sample location has yielded comparable high element anomalies in both the top-soil and sub-soil portions. Both display high concentrations of Pb, Sb and Zn. Importantly, this soil site is close to Tellus Border sample 580537, which, as discussed earlier, yielded high Pb and Zn. These samples are found in close proximity to stream sediments containing notable Au concentrations (Figure 37).

When ranking the soil values based on the main pathfinder elements there is a clear relationship between pH and element levels (Figure 39). The surface environment determines pH with bogs pH ~4 and grassland pH~5.5, therefore, when analysing soil sample values knowledge of the local environment is critical. This relationship is likely to be the reason for low element values in the Tellus Border dataset across Co. Donegal (Section 4, Figure 9).

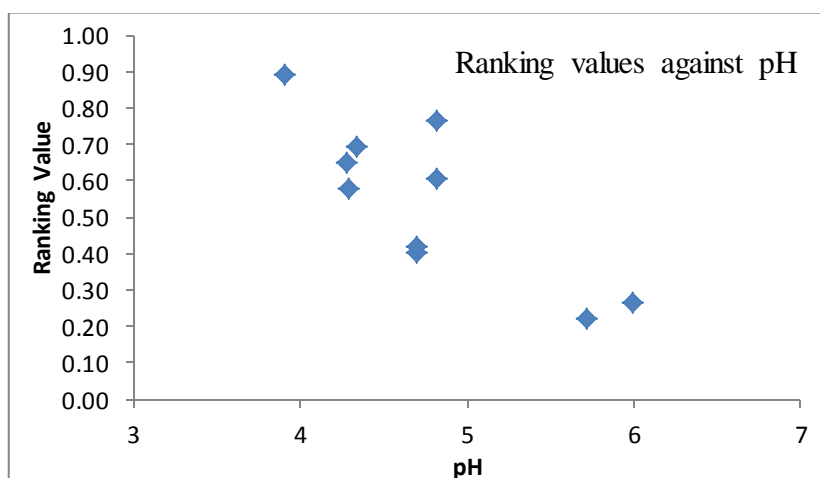


Figure 39: The relationship between ranked anomalies and pH for soil samples in Millford

In summary, the area around Tellus Border sample 580537 yielded a float sample with raised Cu, top-soil and sub-soil Zn and Pb anomalies and multiple stream sediments containing notable Au. This area straddles the Slieve Tooley and Termon Formations and is close to a major NE trending fault.

6.4. Shercock

6.4.1. Introduction

The Shercock target area is the furthest east, located in NW Cavan on the border with Monaghan just north of the town of Shercock (Figure 40). Large towns of Castleblaney and Carrickmacross are found to the east of the target area. Due to the surrounding large settlements, the road network is good and covers the entire area of interest. The geomorphology of Cavan and Monaghan is dominated by rolling drumlins divided by small loughs and streams. The majority of the fieldwork was carried out on the Monaghan side of the border.

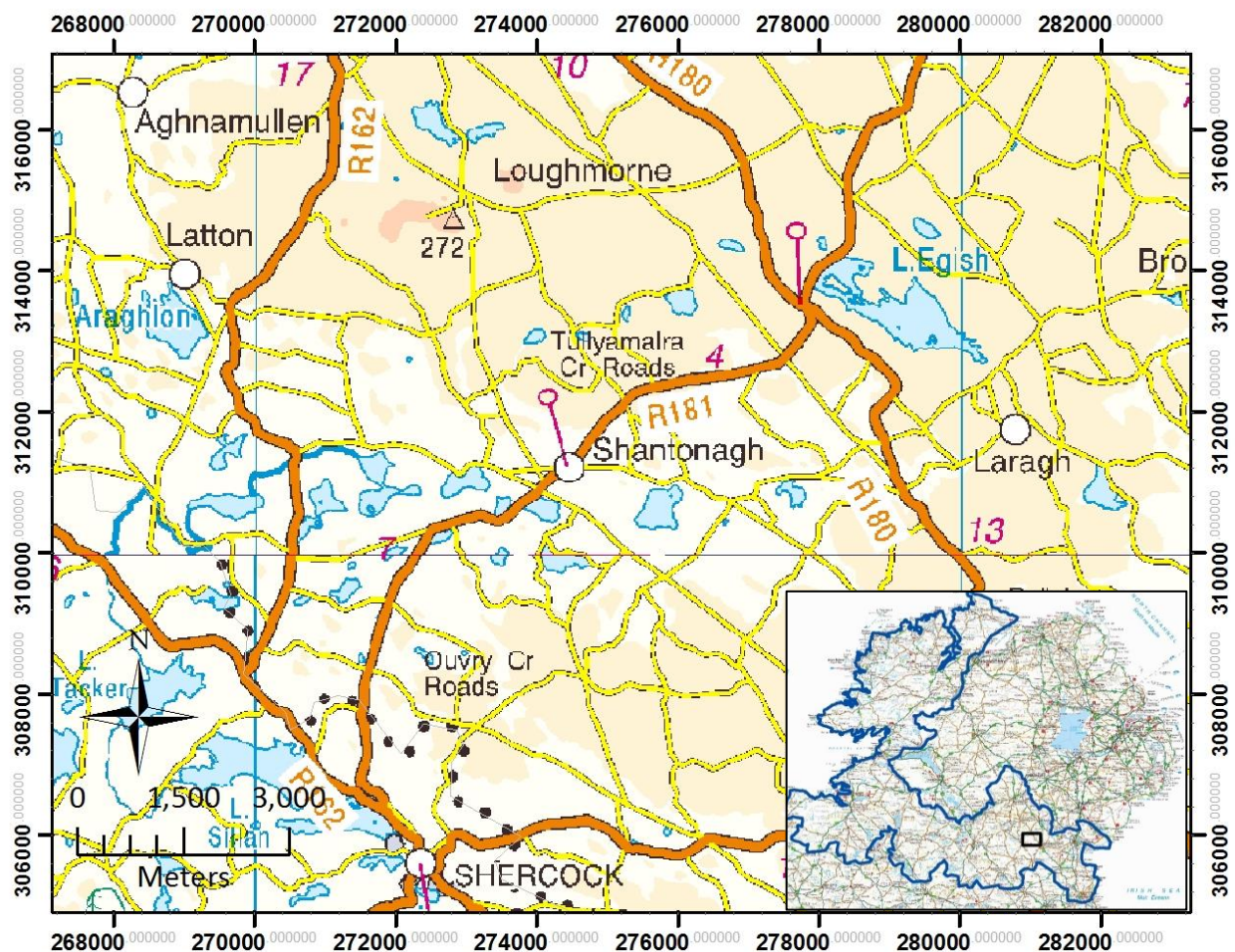


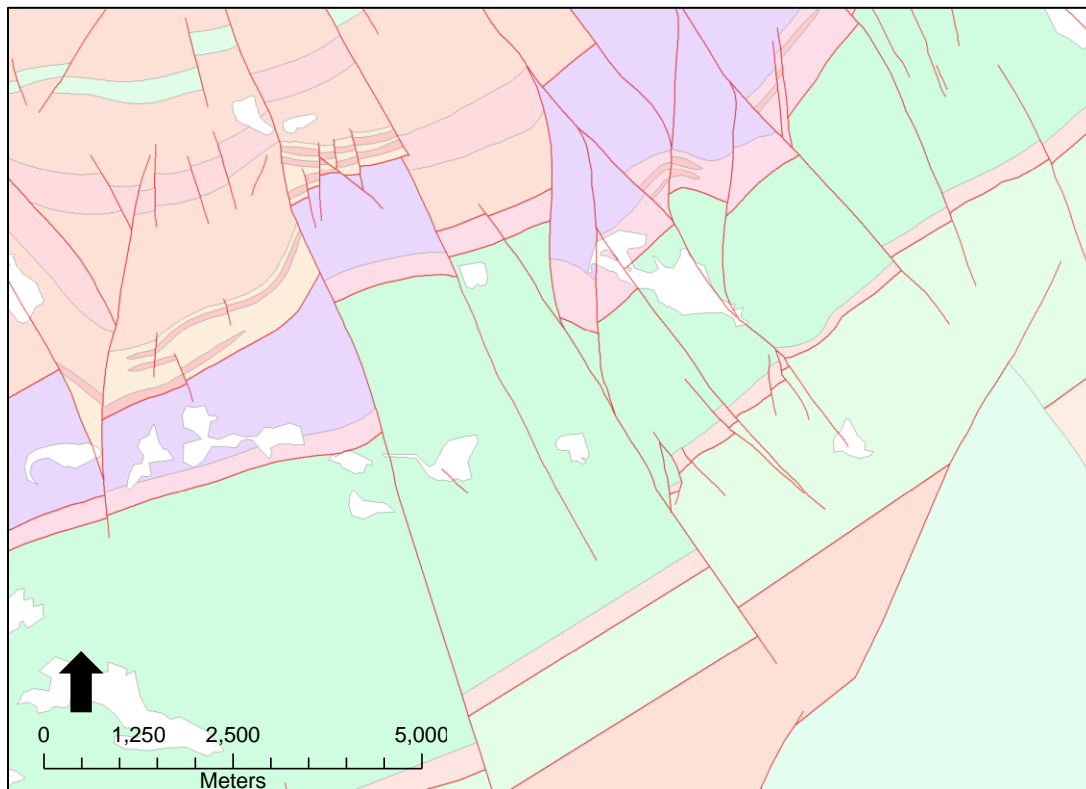
Figure 40: Locality map of the Shercock target area, with a sub-set map of its location within the border region.

6.4.2. Local Geology

The local geology is dramatically different from that of the other targets, in terms of lithology and age. The area is dominated by Lower Palaeozoic sediments of the Longford-Down Massif, primarily turbidite facies mix with fine grained mudstones and shales. Volcanics are found in the form of mafic tuffs, mainly interbedded with black shales of the Carrickree Formation (Figure 41). To the SE of the map lies the Kingscourt fault which shows rocks of

younger age from the Triassic. They are predominately sandstones and gritstones, with old gypsum workings found within them.

The structural geology contains two principle fault orientations, to the NE and NW. There is no age control for the faults, so they cannot be put in context with other faulting of similar orientation across the border region. However, cross cutting relationships suggest that faulting to the NE occurred first. Evidence of mining activity to the north, past and present, can be seen at Clontibret and Castleblaney. Clontibret is known for mineralisation of Au-Sb, with the potential for mining activity in the future. Castleblaney is known for old workings of Pb-Ag, with many adits in the area. These factors need to be considered when carrying out any analysis.



<u>Legend</u>	
<u>Age</u>	<u>Lithology</u>
<u>Lower Paleozoic</u>	Carrickatee Formation
	Castlerahan Formation
	Kehernaghkilly Formation
	Laragh Formation
	Lough Avaghon Formation
	Mullanalt Member
	Oghill Formation
	Shercock Formation
	Taghart Mountain Formation
	Volcanics

Figure 41: Detailed Geological map of the Shercock target area

The glacial maps (Figure 42) indicate that material located within the target area may have been partially shifted from the NW. This would imply that the known mineralisation to the north could have influenced anomalies in the area.

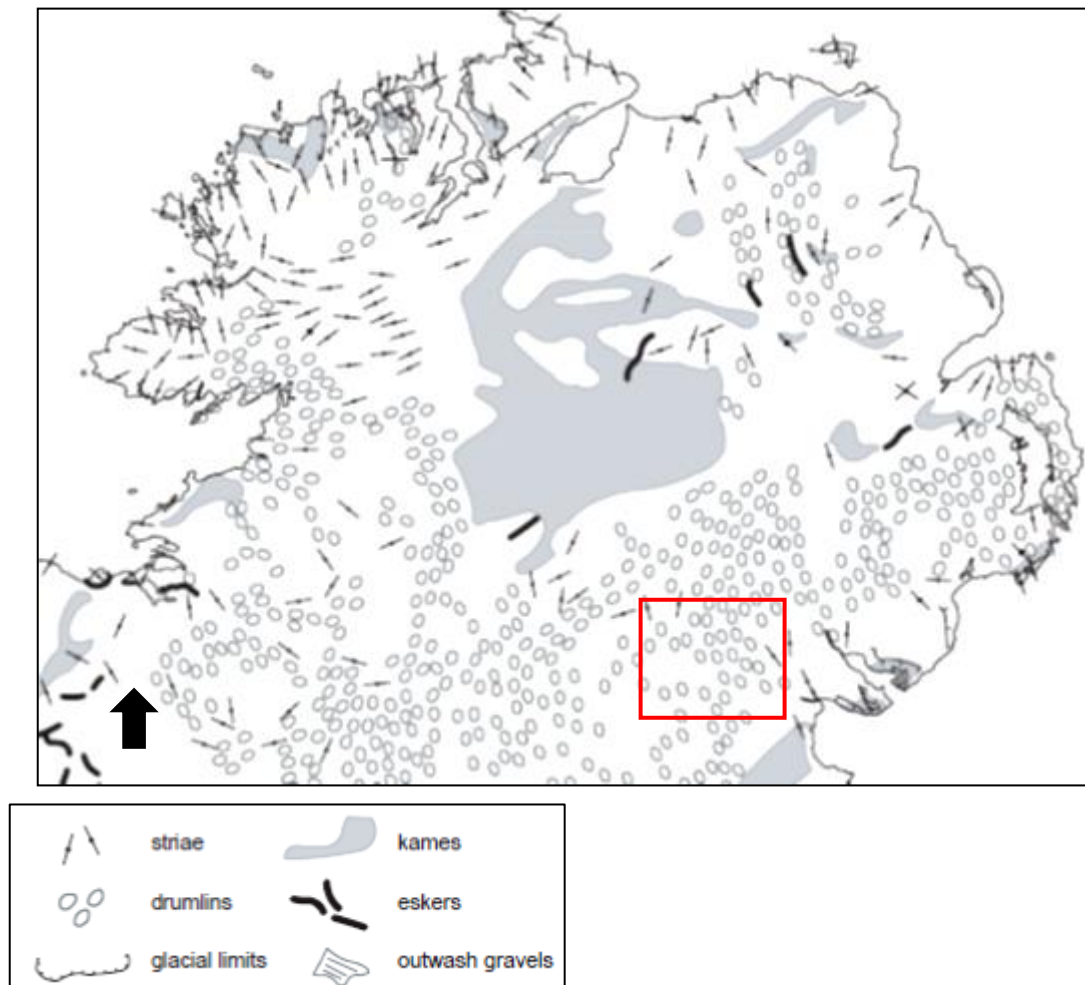


Figure 42: Map displaying the trend of glacial movements in the Shercock target, with the dominant orientation being NNW-SSE. (Clark, 2008)

6.4.3. Existing data analysis

6.4.3.1. Knowledge Driven Exploration

When identifying potential sites for exploration, the areas which yield greatest potential tend to be located near to known areas of mineralisation. The nearby mineral deposits at Castleblaney and Clontibret were used as a model to follow, and a close comparison can be made between features found at the two locations and at Shercock.

Key features at Clontibret and Castleblaney:

- Major NW trending faults
- Minor faults running parallel to major faults
- Regional NE trending lineaments
- Sandstone to turbidite type facies

Key features at Shercock:

- Major NW trending faults
- Minor faults running parallel to major faults
- Turbidite type facies
- No known mineral occurrences in area

The models from each site will be taken into account during the data analysis phase.

6.4.3.2. Data Driven Exploration

The data from both top-soil and stream sediment samples show high anomalies within the 80.2 km² region (Table 47), especially to the north around Clontibret. The size of these anomalies overshadow the more subtle high values found at Shercock. The stream sediment data demonstrate similar trends in areas adjacent to Shercock, such as the Bailieborough area to the south which indicates high Ag values. Considering the styles of mineralisation in areas to the north, a range of elements were included in the detailed analysis. The principle element anomalies that resulted in this area being considered were top-soil and stream sediment As, Ag, Cu, Sb and Zn values. These relationships are looked at in more detail. The top-soils will be analysed first, with sample locations shown in Figure 43 and data for the main pathfinders displayed in Table 48.

Summary of Shercock target area:					
	Element	Overall average (ppm)	Target area average (ppm)	Max	Min
Top-soil	As	6.50	15.25	37.19	3.91
	Ag	0.08	0.12	0.24	0.06
	Hg	0.10	0.12	0.27	0.06
	Sb	0.35	0.75	1.63	0.19
	Mo	1.38	2.11	6.28	0.9
	Zn	54.23	84.86	117.00	52.00
	Pb	25.83	12.93	94.03	23.15
	Cu	22.66	49.62	77.27	13.19
	MnO	461.72	734.86	1440.94	245.71
	Cd	0.41	100.07	0.64	0.21
	<i>Other selected elements with significant difference.*</i>	Elevated: Al%, Ba, Cr, Fe%, Li, Ni, P, V, Zr, Be, Ce, Co, La, Rb, Sc, Th	Depleted: Se, Sr		
Stream Sediment	As	15.24	23.71	72.30	5.20
	Mo	2.12	2.51	6.20	0.80
	Ag	0.28	0.29	0.60	0.10
	Sb	0.82	1.61	4.20	0.60
	Cu	26.86	43.72	165.50	17.60
	Zn	141.37	214.74	412.80	113.20
	Pb	30.67	38.75	125.40	23.30
	Cd	0.79	1.10	2.30	0.40
	MnO%	0.51	1.25	412.80	0.08
	<i>Other selected elements with significant difference.*</i>	Elevated: Co, Cr, Ni, Ba, Sn	Depleted: CaO, Cl, Br, Sr, Zr, Hf, I		

Table 47: Summary table for Tellus Border geochemical data relating to the Shercock target area.

Sample_ID	Ag_mgkg	As_mgkg	Hg_mgkg	Mo_mgkg	Sb_mgkg
582303A	0.20	22.40	0.09	6.28	1.63
582306A	0.12	8.53	0.09	1.31	0.78
582339A	0.09	26.10	0.08	1.29	1.13
582348A	0.13	7.61	0.27	0.99	0.44
582362A	0.24	13.15	0.07	2.69	1.13
582372A	0.10	10.38	0.15	1.82	0.54
582375A	0.13	11.30	0.12	2.20	0.71
582380A	0.10	28.87	0.13	2.28	0.61
582383A	0.14	7.61	0.16	1.44	0.47
582386A	0.11	14.08	0.12	2.43	0.44
582389A	0.12	9.46	0.14	1.77	0.45
582394A	0.16	15.00	0.17	3.82	0.66
582463A	0.17	25.17	0.10	2.03	0.84
582342A	0.07	8.53	0.06	2.06	0.65
582385A	0.09	12.23	0.11	1.92	0.77
582323A	0.12	18.70	0.08	2.52	1.21
582354A	0.10	37.19	0.07	1.62	1.05
582368A	0.09	15.00	0.10	1.25	0.82
582397A	0.06	3.91	0.07	0.90	0.19
582405A	0.12	14.08	0.15	2.57	0.89
582475A	0.13	17.78	0.11	2.18	0.55
582478A	0.09	8.53	0.10	1.06	0.44
area average	0.12	15.25	0.12	2.11	0.75

Table 48: Summary of Au pathfinder elements from top-soil data in the Shercock target.

As displayed in Table 48, Au pathfinder elements show elevated values for the area, when compared with the whole data range. The Ag data reveals good consistency across the set. The correlation matrix does not indicate a strong relationship between As and Ag (Table 49). Despite this, samples with the most distinct element anomalies appear to show good correlation with each other, e.g. 582303A, 582362A and 582463A in Table 48. A strong positive correlation is evident between As and Sb, less so with Sb-Mo and Ag-Mo. There is weak negative correlation for Hg-Sb which was not observed previously.

	<i>Ag_mgkg</i>	<i>As_mgkg</i>	<i>Hg_mgkg</i>	<i>Mo_mgkg</i>	<i>Sb_mgkg</i>
<i>Ag_mgkg</i>	1.000				
<i>As_mgkg</i>	0.312	1.000			
<i>Hg_mgkg</i>	0.236	-0.170	1.000		
<i>Mo_mgkg</i>	0.611	0.479	-0.028	1.000	
<i>Sb_mgkg</i>	0.498	0.722	-0.297	0.575	1.000

Table 49: Correlation matrix for Au pathfinder elements in top-soils for the Shercock target

Sample_ID	Cu_mgkg	Mn_mgkg	Zn_mgkg	Pb_mgkg	Cd_mgkg
582303A	47.76	849.55	82.00	34.14	0.35
582306A	45.84	245.71	69.00	94.03	0.64
582339A	40.57	435.08	103.00	29.96	0.44
582348A	65.30	255.67	52.00	23.78	0.42
582362A	34.89	959.19	70.00	27.60	0.25
582372A	77.27	451.70	102.00	28.96	0.44
582375A	45.03	892.75	95.00	26.33	0.26
582380A	55.27	1440.94	88.00	26.87	0.30
582383A	40.16	330.43	82.00	37.32	0.52
582386A	57.09	768.99	95.00	28.60	0.40
582389A	69.05	861.18	93.00	27.78	0.46

Table 50: Summary table of base metal pathfinder elements in top-soils for Shercock

The results of the base metal analysis are equally as positive, with all elements except for Cd above the total data average (Table 50). Cu-Zn-Mn data show the greatest increase, with only moderate Pb concentrations. The Pb levels may indicate that glacial enrichment from the mine at Castleblaney has not significantly contaminated the area. The correlation matrix for the base metal elements does not generate the positive results expected (Table 51). The best correlation is found between Pb and Cd, this is a relationship that is apparent in the north. Other element associations include Mn-Zn, common in geochemical analyses, and Cu-Cd. The poor relationship between Zn and Pb may reflect the contrasting mobility of the elements.

	<i>Cu_mgkg</i>	<i>Mn_mgkg</i>	<i>Zn_mgkg</i>	<i>Pb_mgkg</i>	<i>Cd_mgkg</i>
<i>Cu_mgkg</i>	1.000				
<i>Mn_mgkg</i>	0.274	1.000			
<i>Zn_mgkg</i>	0.198	0.448	1.000		
<i>Pb_mgkg</i>	0.051	-0.304	-0.019	1.000	
<i>Cd_mgkg</i>	0.552	-0.236	0.175	0.587	1.000

Table 51: Correlation matrix for base metals in the Shercock area

Another correlation matrix was calculated to test the relationships between base metal and Au pathfinder elements (Table 52). The analysis shows weak to moderate positive correlations, with As-Mn showing the greatest correspondence (Table 52). The positive relationship

between Ag and Cu is interesting due to their contrasting mobilities. If these anomalies are related to mineralisation in the north then the transport distance of the two elements should differ.

	<i>Pb_mgkg</i>	<i>Cu_mgkg</i>	<i>Mn_mgkg</i>	<i>Zn_mgkg</i>	<i>Ag_mgkg</i>	<i>As_mgkg</i>	<i>Sb_mgkg</i>
Pb_mgkg	1.000						
Cu_mgkg	0.051	1.000					
Mn_mgkg	-0.304	0.274	1.000				
Zn_mgkg	-0.019	0.198	0.448	1.000			
Ag_mgkg	0.315	0.321	0.274	-0.125	1.000		
As_mgkg	0.010	0.335	0.613	0.317	0.312	1.000	
Sb_mgkg	0.229	0.299	0.443	0.193	0.498	0.722	1.000

Table 52: Correlation matrix for both pathfinder groups in Shercock top-soils.

The stream sediment sample locations and data are displayed in Figure 44 and Table 53. Notable samples include 585602C (raised Mo, Sb and As); 585660C (raised Mo and Sb); 585908C (raised Ag) and 585931C (raised As and Sb).

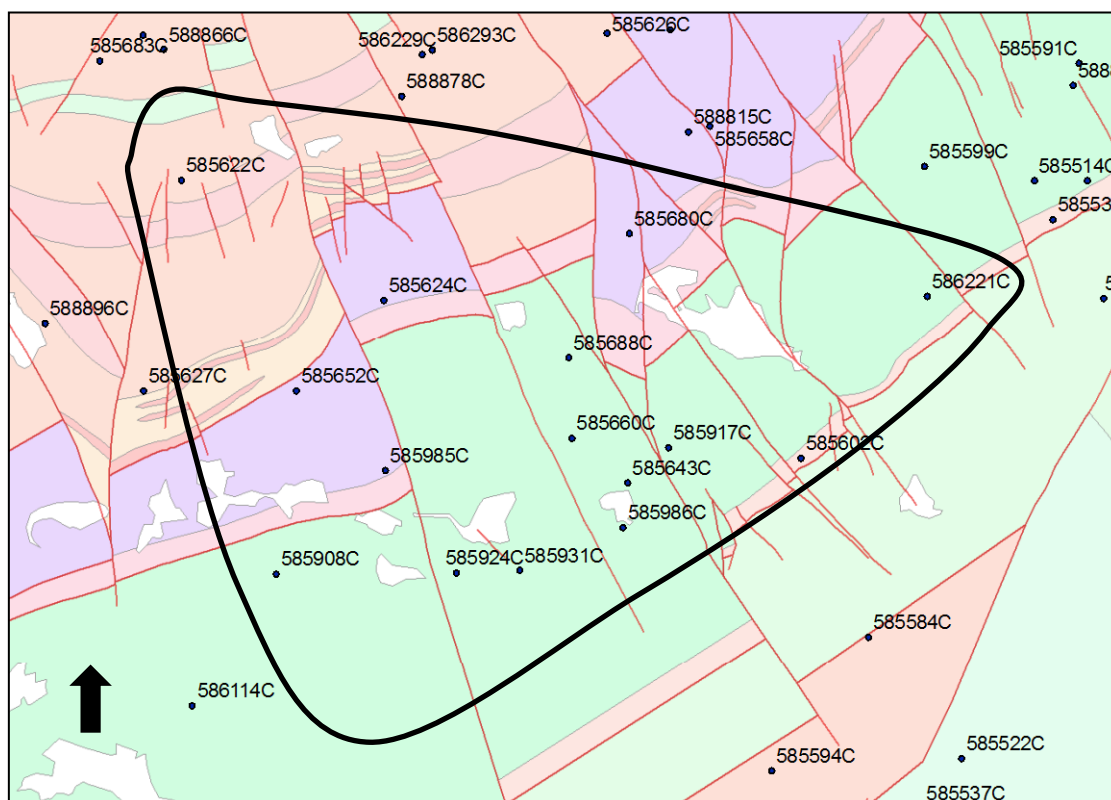


Figure 44: Sample locality map of Tellus Border stream sediment samples

Sample_ID	As_mgkg	Mo_mgkg	Ag_mgkg	Sb_mgkg
585602C	46.9	6.2	0.4	4.2
585621C	11.3	0.8	0.2	2.3
585622C	9.1	1.2	0.25	0.6
585624C	19.5	2.2	0.3	0.9
585652C	14.5	1.4	0.4	1
585680C	9	3	0.25	0.8
585688C	15	2.5	0.25	1.6
585617C	5.2	0.9	0.1	0.6

585643C	20.4	3	0.3	1.6
585660C	32.9	3.8	0.25	1.8
585908C	12.8	2	0.6	1
585917C	25.1	2.4	0.25	1.8
585924C	36	2.3	0.3	1.9
585931C	72.3	1.1	0.25	2.1
585985C	22.3	2.9	0.25	2
585986C	27	4.5	0.25	1.6

Figure 44: Stream sediment sample locations in the Shercock target area

Table 54 shows similar trends within the stream sediment data as the top-soils, with a strong correlation between As and Sb. Comparisons of element associations found at the Sb mine to the north can be made, enhancing this target areas prospectivity. Other elements show weak to moderate positive correlations.

	<i>As_mgkg</i>	<i>Mo_mgkg</i>	<i>Ag_mgkg</i>	<i>Sb_mgkg</i>
<i>As_mgkg</i>	1.000			
<i>Mo_mgkg</i>	0.460	1.000		
<i>Ag_mgkg</i>	0.363	0.406	1.000	
<i>Sb_mgkg</i>	0.766	0.449	0.240	1.000

Table 54: Correlation matrix for Au pathfinder elements in the Shercock stream sediments

The summary of base metal pathfinder elements in stream sediment samples shows very positive results (Table 55). Each element demonstrates a large increase from the average, with Zn and Cu being the most significant. Certain samples stand out due to their elevated values, such as 585602C. This sample, taken in the Laragh black shale formation, also indicates raised values in the Au pathfinder analysis table, thus displaying good consistency of high multi element anomalies.

Sample_ID	MnO_ %	Cu_mgkg	Zn_mgkg	Pb_mgkg	Cd_mgkg
585602C	1.492	165.5	407.3	125.4	1.8
585621C	0.392	28.4	113.2	23.3	0.4
585622C	0.525	17.6	171.7	28.9	0.8
585624C	0.257	33.3	161.8	37.7	0.7
585652C	0.527	38.3	235.6	33.8	0.9
585680C	0.084	40.5	187.5	39.5	1.7
585688C	0.647	48.9	202.7	33.2	1.1
585617C	0.597	22.9	412.8	45.5	2.3
585643C	1.283	33.5	178.4	28	1
585660C	1.527	43.8	245.9	42.5	1
585908C	1.016	25.7	165.7	27.3	0.7
585917C	1.465	60	253.8	49.1	1.3
585924C	2.559	33	168.3	23.4	1.3
585931C	0.738	45.3	178.4	27.8	1
585985C	1.394	28.1	210.2	29.9	0.9
585986C	5.486	34.7	142.6	24.7	0.7

Table 55: Summary of base metal pathfinders in the Shercock target area stream sediments

Strong positive correlations are found between the main base metals (Table 56), particularly Cu-Pb, Zn-Pb-Cd. This was not expected due to contrasting element mobility, and suggests a local source for the anomalous values, either from contamination or mineralisation.

	<i>MnO_%</i>	<i>Cu_mgkg</i>	<i>Zn_mgkg</i>	<i>Pb_mgkg</i>	<i>Cd_mgkg</i>
<i>MnO_%</i>	1.000				
<i>Cu_mgkg</i>	0.172	1.000			
<i>Zn_mgkg</i>	0.075	0.484	1.000		
<i>Pb_mgkg</i>	-0.047	0.778	0.816	1.000	
<i>Cd_mgkg</i>	-0.043	0.397	0.817	0.616	1.000

Table 56: Correlation matrix for base metal pathfinders in the Shercock target area stream sediments

The correlation matrix for both pathfinder groups shows an overall weak to moderate positive correlation (Table 57), with similar patterns to the top-soil data. Again, Zn-Ag shows a weak negative correlation, which could be explained by mobility but this is unlikely considering the other element relationships.

	<i>MnO_%</i>	<i>Cu_mgkg</i>	<i>Zn_mgkg</i>	<i>Pb_mgkg</i>	<i>As_mgkg</i>	<i>Ag_mgkg</i>	<i>Sb_mgkg</i>
<i>MnO_%</i>	1.000						
<i>Cu_mgkg</i>	0.172	1.000					
<i>Zn_mgkg</i>	0.075	0.484	1.000				
<i>Pb_mgkg</i>	-0.047	0.778	0.816	1.000			
<i>As_mgkg</i>	0.537	0.594	-0.006	0.160	1.000		
<i>Ag_mgkg</i>	0.141	0.294	-0.205	0.051	0.363	1.000	
<i>Sb_mgkg</i>	0.504	0.704	0.045	0.280	0.766	0.240	1.000

Table 57: Correlation matrix for both pathfinder groups in stream sediments of the Shercock target area.

The main concern for this target area is the risk of contamination from historic and current mining activity to the north. A good way of testing this is to consider the abundance of elements with contrasting mobilities, such as Cu and Pb. The data suggests a strong positive relationship between the two, if sourced from northern mines the discrepancy between the elements would be greater (see Appendix for further discussion and analysis). This suggests that contamination from mining activity to the north has not significantly raised pathfinder values, but may have increased the background levels of each element. If the impact of the mines had been severe, it may have been possible to trace the anomalous values southwards in the direction of ice flow and find a general decrease in element concentration. The outcome of our preliminary analysis enhances the areas prospectivity for both Au-Ag and base metal style mineralisation.

6.4.4. Fieldwork

The target area was selected due to high geochemical anomalies across a range of element groups. Unlike Millford and Glenties, the Shercock target area has available geophysical data which can also be used as an exploration tool to follow up any geochemical anomalies. The main targets are the NW trending faults which have a similarity with the fault controlled mineralisation at Clontibret and Castleblaney. Due to the nature of the landscape, limited outcrop in the area restricted mapping and geological interpretations, making stream sediment and float samples of even greater significance. The following fieldwork objectives were set:

- Target areas where streams cross mapped faults
- Identify indications of glacial movements in the topography
- Identify any causal links between bedrock and geochemical anomalies
- Target specific areas of high anomalies to look for contamination or bedrock exposure

The limited outcrop was the biggest restriction during field exploration which resulted in limited assessment of lithologies and structural geology. However, in places outcrop was of good quality and allowed a brief glimpse of small scale structural features which were analysed. Figure 45 shows typical overburden, with thickness >2 m.



Figure 45: Photograph of typical overburden in Shercock area

Streams, and roadside rock piles were useful sources of float material although potentially derived from distal sites. The majority of float material consisted of mudstones and shales, which match well with the local mapped lithologies. The stream sediment samples were widespread and difficult to extract, mainly due to the overgrown nature of many streams and rivers. In certain areas re-sampling of Tellus Border survey points was carried out to assess any contrast in results. Bedrock sampling was possible in some upland areas.

Formation	Lithology	Description
Lough Avaghon Formation	Mudstone	Fine grained mudstone showing massive to no bedding. Pyrite commonly associated as disseminations.
	Conglomerate	Very coarse material. Two types of veining apparent, quartz and calcite veins. Shows calcite on inside with rims of quartz. Pyrite associated with calcite more than quartz. Veining often exhibits brecciation.
Oghill Formation	Micro-conglomerate	Poorly sorted fine to coarse conglomerate with alternating layers of mudstone. Minor disseminations found in conglomerate but not in mudstone.
Kehemaghkilly Formation	Mudstone	Light in colour and less laminated than other mudstones in the area. Narrow veinlets within samples heavily hematized. Fewer laminations resulted in less deformation and erosion. Minor disseminations of sulphide

	Black shale	Distinguished by abundant pyrite along fine laminations. Also very dark colour easily separates unit from mudstone. Pyrite possibly orthogenic, no evidence to suggest otherwise. Minor stringer veins but not associated with mineralisation.
--	-------------	--

Table 58: Summary of mapped units and formations in the Shercock area.

Despite poor exposure, the units studied and sampled provided a good understanding of the local geology. The most common units are variations between mudstones, shales and conglomerate type facies. Mineralisation was common throughout the target area, mainly minor disseminations within specific shale units. Pyrite is the dominant sulphide mineral, with minor arsenopyrite. The photographs in Figure 46 illustrate the main forms and occurrences of sulphide mineralisation. As well as the disseminated pyrite, the fine quartz veins that occur within the shale units display signs of mineralisation. The thin veins are heavily hematized on the surface, with visible pyrite in places. The occurrences seem to be associated with minor fractures, as minor offsets can be seen at contact with host rock. The veins themselves also appear offset, indicating multiple phases of deformation throughout the units geological history.

During fieldwork there was the chance to analyse the poor correlation between top-soil and stream sediment anomalies. Small observations in the field concluded that due to the overgrown nature and low flow rate of many streams, the type of material found may not be fully representative of underlying bedrock. This theory was further analysed by comparing top-soil values with sub-soil values and elemental background levels with bedrock composition.



Figure 46: photographs showing the occurrence of vein hosted mineralisation in the Shercock target area.

6.4.5. Results

The results reveal significant relationships in geochemistry of the target area. Bedrock samples show small anomalies across a range of lithologies with raised values of Cu, Ag, Mo, Sb and Au (Table 59; Figure 47). A strong correlation between Sb and Mo can be observed easily with values showing marked increase in black shale units throughout the area (OM-13-PS-074). The quartz vein material, shown in Figure 46, contains raised Cu, which may suggest minor amounts of chalcopyrite. The well documented abundant pyrite within shale units appears barren, with little signs of base metal or Au pathfinder concentrations above background levels. Small increases in Cu and As may be related to minor levels of arsenopyrite and chalcopyrite. Although not reported in Table 59, high Ni values (154 ppm) in the area have a strong association to the volcanic units, mainly rhyolite, within the sedimentary formations. In terms of association of anomalous values with contamination, the high background levels in the bedrock may rule out the possibility of large scale element concentrations from the north. However, when analysing the stream sediment results, contamination cannot be ignored. The Au values from bedrock are close to its LLD, but values in stream sediments can be found close to 1 ppm showing little association with bedrock. This could be related to the type of material being predominately of glacial origin and not from the local bedrock. Other elements which demonstrate a contrast between sample types include Zn and Mo, which are elevated within stream sediments. This may be related to the mobility of these elements, potentially being transported over large distances. It should be noted that not all lithologies in the target area were sampled, so caution should be applied when comparing these two datasets. Results from the selected Tellus Border samples (GSI archive) reveal few high end anomalies in Table 60. The sub-soils showed good Ag concentrations of around 0.3 ppm with base metals above background values. There is good correspondence between top-soil and sub-soils. The most encouraging sample was 582303, showing elevated concentrations of Cu and Sb, but as mentioned earlier levels of Sb have a strong correlation with the shale units in this area. Panned concentrate samples indicated below background levels for most elements of interest. Only three samples were analysed but they show little correlation with the Au levels witnessed from the stream sediment samples collected.

SAMPLE	Type	Lithology	grams weight	ppm Au	ppm Ag	ppm As	ppm Cu	ppm Hg	ppm Mo	ppm Pb	% S	ppm Sb	ppm Zn
OM-13-PS-057	Float	quartzite	350	<0.001	0.05	5.5	10.4	0.04	0.3	5.5	0.3	0.3	23
OM-13-PS-058	Float	mudstone	371	0.001	0.06	5.7	39.8	0.09	0.34	20.6	0.33	0.29	104
OM-13-PS-059	Float	quartz	73	<0.001	<0.01	1.3	19.7	0.03	0.24	11.6	0.04	<0.05	17
OM-13-PS-060	Float	mudstone	234	0.006	0.11	17.1	68	0.06	0.69	26.5	0.96	2.65	97
OM-13-PS-061	Float	mudstone	444	<0.001	0.01	3.3	27.2	0.04	0.32	8	0.14	0.25	65
OM-13-PS-062	Float	rhyolite	381	<0.001	0.01	11.4	31.9	0.04	0.06	6.1	0.36	5.47	51
OM-13-PS-063	Float	shale	290	0.035	0.28	87.3	87.7	0.06	17.05	51.3	2.25	13.5	41
OM-13-PS-064	Float	mudstone	179	<0.001	0.04	1.8	23.3	0.05	0.33	3.1	0.72	0.95	53
OM-13-PS-065	Float	turbidite	390	0.002	0.18	7.3	60.2	0.05	2.12	7.1	0.64	1.45	95
OM-13-PS-068	Bedrock	micro- conglomerate	416	<0.001	0.1	10.1	23.3	0.03	0.31	11.1	1.08	3.55	42
OM-13-PS-070	Bedrock	mudstone	341	<0.001	0.08	10.3	29.6	0.04	0.89	18.9	0.41	0.36	87
OM-13-PS-072	Bedrock	micro- conglomerate	339	<0.001	0.06	5.1	29.3	0.03	0.33	16.2	0.06	<0.05	66
OM-13-PS-073	Bedrock	shale	99	<0.001	0.2	50.7	48.5	0.04	0.9	29.9	0.86	0.72	45
OM-13-PS-074	Bedrock	black shale	460	0.003	0.43	38.1	89.2	0.07	8.68	26.4	2.53	4.78	66
OM-13-PS-075	Bedrock	quartz vein	83	<0.001	0.08	9.8	133.5	0.03	1.24	16.5	0.46	0.46	40
OM-13-PS-076	Bedrock	mudstone	221	<0.001	0.14	10.8	38.5	0.05	1.25	16.7	0.67	0.69	86

Sample ID	Type	Grain size	grams weight	ppm Au	ppm Ag	ppm As	ppm Cu	ppm Hg	ppm Mo	ppm Pb	% S	ppm Sb	ppm Zn
OM-13-PS-066	SS	fine	537	0.952	0.07	19.6	35.7	0.04	2.09	43.2	0.1	1.27	96
OM-13-PS-071A	SS (dup)	fine	339	0.638	0.26	9.5	22.1	0.02	1.19	24.4	0.04	0.59	121
OM-13-PS-071B	SS (dup)	fine	330	0.282	0.06	12.1	20.4	0.03	1.24	35.2	0.03	0.63	120
OM-13-PS-077	SS	medium	511	0.227	0.31	29.7	31.6	0.02	2.75	77.2	0.04	0.86	236

Sample ID	type	Weight	pH	pH (HCl)	ppm Au	ppm Ag	ppm As	ppm Cu	ppm Hg	ppm Mo	ppm Pb	% S	ppm Sb	ppm Zn
OM-13-PS-234	topsoil	962	5.37	5.08	0.001	0.12	11	45.6	0.1	1.22	28.8	0.08	0.68	89
OM-13-PS-235	subsoil	680	6.17	4.65	0.003	0.03	12.5	33.3	0.09	0.65	27.2	0.01	0.82	96
OM-13-PS-236	topsoil	1009	5.78	4.8	0.002	0.1	9.2	60.6	0.12	0.86	31.4	0.08	0.53	80
OM-13-PS-237	subsoil	675	6.02	4.9	0.001	0.03	5.3	25	0.02	0.66	34.2	0.01	0.65	119
OM-13-PS-238	topsoil	1082	5.47	4.51	0.002	0.1	8.6	42.5	0.12	0.66	29.3	0.06	0.64	65
OM-13-PS-239	subsoil	894	5.79	4.46	0.002	0.06	8.3	22.8	0.08	0.65	20.6	0.03	0.59	72
OM-13-PS-240 A	topsoil	443	5.24	4.45	0.001	0.08	6.6	42.1	0.1	0.68	31.1	0.05	0.62	84
OM-13-PS-240 B	topsoil	443	5.24	4.45	0.002	0.09	6.8	41.4	0.12	0.7	30.3	0.05	0.7	84
OM-13-PS-241	subsoil	1100	5.45	4.21	0.001	0.1	5.9	28.3	0.1	0.65	26.7	0.04	0.48	69
OM-13-PS-242	topsoil	789	4.95	4.14	0.01	0.12	9.6	63.6	0.12	0.73	32.7	0.07	0.6	70
OM-13-PS-243	subsoil	1198	5.2	4.13	0.001	0.07	6.2	25.2	0.05	0.61	31.8	0.02	0.38	98

Total number of samples = 31
soil samples = 10
sediment samples = 4
whole rock samples = 16

Table 59: Summary table showing new sample results for the Shercock target.

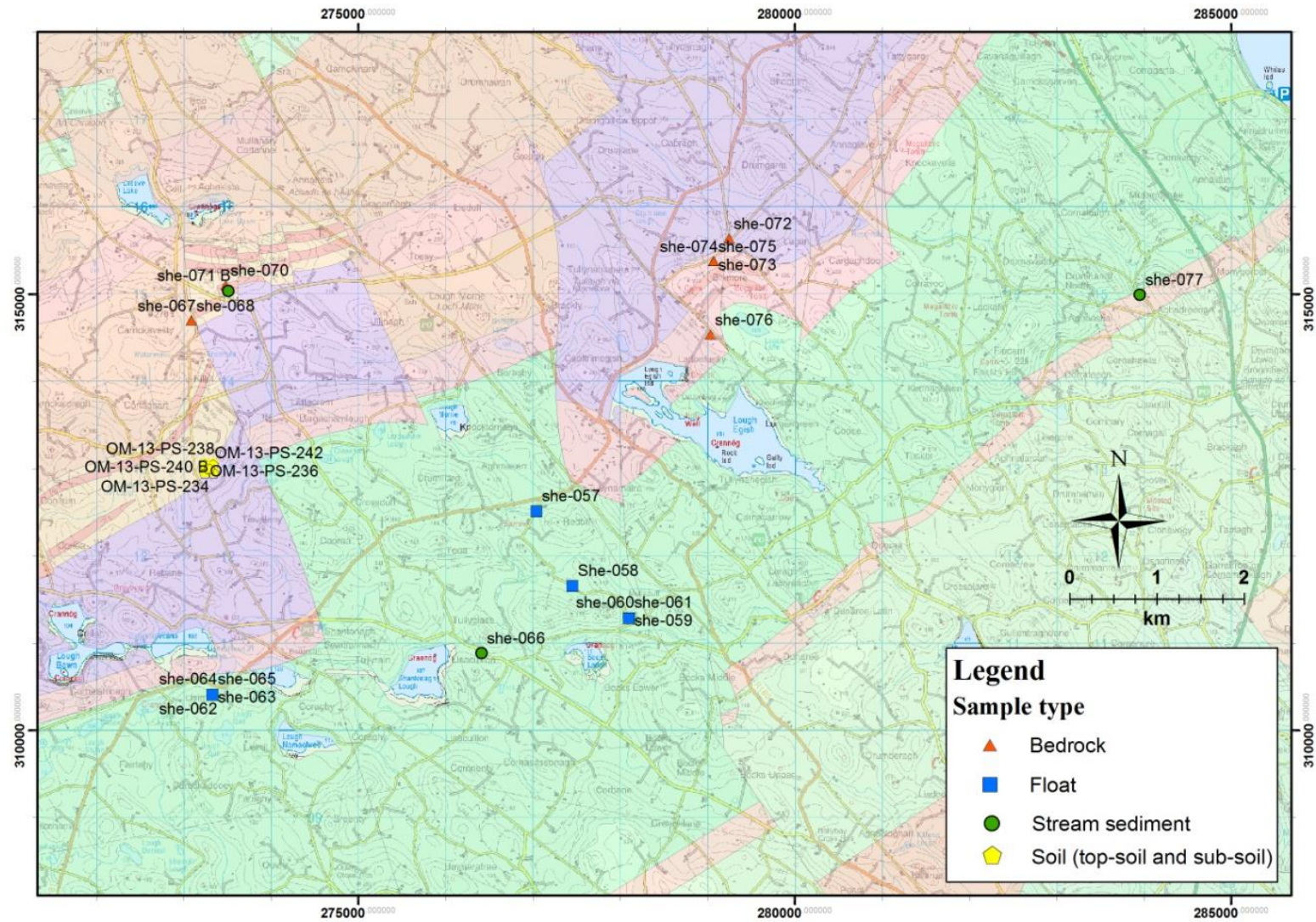


Figure 47: Map showing location of new samples collected in the Shercock target.

Sample type	ID	Au	Ag	As	Hg	Sb	Cu	Mo	Pb	Zn
sub-soil	582399 -S	0.002	0.29	16.2	0.21	0.89	71.5	1.48	66.4	54
	582362 -S	0.002	0.31	16.9	0.11	1.87	35.7	2.29	28.4	72
	582303 -S	0.002	0.31	28	0.13	2.02	53.3	6.36	42.9	86
panned conc.	585688	Na	0.04	16.5	0.02	0.42	57.6	1.51	6.4	76
	585660	Na	0.02	8.7	0.01	0.4	13.6	1.11	10.1	95
	585662	0.013	0.04	2	0.02	0.11	16.9	0.16	16.7	163
Stream-sediment	585688C	Na	0.25	15	Na	1.6	48.9	2.5	33.2	202.7
	585660C	Na	0.25	32.9	Na	1.8	43.8	3.8	42.5	245.9
	585662C	Na	0.2	4.3	Na	0.4	38.6	0.6	32.6	193.9
top-soil	582399	Na	0.21	14.08	0.26	0.60	94.80	1.96	62.77	80.00
	582362	Na	0.24	13.15	0.07	1.13	34.89	2.69	27.60	70.00
	582303	Na	0.20	22.40	0.09	1.63	47.76	6.28	34.14	82.00

Table 60: Comparison of selected sub-soil and panned concentrate samples with the associated top-soil and stream sediment samples in the Shercock target

A soil grid was constructed in the west of the target area, around a Tellus Border sample (582373) displaying high Ag, As and base metals. The soil samples were taken from hard but easily penetrable ground. The samples were generally dry with large fragments of shale and mudstone. Results do not show any significant anomalies (Table 59). As with Tellus border values for the region, the Cu concentrations are above background levels, however, no other base metals stand out. There appears to be a strong lithological control with high Ni and Cr values likely to be sourced from the local volcanic intrusions (see Appendix). The Tellus Border Pb anomalies are not replicated in the new data. The Shercock soil results demonstrate significantly lower values for key elements in sub-soils compared with top-soils (Table 61). Each value within the dataset was ranked with lower ranking scores corresponding to higher element anomalies. The high concentrations of elements in the top-soil may be due to the glacial reworking of the upper layers over time, whereas the sub-soils have been subject to less alteration and enrichment. The table below summaries the results for the soil analysis, notice the comparatively high pH values compared with Millford and Manorhamilton.

Sample ID	type	Weight (g)	pH	pH (HCl)	Score		
OM-13-PS-235	subsoil	680	6.17	4.65	0.49	average score	
OM-13-PS-237	subsoil	675	6.02	4.9	0.57		
OM-13-PS-239	subsoil	894	5.79	4.46	0.75		
OM-13-PS-241	subsoil	1100	5.45	4.21	0.72		
OM-13-PS-243	subsoil	1198	5.2	4.13	0.68		
OM-13-PS-234	topsoil	962	5.37	5.08	0.28	subsoil	0.64
OM-13-PS-236	topsoil	1009	5.78	4.8	0.43	topsoil	0.44
OM-13-PS-238	topsoil	1082	5.47	4.51	0.54		
OM-13-PS-240 A	topsoil	443	5.24	4.45	0.53		
OM-13-PS-240 B	topsoil	443	5.24	4.45	0.43		
OM-13-PS-242	topsoil	789	4.95	4.14	0.40		

Table 61: Comparison between major element values in top- and sub-soils within the Shercock target.

7. Summary and Conclusion

A thorough analysis of the geochemical datasets generated through the Tellus Border project identified several areas containing clusters of samples with multiple raised pathfinder element anomalies. This data was used in conjunction with the new geophysical maps to determine the most prospective areas (Section 4). Four target areas were defined for further detailed investigation, however, it must be stressed that these represent only a fraction of the ground classified as highly prospective through this work. Prior to the start of the fieldwork phase, a series of objectives were set for each area and these determined the exploration strategy. The main aim was to identify potential sources of major element anomalies through comparison of geochemical signatures for local bedrock with top-soil and stream sediment values. This process was hindered by variable outcrop in each target area, in particular lithological compositions were difficult to determine within the Manorhamilton and Shercock regions. Despite poor exposure, no major sources of human derived contamination were identified.

The Manorhamilton prospect was originally based on high levels of Au pathfinder elements within top-soils, with the NE trending faults and Dalradian meta-sediments designated as potential sources for the anomalies. Few bedrock samples were found and these did not contain Au above detection limits, however, one sample did show significantly raised values for Au pathfinder elements Ag, As and Sb. Stream sediments yielded more positive results, which is likely to be due to the concentration of denser more resistant sulphides. The evidence suggests a genetic link between stream sediment values and a bedrock source, particularly psammite units adjacent to the major NE trending faults. The spatial relationships of high anomalies with the aforementioned faults also back up this theory. Soil samples in the west of the target, overlying the Dalradian Meelick unit, indicate raised Au pathfinder elements, specifically for Sb.

The Glenties target area was selected because of its ideal geological setting and high geochemical anomalies of Ag and As within stream sediments. The fieldwork evidence suggests that this area remains highly prospective due to observed mineralisation and anomalous precious metal values derived from whole rock analysis. Stream sediments display high Au contents and the prospectivity of the target is supported by raised pathfinder values for Au, Ag and Sb over a large region. The source of these anomalies is attributed to a quartz vein taken from a large boulder, most likely from proximal quartzite formations. Values for Pb are also significant in float and stream sediments, often combined with raised Ag. The other style of mineralisation noted throughout the area was Cu mineralisation of quartz veins within dolerite pods. It is possible that these mineralised veins could be present outside of the dolerite, within the adjacent meta-sediments. The shape and orientation of this phase of veining may be different due to contrasting rheological properties of the host rocks. However, Cu mineralisation may only be limited to the dolerite pods if the metal has been scavenged from the host rock along with Fe and sulphur. Evidence for Cu style mineralisation is as yet unidentified within the meta-sediment formations.

Significant concentrations of Au, Ag, Sb and Pb are noted for stream sediments within the Millford target area. The source of these anomalies seems to be linked to the Slieve Tooley

Formation. Any outcrop of the formation appears barren but several samples show thin stringers of black material rich in pyrite. Aside from high values in stream sediments, the same region indicates high promise in soil concentrations of pathfinder elements, specifically Sb, Pb and Zn, good correlation between sample types shows that this area is highly prospective.

The Shercock target area was interpreted with caution, due to the potential of contamination from the northern mineral districts. This issue was investigated through careful analysis of pathfinder element concentrations between Shercock and the region to the north. No geochemical trails were found and correlation was identified between elements of contrasting mobilities suggesting that contamination is not significant. The comparison between local geology and geochemical data is complicated by scarce bedrock exposure. However, the new stream sediment samples collected do show similar results to the Tellus Border samples indicating minor Au, however, it is likely that this material has been washed out and eroded from thick glacial overburden. Raised levels of Ag, Sb and Cu in Tellus Border sub-soils are encouraging, however, soil grids generated in this project did not identify any significant anomalies. Bedrock and float samples of black shale contain raised Ag, Sb, Mo and Cu. The bedrock sample is derived from a heavily faulted block in the north of the target area.

The results from this project demonstrate that many areas within the border region are highly prospective for base and precious metals. All four of the target areas examined showed promise and built on the positive results from the Tellus Border survey. In each case, raised pathfinder element anomalies shown in the Tellus Border datasets were supported by anomalous levels of Au and Ag in the regions studied. Throughout the project the question of accuracy and reliability of geochemical data for representing the underlying geology has been investigated. Geochemistry has been a highly useful tool in delineating potential sources of mineralisation. The four chosen target areas were only a small number of potential target areas which met the right criteria for further analysis. The four areas selected are ranked below in order of prospectivity, based on geochemistry, geology and theoretical interpretations:

1. Glenties, Co. Donegal - Au-Ag and Cu mineralisation
2. Millford, Co. Donegal - Au-Ag mineralisation
3. Manorhamilton, Co. Leitrim - Au mineralisation
4. Shercock, Co. Monaghan - Au and base metal mineralisation

Of the preliminary target areas shown in Section 4 several areas should be noted for special consideration, including Ballyshannon and Pettigoe. Both of these would benefit from high resolution sampling in soils and stream sediments.

Whether this project achieves its main aims of generating investment and interest in the Republic of Ireland remains to be seen. However, it is clear from the results that the border region hosts some highly prospective areas for Au and base metal mineralisation.

8. References

- Andrew-Jones, D. (1968). *Application of Geochemical Techniques to Mineral Exploitation*, s.l.: Colorado School of Mines.
- Clennon, K.K. (2013). *Geochemical Data User Guide*, Dublin: Geological Survey Ireland.
- Clifford, J.A., Earls, G., Meldrum, A.H. and Moore, N. (1992). Gold in the Sperrin Mountains, Northern Ireland: an exploration case history.
- Cole, G.A.J., (1922). Memoir and Map of Localities of Minerals of Economic Importance and Metalliferous Mines in Ireland. *Department of agriculture and Technical Instruction For Ireland*. Dublin.
- Cooper, M.R., Crowley, Q.G., Hollis, S.P., Noble, S.R. and Henney, P.J. (2013). A U-Pb age for the Late Caledonian Sperrin Mountains minor intrusions suite in the north of Ireland: timing of slab break-off in the Grampian terrane and the significance of deep-seated, crustal lineaments. *Journal of the Geological Society, London*. Doi 10.1144/jgs2012-098.
- Cruise, M. and Farrell, L.P.C. (1993). Exploration focus – Clontibret. MINFO 10/93, Exploration and Mining Division, Department of Transport, Energy and Communication, 4pp.
- Damman, A. (1978). Distribution and movement of elements in ombrotrophic peat bogs. *Oikos*, pp. 480-495.
- Exploration and Mining Division Ireland (2005). The “Top 55” Deposits. Department of Communications, Marine and Natural Resources.
- GSI, (2006). *Land of Mineral Opportunities*, Dublin: Geological Survey Ireland.
- Lusty, P.A.J., McDonnell, P.M., Gunn, A.G., Chacksfield, B.C. and Cooper, M. (2009) Gold Potential of Dalradian Rocks of north-west Northern Ireland: Prospectivity Analysis using Tellus Data, Keyworth, UK: British Geological Survey.
- Parnell, J., Earls, G., Wilkinson, J.J., Hutton, D.H.W., Boyce, A.J., Fallick, A.E., Ellam, R.M., Gleeson, S.A., Moles, N.R., Carey, P.F. & Legg, I. (2000). Regional fluid flow and gold mineralization in the Dalradian of the Sperrin Mountains, northern Ireland. *Economic Geology*, Vol 95, pp. 1389-1416.
- Smith, M.H., Furlong, D. and Sweeney, J. (2003). The Longford-Down Massif- A New in the Appalachian, Caledonian Orogen, Dublin: Conroy Diamonds and Gold, PLC.
- Soper, N.J. (1994). Neoproterozoic sedimentation on the northeast margin of Laurentia and the opening of Iapetus. *Geological Magazine*, 131, 291-299.
- Steed, G.M. and Morris, J.H. (1997). Isotopic evidence for the origins of a Caledonian gold-arsenopyrite-pyrite deposit at Clontibret, Ireland. *Trans. Instn. Min. Metall. (Sect. B: Appl. Earth Sci.)*, Vol 106, pp 109-118.

Stone, P., Cook, J.M., McDermott, J.J., and Simpson, P.R. (1995). Lithostratigraphic and structural controls on distribution of As and Au in the southwest Southern Uplands, Scotland. Trans. Instn. Min. Metall. (Sect B., Appl. Earth Sci.) Vol 104, pp111-119.